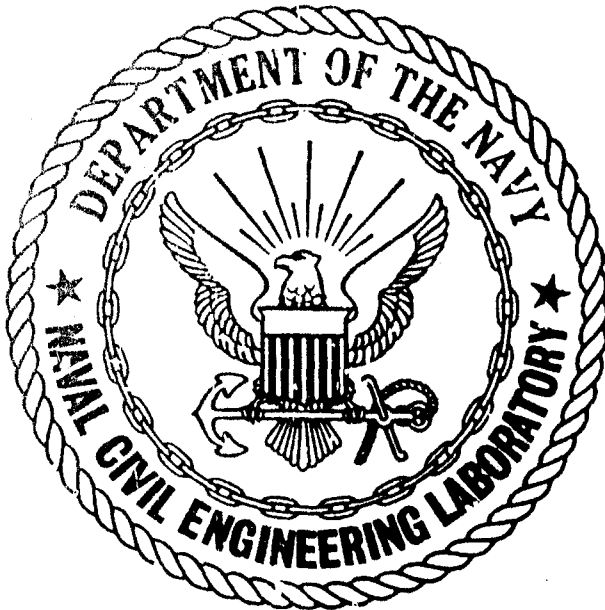


AD 747657



**CR 72.018**

NAVAL CIVIL ENGINEERING LABORATORY  
Port Hueneme, California

Sponsored by  
NAVAL ELECTRONIC SYSTEMS COMMAND

DEVELOPMENT AND SHOCK TUBE TEST  
ANALYSIS OF PISTON PLATE AIRBLAST  
VALVE

7 April 1972

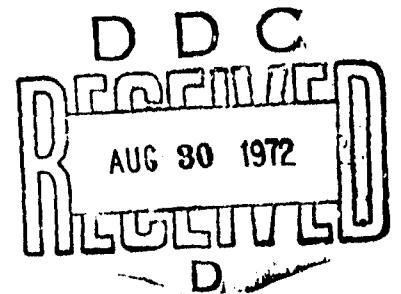
An Investigation Conducted by

THE CLARK VALVE COMPANY  
Albuquerque, New Mexico 87111

N62399-70-C-0009

Approved for public release;  
distribution unlimited.

Reproduced by  
NATIONAL TECHNICAL  
INFORMATION SERVICE  
U.S. Department of Commerce  
Springfield VA 22151



143

0

UNCLASSIFIED

Security Classification

DOCUMENT CONTROL DATA - R & D

(Security Classification of title, body of abstract and indexing annotation must be entered when the overall report is classified)

1. ORIGINATING ACTIVITY (Corporate author) <b>THE CLARK VALVE COMPANY</b> 11916 El Solindo, N. E. Albuquerque, New Mexico 87111		2a. REPORT SECURITY CLASSIFICATION <b>Unclassified</b>	
		2b. GROUP	
3. REPORT TITLE <b>DEVELOPMENT AND SHOCK TUBE TEST ANALYSIS OF PISTON PLATE AIRBLAST VALVE</b>			
4. DESCRIPTIVE NOTES (Type of report and inclusive dates) <b>Final Report on work in interval March 26, 1970 to April 7, 1972.</b>			
5. AUTHOR(S) (First name, middle initial, last name)  <b>Robert O. Clark</b>			
6. REPORT DATE <b>April 7, 1972</b>	7a. TOTAL NO OF PAGES <b>140</b>	7b. NO OF REFS <b>10</b>	
8a. CONTRACT OR GRANT NO <b>Contract No. N62399-70-C-0009</b>	9a. ORIGINATOR'S REPORT NUMBER(S)  <b>3</b>		
b. PROJECT NO <b>Work Unit 63-007</b>	9b. OTHER REPORT NO(S) (Any other numbers that may be assigned this report)  <b>CR 72.018</b>		
10. DISTRIBUTION STATEMENT  <b>Approved for public release; distribution unlimited</b>			
11. SUPPLEMENTARY NOTES		12. SPONSORING MILITARY ACTIVITY <b>U. S. Naval Civil Engineering Laboratory</b> <b>Port Hueneme, California 9304</b>	
13. ABSTRACT <p>An airblast valve utilizing the piston plate principle is conceptually designed for use in a blast hardened air entrainment system. Primary features of this valve are the elimination of the extensive delay path external to the valve housing, the elimination of the debris pit and auxiliary power to help close the valve, insensitivity to ground shock even if some distortion of the valve housing occurs, and several less significant features (U).</p> <p>One dimension of the valve is independent of scaling properties. This dimension was reduced about one-sixth to design a sectional test valve that would adapt to a high pressure shock tube without changing any performance characteristics associated with normal ventilation flow or shock interaction.(U).</p> <p>The sectional test valve is stress analyzed for static pressure up to 1,500 psi and dynamic interacting high pressure shock on the closure mechanism (U).</p> <p>The sectional test valve was constructed according to the included shop drawings for tests in a high pressure shock tube. The first series of tests showed three problem areas or performance faults and indicated likely methods of solution. The second test series validated these methods of solution. Finally, repeated shock waves were applied up to the incident pressure of 250 psi (1,640 psi reflected pressure) successfully (U).</p> <p>The normal ventilation pressure head loss through the valve was found to be exceptionally low at 0.73 inches of water for 500 cfm (U).</p> <p>The resulting recommended modification applied to the prototype is expected to more than satisfy government specifications and requirements of the blast valve (U).</p>			

ia

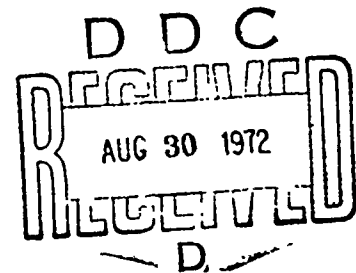
14 KEY WORDS	LINK A		LINK B		LINK C	
	ROLE	WT	ROLE	WT	ROLE	WT
1. Airblast Valve Tests						
2. Piston Plate Airblast Valve						
3. Design, Performance Characteristics, and Shock Tests of Fast Acting Airblast Valve						
4. A Thin Plate Closes by Shock so Rapidly that a Blast Valve Based on this Principle Needs no Extensive Delay Path						
5. Shock Tube Tests to 250 psi Incident on Closure Valve						
6. Weapons Systems						
7. Blast Valve						
8. Blast Closure Valve						
9. Blast Hardened Facilities						

*IL*

DEVELOPMENT  
and  
SHOCK TUBE TEST ANALYSIS  
of  
PISTON PLATE AIRBLAST VALVE

by

THE CLARK VALVE COMPANY  
11916 El Solindo, N. E.  
Albuquerque, New Mexico 87111

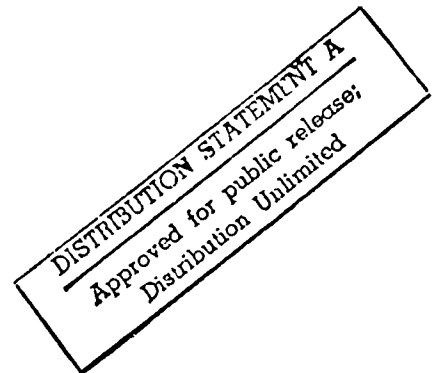


N.C.E.L. Contract No. N62399-70-C-0009

April 7, 1972

Prepared for

THE NAVAL CIVIL ENGINEERING LABORATORY  
Port Hueneme, California 93041



*lc*

## FOREWORD

This report constitutes a portion of the Project Clarinet-Sanguine facilities research program which was accomplished through NCEL by contractual and in-house effort. The facilities research program was sponsored by the Earth Sciences Division of the Office of Naval Research (ONR) under their field projects program. ONR was charged by the Sanguine Division of the Naval Electronic Systems Command with the general management of the overall research program for Project Sanguine.

This facilities research program consists of work units as follows:

- Facility System Study
- Air Entrainment System
- Water Wells
- Air System Components
- Fuel Storage Containers
- Computer Output Display
- Hardness of Buried Cable
- Vertical Grounds

These work units encompass areas in which improved technology was needed or in which significant cost reduction might be achieved through improvement in extant knowledge. The research program at NCEL was initiated in early November 1968.

General direction of the program was provided by Dr. T. P. Quinn and his staff of the Earth Sciences Division, ONR, with the counsel of Messrs. W. J. Bobisch and W. W. Pinkerton of the Naval Facilities Engineering Command. Mr. J. R. Allgood of NCEL served as project coordinator. Messrs. D. E. Williams and J. A. Norbutas served as contract monitors for the work described in this report.

The Clark Valve Company project engineer was Mr. Robert Clark. Principal contributors to the report were Messrs. Robert Clark and Wayne McMurtry. A portion of the work was done under subcontract by Mechanics Research Incorporated.

## ABSTRACT

An airblast valve utilizing the piston plate principle is conceptually designed for use in a blast hardened air entrainment system. Primary features of this valve are the elimination of the extensive delay path external to the valve housing, the elimination of a sensor and auxiliary power to help close the valve, insensitivity to ground shock even if some distortion of the valve housing occurs, and several less significant features.

One dimension of the valve is independent of scaling properties. This dimension was reduced about one-sixth to design a sectional test valve that would adapt to a high pressure shock tube without changing any performance characteristics associated with normal ventilation flow or shock interaction.

The sectional test valve is stress analyzed for static pressure up to 1,500 psi and dynamic interacting high pressure shock on the closure mechanism.

The sectional test valve was constructed according to the included shop drawings for tests in a high pressure shock tube. The first series of tests showed three problem areas or performance faults and indicated likely methods of solution. The second test series validated these methods of solution. Finally, repeated shock waves were applied up to the incident pressure of 250 psi (1,640 psi reflected pressure) successfully.

The normal ventilation pressure head loss through the valve was found to be exceptionally low at 0.73 inches of water for 500 cfm.

The resulting recommended modification applied to the prototype is expected to more than satisfy government specifications and requirements of the blast valve.

## CONTENTS

I.	INTRODUCTION	
	1. Discussion	1
	2. Background	2
	3. Purpose	3
	4. Performance	4
II.	PLATE DESIGN OF MODEL VALVE	
	1. General Comments	6
	2. Cover Plate	7
	3. Access Door	13
	4. Baffle Plate	16
	5. Side Plates	21
	6. Bottom Plate	22
	7. Test Door	23
	8. Top Plate	23
	9. Inlet Tube	24
	10. Typical Grid Plate	27
	11. Grid Support Plate	31
III.	ANALYSIS OF PISTON PLATE	
	1. General Considerations	35
	2. Required Closure Time	37
	3. Approximate Closure Time	38
	4. Impact Velocity	41
	5. Static Stability	42

IV.	1. P AND STUD DESIGN	
	1. General Comments	46
	2. General Analysis	48
	3. Stud Selection	51
	4. Bolt Design	54
V.	DESIGN AND ANALYSIS OF PROTOTYPE	
	1. Introduction	59
	2. Baffle and Baffle Support Plates	60
	3. Inlet Side Plates and Stiffeners	64
	4. Cylindrical Wall	69
	5. Semi-Elliptical Head	75
	6. Exit: Side and End Plates and Stiffeners	80
	7. Concluding Remarks	87
VI.	VALVE CONSTRUCTION AND ANALYSIS OF FIRST TEST SERIES	
	1. Construction of Sectional Test Valve and its Modification	88
	2. First Test Series	89
	3. Evaluation of First Test Series	90
	4. Pressure Head Loss	93
VII.	SECOND TEST SERIES	
	1. Discussion	98
	2. Evaluation of Second Test Series	100

VIII. RECOMMENDED MODIFICATIONS OF THE VALVE	
1. Reflected Backpressure	105
2. Impact Grid	108
3. Double Diaphragm Arrangement and Triple Diaphragm	109
4. Backup Grid	111
5. Elastic Impact Layer	111
IX. CONCLUSIONS AND RECOMMENDATIONS	113
REFERENCES	115

FIGURES 1 through 20

## I. INTRODUCTION

### 1. Discussion

This is the final report on the development and shock tube test analysis of the piston plate airblast valve by The Clark Valve Company, under a contract to The Naval Civil Engineering Laboratory.

Work on this project began on March 26, 1970, and has required slightly over two years to complete. The work was divided into two phases in which the second phase was contingent upon the successful completion of the first. A draft report was written on each phase and was approved by the government. Both reports, with some additions and changes, are included in this report.

Phase I consisted of designing the prototype valve and the sectional-test-valve with stress analyses and consistent with specifications and service parameters.

Phase II consisted of the construction of the sectional-test-valve and an analysis of the test results, with recommendations for modifying the original prototype design.

For the most part, the order of contents of this report is consistent with the time sequence of the work.

The stress analysis and design drawings were done by Mechanics Research, Incorporated.

The sectional-test-valve was constructed by Gaddis Machine Service of Albuquerque, New Mexico.

The shock tube tests were done through the Air Force Weapons Laboratory at the Civil Engineering Research Laboratory, Albuquerque,

New Mexico.

Results of the planned tests showed that problems encountered would require additional tests to prove corrective measures. This resulted in a second test series and test report from the testing agency.

## 2. Background

The principle of this piston plate valve is based on an invention by R. O. Clark called, "Shock Closure Valve," Patent Number 3,115,155, in which a thin spring material is used as a closure mechanism against high pressure. The adaptation of this principle in a blast valve is pending patent under serial number 191979. This blast valve was a technological development that has evolved to the present design, the performance of which is the objective of this project.

The prototype design shown in Figure 1 has many features that are superior to any other known shock actuated valve intended for the same service and hardness. The heart of this superior performance lies with its very fast acting closure mechanism and the resulting short delay path contained within the valve housing. Other advantages resulting from the fast closure are described in the following.

1) Reduction of vulnerable target size by the elimination of the large area needed by the extensive delay path.

2) Minimum vulnerability to ground shock by the absence of movable parts that are possible to a. Even if the outer housing were permanently distorted by ground shock, the closure mechanism would show little or no effects.

3) The auxiliary power required by most valves to aid the low pressure closing cycle is not used in this valve.

These and other advantages of the fast closure system will become more apparent as the construction is understood.

### 3. Purpose

The purpose of this investigation was to prove that the proposed valve could perform properly under high pressure airblast loading. The prototype valve was designed as a unit that would be expected to have a normal ventilation capacity of 3,330 cfm, so that three units would be used in a system requiring 10,000 cfm. This prototype was too large to adapt to a high pressure shock tube for testing and also expensive to construct. Therefore, the smaller valve was designed by reducing one dimension without reducing the others, and without changing the scale that would affect its interaction with the shock. This meant that processes such as the closing time, closing impact velocity, and momentum per unit area of the diaphragm, would be the same in the test valve as in the prototype.

#### 4. Performance

Besides the advantage of this valve over other valves that was discussed previously, its mechanical simplicity provides still other advantages. Since there are no sliding parts, lubrication is not needed, and the only maintenance required is removal of dust that would accumulate in a ventilating system, especially in the grid of the valve. Maintenance is facilitated by removal of the entire closure mechanism from the valve housing. Also, there should be a sink at a low point in the valve to remove cleaning fluid. The absence of sliding parts in the valve allow paint to be used as corrosion protection. Stainless materials can also be used to prevent corrosion in the valve.

The valve is to have an overpressure protection from 5 psi to 1,000 psi reflected shock pressure. The criterion of protection is that no more than 5 psi of shock with a positive duration of 3 milliseconds may be exceeded in the protected side of the valve. The valve should be designed to contain a static pressure of 1,500 psi.

Other elements included in the prototype valve, but not in the sectional-test-valve, are a manual or sensory actuated method of closure and a negative phase closure. These elements were not included in the test valve because they did not pertain to the objective of the investigation and, therefore, may be changed. Preliminary designs of these other elements are shown in Figure 1 under "positive closure" and "negative closure."

Figure 2 shows a sectional view of the sectional-test-valve.

Figures 3 through 5 show the design drawings of the original prototype valve. Figures 6 through 14 are a complete set of shop drawings of the sectional-test-valve.

The static and dynamic stress analysis of the prototype and sectional-test-valve are given in the following sections.

## II. PLATE DESIGN OF MODEL VALVE

### 1. General Comments

In analyzing the components of the blast valve as shown on the design drawings, a static internal pressure of 1,500 psi is used. Various combinations of boundary conditions are considered so that the governing condition can be determined to ensure that the yield stress is not exceeded.

In the following sections, the components are treated separately. Sketches are presented for convenience, but for detailed dimensions, the design drawings should be used.

The primary reference for the plate analysis is Timoshenko and Woinowsky-Krieger (Reference 1), and notation and resultant maximum moments are taken directly from this source.

Since two of the principal stresses are usually of the same sign and the transverse normal stress is assumed to be zero, the maximum difference between the principal stresses will just be the maximum principal stress. The purpose of the analysis is to show that this stress is less than the yield stress for all cases.

It is assumed that for most cases, the membrane stress can be ignored in comparison with the bending stress.

The pictorial views and design drawings, though not specifically referred to in the analysis, may aid in understanding the areas under consideration. These figures are at the end of the report.

2. Cover Plate

a. Geometry

Length =  $73 \frac{1}{2}$ "

Width = 50"

Thickness =  $1 \frac{1}{2}$ "

b. Material

USS T1 Steel

$\sigma_y = 100,000$  psi

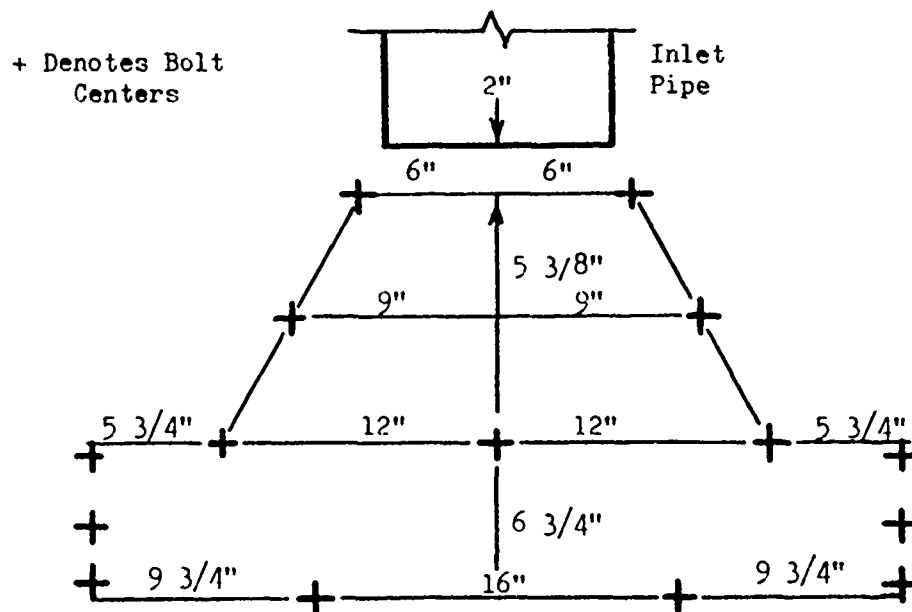
$\sigma_u = 115,000$  psi

c. Design Load

Internal Pressure = 1,500 psi

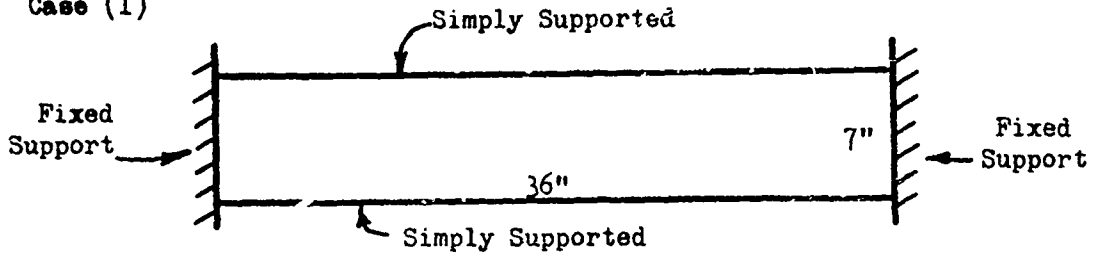
One critical span will be that area next to the piston plate

where we have the following bolt geometry:



Since an exact analysis would not be feasible, consider the following possible approximations for plate segment geometries and boundary conditions:

Case (1)

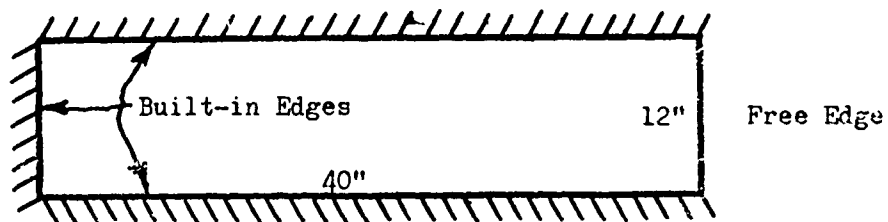


Case (2) Plate segment 24" x 12" considered simply-supported on all 4 sides

Case (3) Plate segment 24" x 12" considered built-in on all 4 sides

The span next to the inlet pipe can be closely approximated by

Case (4)



These loading conditions should yield a conservative approximation for the maximum stress in the plate.

d. Analysis

Case (1) With  $b = 36''$        $a = 7''$

$$\frac{b}{a} = \frac{36}{7} = 5$$

and from page 187, Reference (1), the maximum moment is

$$(M)_{\max} = 0.1250qa^2$$

The maximum stress is

$$(\sigma)_{\max} = \frac{6(M)_{\max}}{h^2}$$

With

$$q = 1,500 \text{ psi}$$

$$h = 1 \frac{1}{2} \text{ inches}$$

we get

$$\begin{aligned} (\sigma)_{\max} &= 0.125 \times 1500 \times 49 \times \frac{(3)^2}{(2)^2} \\ &= 25,000 \text{ psi} \end{aligned}$$

Case (2)

$$\text{Let } b = 24'' \quad a = 12''$$

$$\text{Then } b/a = 2 .$$

From Reference (1), page 119, the maximum moment is

$$(M)_{\max} = .102qa^2$$

Hence,

$$\begin{aligned} (\sigma)_{\max} &= .102qa^2 \times \frac{6}{h^2} \\ &= .102 \times 1500 \times 12 \times 12 \times 6 / (2)^2 \\ &= 59,000 \text{ psi} \end{aligned}$$

Case (3)

$$\text{Let } b = 24'' \quad a = 12''$$

$$\text{Then } b/a = 2$$

From Reference (1), page 202, the maximum moment is

$$(M)_{\max} = 0.0829qa^2$$

Hence,

$$\begin{aligned} (\sigma)_{\max} &= 0.0829qa^2 \times \frac{6}{h^2} \\ &= 48,000 \text{ psi} \end{aligned}$$

Case (4)

Let  $b = 40''$        $a = 12''$

Then  $b/a = 3$  .

From Reference (1), page 215, the maximum moment for  $b/a = 1.5$  is

$$(M)_{\max} = .0842qa^2$$

and

$$(\sigma)_{\max} = 49,000 \text{ psi}$$

For  $b/a = 1.5$ , the maximum stress would probably be less.

e. Remarks

In addition to the bending stress, we should include a membrane stress due to the reaction forces from the edge plates.

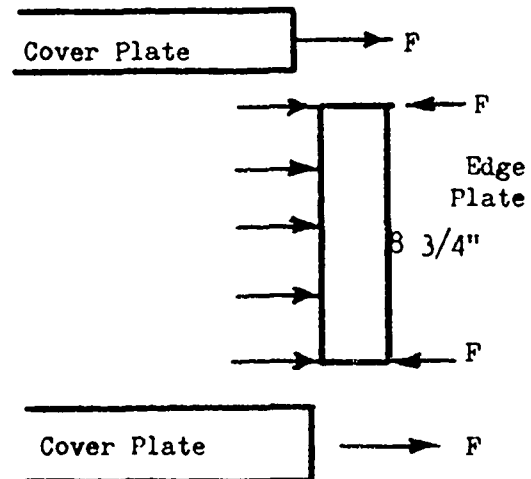
This stress would be approximately given by

$$(\sigma)_{\text{mem}} = F/2''$$

Where  $F$  is the edge force per unit inch.

$$F = 1500 \times \frac{8\frac{3}{4}}{2}$$

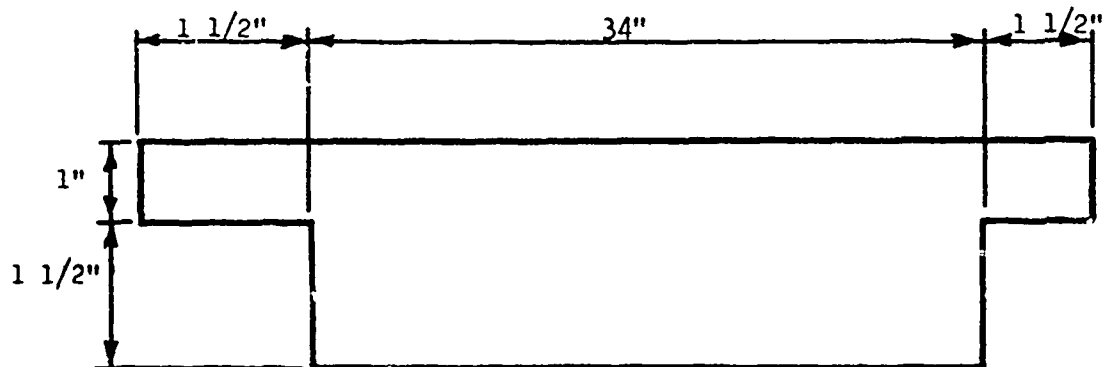
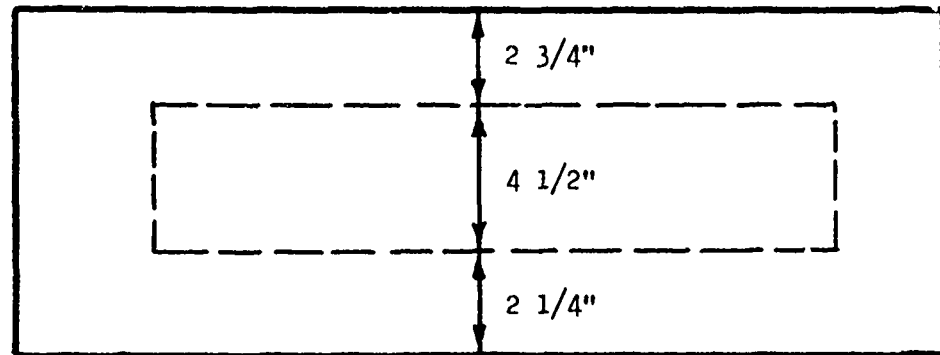
$$(\sigma)_{\text{mem}} = 4,400 \text{ psi}$$



Also, the effect of other stress components should be considered by means of three-dimensional Mohr's circles. However, essentially no additional critical possibilities will arise in this manner. The maximum difference in principal stresses will still be less than 65,000 psi which is well below the yield stress.

3. Access Door

a. Geometry



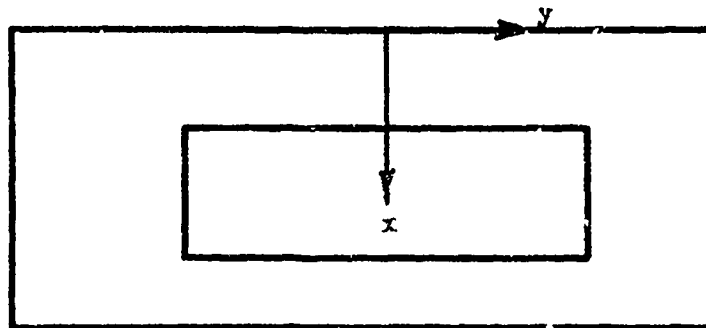
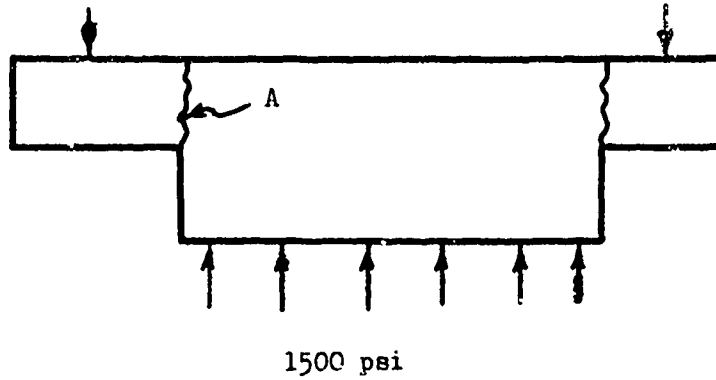
b. Material

USS T1 Steel

$$\sigma_y = 100,000 \text{ psi}$$

$$\sigma_u = 115,000 \text{ psi}$$

c. Design Load



d. Analysis

An important consideration here is that of shear failure along the plane A. The total load is

$$F_T = 1500 \times \left(4\frac{1}{2}\right) \times (34) = 23,000 \text{ lbs.}$$

This force must be transmitted across an area A that is 1 inch wide and whose circumferential length is

$$l = 34 + 34 + 4\frac{1}{2} + 4\frac{1}{2} = 77 \text{ in.}$$

If the resultant force is assumed to be carried uniformly around this area, then the shear force per inch is given by

$$V = \frac{230,000 \text{ lbs.}}{77 \text{ in.}} = 3,000 \text{ lbs./in.}$$

If the shearing stress is distributed parabolically across the plate, then the maximum shearing stress will be

$$\tau_{\max} = \frac{3}{2} V = 4,500 \text{ lbs./in.}$$

Thus the access door will be quite adequate in this regard.

To obtain an approximate expression for the maximum bending stress, assume the door is simply-supported along all four edges. With  $b = 37"$ ,  $a = 9.5"$ , and  $x = 0.3a$ , the maximum moment according to Reference (1), page 118, is

$$(M)_{\max} = .079qa^2$$

Taking  $q = 1500$  psi will be conservative since it may not act over the whole door. With  $h = 1"$ , we get

$$\begin{aligned} (\sigma)_{\max} &= (\sigma)_{\max} \times \frac{6}{h} \\ &= .079 \times 1500 \times (9.5)^2 \times 6 \\ &= 64,000 \text{ psi} \end{aligned}$$

which is less than  $\sigma_y$ .

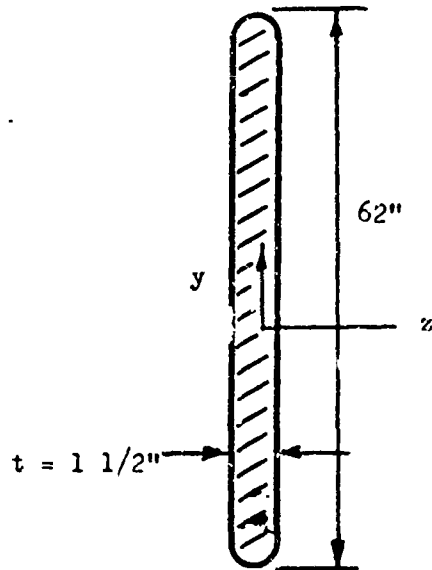
#### 4. Baffle Plate

##### a. Geometry

$$\text{Length} = 62''$$

$$\text{Width} = 8\frac{3}{4}''$$

$$\text{Thickness} = 1\frac{1}{2}''$$

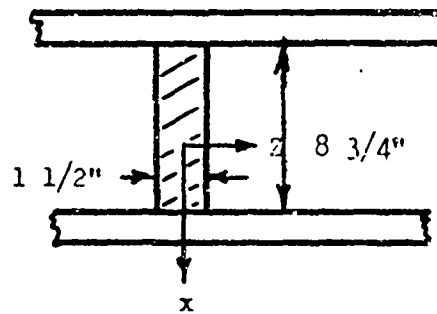


##### b. Material

US Steel T1 Steel

$$\sigma_y = 100,000 \text{ psi}$$

$$\sigma_u = 115,000 \text{ psi}$$



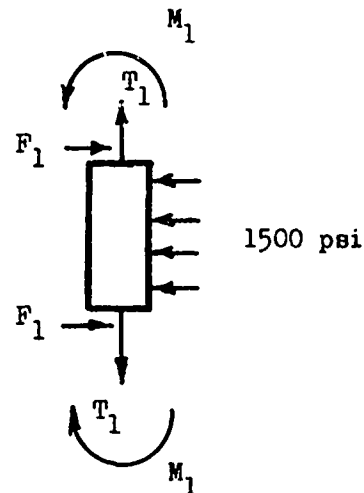
##### c. Design Load

For convenience, assume a single baffle plate on each side.

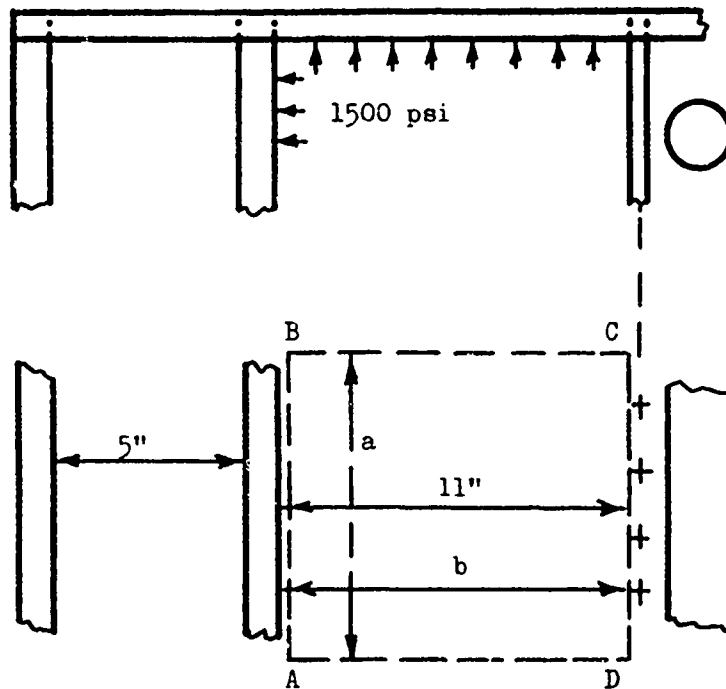
Case (1) No pressure between Baffle Plate and Side Plate

Assume a maximum internal pressure of 1500 psi, plus a force  $T_1$  per inch due to the pressure on the cover plates

on the interior side of the baffle plate and a moment  $M_1$  due to the connection between the baffle plate and the cover plate.



Assume that the force  $T_1$  is the contribution of the pressure acting on the cover plate on an area bounded by the baffle plate and a line halfway between the baffle plate and the line of bolts next to the inlet pipe.



$$\text{Now } T_1 = 1500 \times \frac{11}{2} = 8,250 \text{ lbs./in.}$$

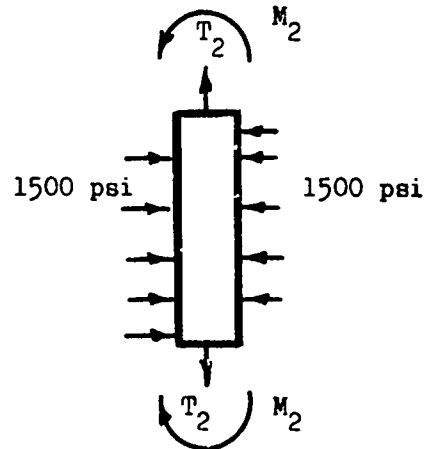
To obtain an upper bound for  $M_1$ , consider a portion ABCD of the cover plate. Assume the edge AB is built in and the other three edges are simply supported for a conservative approach. Take  $a = 42''$  and  $b = 11''$ . Then  $b/a = \frac{1}{3}$  and according to Table 32, page 194 of Reference (1), the maximum moment is

$$\begin{aligned} M_1 &= 0.123qb^2 \\ &= 0.123(1500)(11)^2 \text{ in.lbs./in.} \\ &= 22,300 \text{ in.lbs./in.} \end{aligned}$$

#### Case (2) Pressure between Baffle Plate and Side Plate

Here the force  $T_2$  per inch along the baffle plate will be

$$\begin{aligned} T_2 &= 1500 \left( \frac{11}{2} + \frac{5}{2} \right) \\ &= 12,000 \text{ lbs./in.} \end{aligned}$$



The moment  $M_2$  will be the moment  $M_1$  minus the moment  $M_1$  computed for the edge of a plate fixed on two sides that spans the area between the baffle plate and the side plate. For this case, a reasonable design approximation would be

$$M_1' = \frac{1}{12} q(b')^2$$

where  $b' = 5''$ . Then

$$M_1' = \frac{1}{12} \times 1500 \times 5 \times 5$$

$$= 3,100 \text{ in.lbs./in.}$$

and

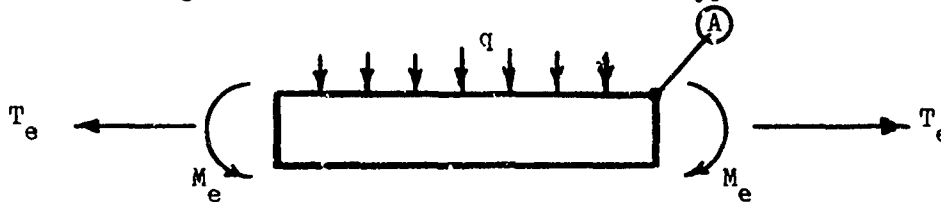
$$M_2 = 22,300 - 3,100$$

$$= 19,200 \text{ in.lbs./in.}$$

d. Analysis

Suppose we consider a segment of the baffle one inch long.

Then the loading on this "beam" would be of the type shown.



The maximum value of the axial stress component is given by

$$(\sigma)_{\max} = \frac{1}{1 - \nu^2} \left\{ \frac{T_e}{A} + \frac{Mc}{I} \right\}$$

where the factor  $\frac{1}{1 - \nu^2} = \frac{9}{8}$  is included to account for the fact that we more closely approximate a case of plane strain rather than plane stress. For this situation

$$A = 3/2 \text{ in.}^2$$

$$c = 3/4 \text{ in.}$$

$$I = (1/12) (3/2)^3 = 27/96 \text{ in.}^3$$

The critical stress will occur on the edge at the end of the beam (point A). Stresses at interior points will be smaller in absolute value.

Case (1)  $T_e = T_1$

$$M_e = M_1$$

$$(\sigma)_{\max} = \frac{9(8,250}{8(\frac{3}{2} + \frac{22,300}{27/96} \times 3/4)}$$

$$= 73,000 \text{ psi}$$

Case (2)  $T_e = T_2$

$$M_e = M_2$$

$$(\sigma)_{\max} = \frac{9(12,000}{8(\frac{3}{2} + \frac{19,200}{27/96} \times 3/4)}$$

$$= 67,000 \text{ psi}$$

e. Remarks

The above analysis is applicable to the portion of the baffle plate that roughly parallels the inlet tube. Since the loading on the baffle plate will be less severe towards the end where the piston plate is located, and there are two baffle plates in the region that parallels the inlet tube, the design is quite adequate.

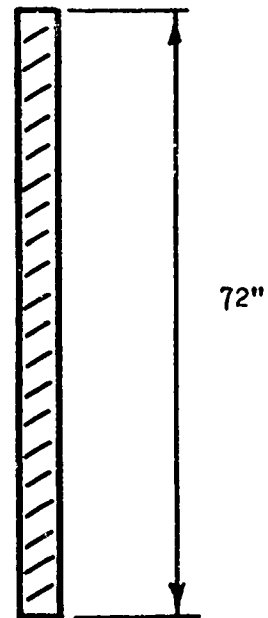
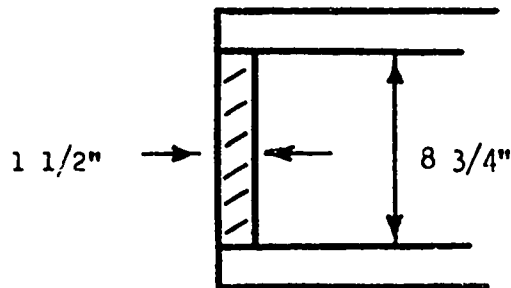
5. Side Plates

a. Geometry

Length = 72"

Width =  $8\frac{3}{4}$ "

Thickness =  $1\frac{1}{2}$ "



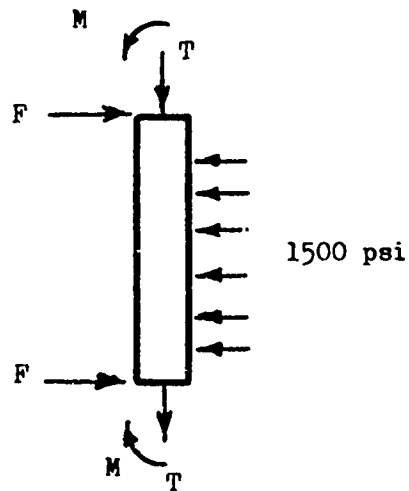
b. Material

USS T1 Steel

$\sigma_y = 100,000$  psi

$\sigma_u = 115,000$  psi

c. Design Load



In a procedure completely analogous to that used for the baffle plate

$$T = 1500 \times \frac{5}{2} = 3750 \text{ lbs./in.}$$

$$M = \frac{1}{12} qb^2 = \frac{1}{12} \times (5)^2 = 3,100 \text{ in.lbs./in.}$$

d. Remarks

This load is not as severe as that considered for the baffle plate. Thus, the design is adequate.

6. Bottom Plate

a. Geometry

Length = 18"

Width =  $8\frac{3}{4}$ "

Thickness =  $1\frac{1}{2}$ "

b. Material

USS T1 Steel

c. Design

See analysis for baffle plate.

7. Test Door

a. Geometry

Length = 18"

Width =  $11\frac{3}{4}$ "

Thickness =  $\frac{1}{2}$ "

b. Material

Mild Steel

c. No Design Load

Plate will hold pressure gages only.

8. Top Plate

a. Geometry

Length = 50"

Width =  $11\frac{3}{4}$ "

Thickness =  $1\frac{1}{2}$ "

b. Material

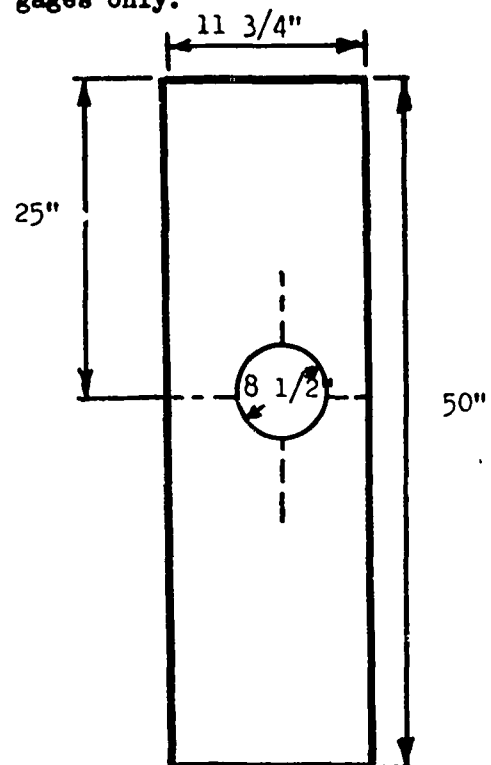
USS T1 Steel

$\sigma_y = 100,000$  psi

$\sigma_u = 115,000$  psi

c. Design Load

The design load is very similar to that of the baffle plate and, hence, the previous computation for maximum stress will be the same. The weld that holds the inlet pipe should adequately compensate for any stress concentrations that might arise because of the presence of the circular hole.



## 9. Inlet Tube

### a. Geometry

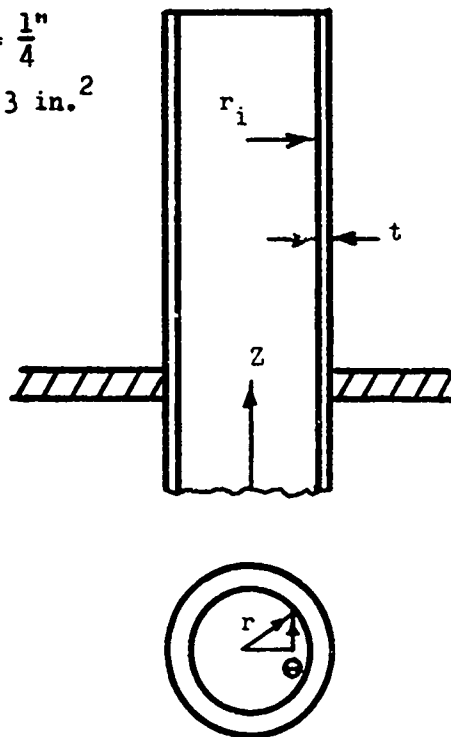
Length = 54"

Inner radius  $r_i = 4"$

Outer radius  $r_o = 4\frac{1}{4}"$

Thickness  $t = r_o - r_i = \frac{1}{4}"$

Inlet area  $A_o = \pi r_i^2 = 50.3 \text{ in.}^2$



### b. Material

1015 CR Steel

$E = 30 \times 10^6 \text{ psi}$

$\sigma_y = 65 \times 10^3 \text{ psi}$  (yield stress)

$\sigma_u = 80 \times 10^3 \text{ psi}$  (ultimate stress)

### c. Design Load

Internal pressure of 1500 psi

\*Values obtained by telephone from Tubesales, Los Angeles, California.

d. Analysis

Thin shell theory is applicable.

Membrane Theory: (Portion of pipe away from entrance)

$$\begin{aligned}\sigma_{\theta} &= \frac{Pr}{t} \\ &= (1500) \frac{(4.125)}{(0.25)} \\ &= 24,750 \text{ psi}\end{aligned}$$

The other maximum principal stresses are

$$\begin{aligned}\sigma_z &= 0 \\ \sigma_r &= -1500 \text{ psi}\end{aligned}$$

From the maximum shear-stress criterion

$$\frac{1}{2} (\sigma_{\max} - \sigma_{\min}) < \frac{\sigma_y}{2}$$

$$\frac{1}{2} (\sigma_{\max} - \sigma_{\min}) = \frac{1}{2} (24,750 + 1500) = 13,200$$

$$< 32,500 \text{ psi}$$

Bending Theory:

$$\sigma_z = \frac{N_z}{t} + \frac{6M_z}{t^2}$$

$N_z, N_{\theta}$  - membrane force resultants

$$\sigma_{\theta} = \frac{N_{\theta}}{t} + \frac{6M_{\theta}}{t^2}$$

$M_z, M_{\theta}$  - bending moment resultants

At the point where the pipe is fastened to the plate, the shell can be considered built in. Here we have [Reference (2), page 139]

$$N_x = 0$$

$$N_\theta = 0$$

$$(M_z)_{\max} = - \frac{2\kappa^2 D}{Et} Pr^2$$

$$(M_\theta)_{\max} = \nu (M_z)_{\max}$$

where

$$\kappa^2 = \left[ \frac{3(1-\nu^2)}{r^2 t^2} \right]^{1/2}$$

$$D = \frac{Et^3}{12(1-\nu^2)}$$

$$(M_z)_{\max} = \frac{-2 \{3(1-\nu^2)\}^{1/2}}{rt} \cdot \frac{Et^3}{12(1-\nu^2)} \cdot \frac{Pr^2}{Et}$$

$$(\sigma_z)_{\max} = \frac{-\sqrt{3}}{(1-\nu^2)^{1/2}} \cdot \frac{Pr}{t}$$

$$= -1.77 \frac{Pr}{t} \quad \text{with } \nu = \frac{1}{3}$$

Maximum shear stress

$$= \frac{1}{2} \left( 1.77 \frac{Pr}{t} \right) = 21,800 \quad 32,500 \text{ psi}$$

This indicates the given design is adequate.

10. Typical Grid Plate

a. Geometry

Assume for the purpose of analysis that each grid plate can be approximated by a beam that is

34" long

4" deep, and

$\frac{1}{4}$ " thick

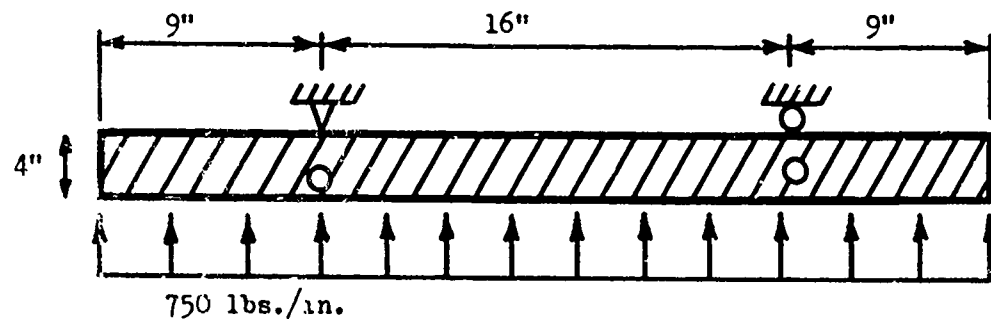
b. Material

USS T1 Steel

$\sigma_y = 100,000$  psi

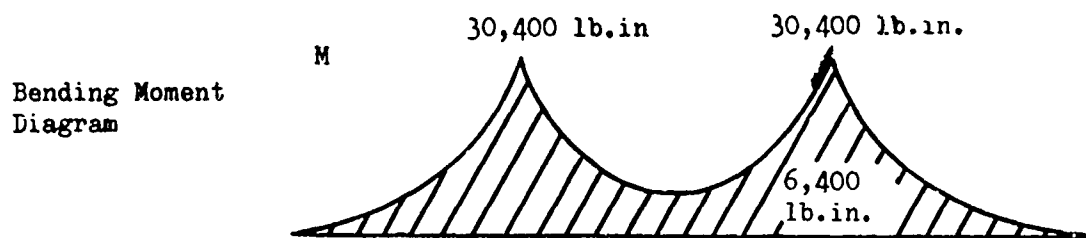
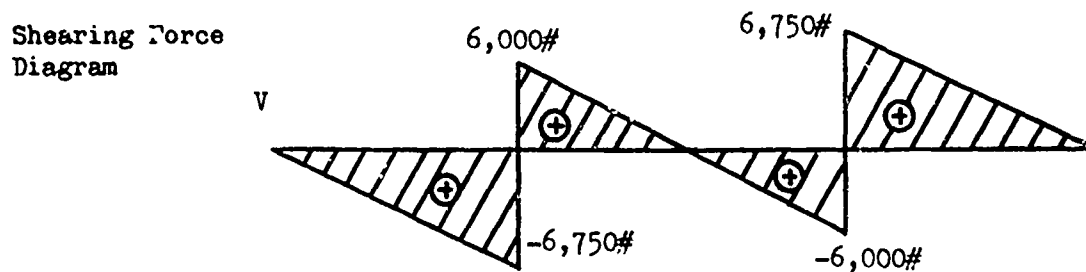
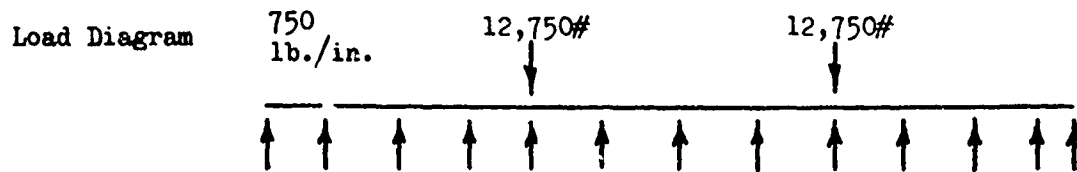
$\sigma_u = 115,000$  psi

c. Design Load



Assume the supports are simply supported which will yield a more conservative estimate of the bending stress than if the supports are taken to be fixed which more closely approximates the actual situation.

d. Analysis



$$(M)_{\max} = 30,400 \text{ lbs./in.}$$

$$(\sigma)_{\max} = (M)_{\max} \frac{c}{I}$$

where

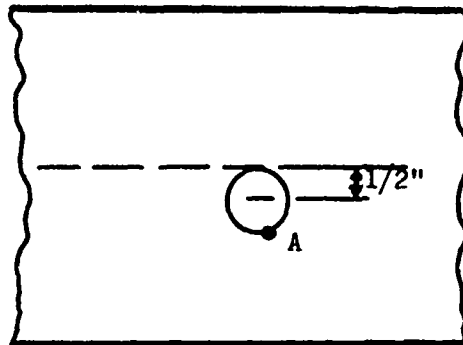
$$c = 2''$$

$$I = \frac{1}{12} \left(\frac{1}{4}\right)(4)^3 = \frac{4}{3} \text{ in.}^4$$

$$\begin{aligned}(\sigma)_{\max} &= (30,400) (2) \left(\frac{3}{4}\right) \text{ psi} \\ &= 45,600 \text{ psi}\end{aligned}$$

which is less than  $\sigma_y$ .

The effect of the bolt hole directly below the support should be analyzed for stress concentrations.



If the hole were not present, the stress at point A would be

$$\begin{aligned}\sigma &= \frac{My}{I} \\ &= (30,400) \left(\frac{1}{3}\right) \\ &= 22,800 \text{ psi}\end{aligned}$$

A stress concentration factor of 3 yields a maximum stress at the edge of the hole of

$$\sigma = 67,400 \text{ psi}$$

$$< \sigma_y$$

e. Remarks

Additional rigidity is provided by the  $\frac{1}{4}$ " plates at the ends of the grid assembly, as well as by the weld to the spacers and the plates that support the grids.

11. Grid Support Plate

a. Geometry

Length = 10"

Width = 8.75"

Thickness = 2"

b. Material

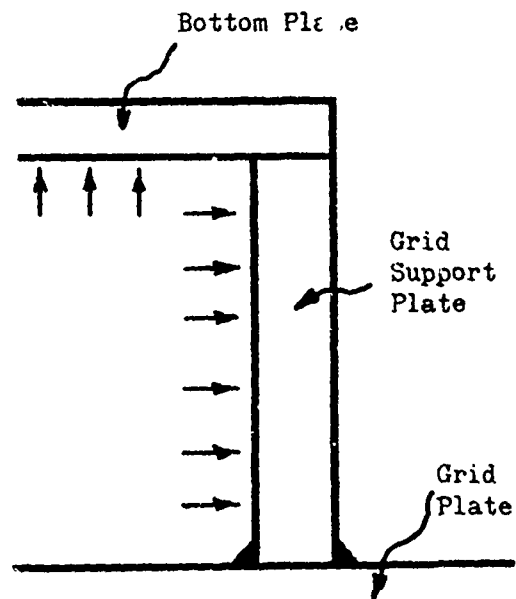
USS T1 Steel

$\sigma_y = 100,000$  psi

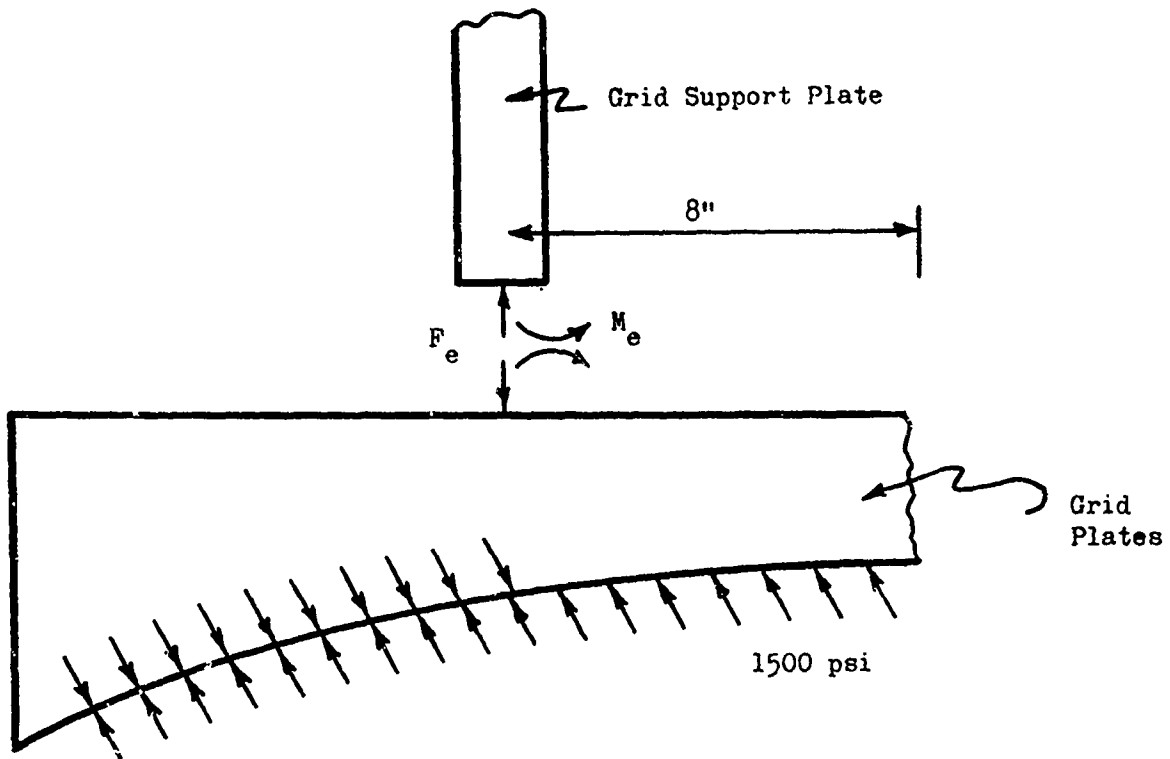
$\sigma_u = 115,000$  psi

c. Design Load

Assume that three edges are built-in and that the edge along the grid is free (Grids will have a slight amount of rotational and lateral freedom).



In addition to the internal pressure, the edge loading transmitted by the grid plate must be taken into account.



The edge force  $F_e$  per inch is equal to

$$F_e = 1500 \times 8$$

$$= 12,000 \text{ l.b./in.}$$

and the maximum possible edge moment  $M_e$  (obtained by assuming the grid plates are rigidly attached) is

$$M_e = \frac{ga^2}{12}$$

With  $a = 16''$ , we get

$$M_e = 32,000 \text{ in.lbs./in.}$$

d. Analysis

With  $b = 10"$ ,  $a = 8.75"$ ,  $h = 2"$ , Reference (1), page 215,  
yields a maximum moment of

$$(M)_{\max} = .086qa^2$$

The maximum bending stress is

$$\begin{aligned}(\sigma)_{\text{bend}} &= \frac{6(M)_{\max}}{h^2} \\ &= \frac{6}{4} (.086) \times 1500 \times (8.75)^2 \\ &= 14,800 \text{ psi}\end{aligned}$$

The uniform compressive stress due to the force  $F_e$  is

$$|(\sigma)_c| = 12,000 \text{ lbs./in.} \times \frac{1}{h} = 6,000 \text{ psi}$$

and the bending stress due to the applied edge moment is

$$\begin{aligned}\sigma_e &= \frac{6M_e}{h^2} \\ &= 48,000 \text{ psi}\end{aligned}$$

Since the full value of these stresses will not occur at the same point in the plate, the maximum stress will be less than the sum

$$(\sigma)_{\max} < 14,800 + 6,000 + 48,000 = 69,000 \text{ psi} < \sigma_y$$

e. Remarks

In addition, a buckling analysis should perhaps be considered. However, because of the small length to thickness ratio and the fact that the plate is well supported on three sides, it is highly likely that buckling will not be a problem.



From geometrical considerations

$$R \sin \beta = 16.25''$$

$$R - R \cos \beta = 2''$$

Solve for R and  $\beta$

$$R^2 \sin^2 \beta = (16.25)^2$$

$$R^2 \cos^2 \beta = (R - 2)^2$$

Add

$$R^2 = R^2 - 4R + 4 + (16.25)^2$$

$$4R = 268$$

$$R = 67''$$

Since  $\beta$  is small, approximate  $\cos \beta$  by a series expansion of order 2 in  $\beta$ .

$$1 - \cos \beta = 2/R$$

$$1 - (1 - \beta^2/2) = 2/R$$

$$\beta^2 = 4/R$$

$$\beta = 0.244 \text{ rad.}$$

To compute the cross-sectional area for the air flow, the magnitude  $2\delta$  is necessary. Again, by inspection

$$R \sin \alpha = 9''$$

$$\delta = R \cos \alpha - R \cos \beta$$

$$\sin \alpha = 9/67$$

$$\cos \alpha = (1 - \sin^2 \alpha)^{1/2} = \frac{1}{67} (67^2 - 9^2)^{1/2} = \frac{66.4}{67}$$

$$R \cos \alpha = 66.4''$$

$$R \cos \alpha = 65''$$

$$\delta = 1.4''$$

## 2. Required Closure Time

As a reference point, choose the end of the inlet pipe.

The minimum distance from the pipe to the horizontal plane containing the edges of the piston plate is

$$L_1 = 16''$$

The minimum path length by which the blast wave could reach the exit portion of the valve is

$$L_2 = l_1 + l_2 + l_3$$

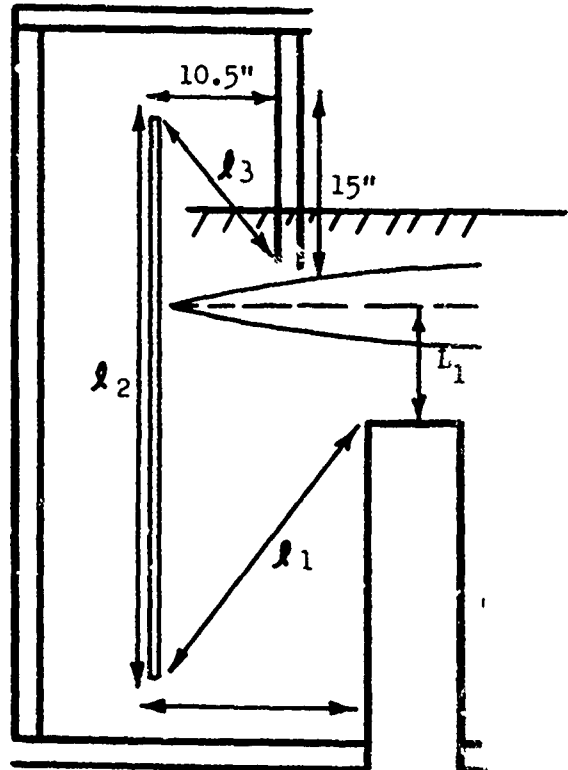
From the given dimensions of the valve,

$$l_1 = (35^2 + 18.5^2)^{1/2} = 40''$$

$$l_2 = 62''$$

$$l_3 = (10.5^2 + 9.5^2)^{1/2} = 14.2''$$

$$L_2 = 116.2''$$



Difference in path lengths  $\Delta L = L_2 - L_1 = 100 \text{ in.} = 8\frac{1}{3} \text{ ft.}$  Assume (conservatively) a shock wave velocity of 2,000 ft./sec. Hence, if no portion of the shock wave is to pass through the valve, the piston plate should close in a time less than the transit time

$$\Delta t = \frac{8\frac{1}{3} \text{ ft.}}{2000 \text{ ft./sec.}}$$

or

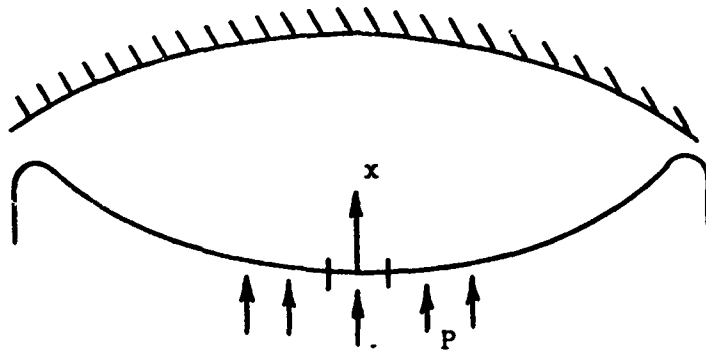
$$\Delta t = 4.16 \text{ ms} \qquad \text{ms} = \text{milliseconds.}$$

### 3. Approximate Closure Time

To compute the closure time of the valve, we make the following assumptions:

- (1) The bending stiffness of the plate can be ignored in comparison to the inertia effect.
- (2) The valve is closed when the center of the piston plate reaches the grid.
- (3) Transverse shear forces can be ignored and, hence, any arbitrary element can be considered independently of the neighboring portion of the plate.

Consider a segment of the plate at the center. For convenience, let the surface area be one square inch. Denote the displacement from the initial position by  $x$  and the pressure by  $P$ . When the valve closes at time  $t = T$  after the blast wave has reached the plate,  $x = 4 \text{ in.}$



Applying Newton's law,  $F = Ma$ , we have

$$P = m\ddot{x}$$

where  $m$  is the mass of the plate per unit surface area. Assuming  $x(0) = 0$  and  $\dot{x}(0) = 0$ , we have

$$\int_0^t P dt_1 = m\dot{x}$$

$$\int_0^t \int_0^t P dt_1 dt_2 = mx$$

At  $t = T$ , let  $x = X$

$$\int_0^T \int_0^{t_2} P dt_1 dt_2 = mX$$

(4) Assume that over the closure time,  $P$  can be approximated by a constant pressure  $P_0$ . Then

$$P_0 \frac{T^2}{2} = mX$$

Let  $\rho$  be the weight density. Then we have

$$\frac{P_0 T^2}{2} = \frac{\rho h}{g} X$$

or

$$T^2 = \frac{2\rho hX}{P_0 g}$$

Suppose we have the following values:

$$x = 4 \text{ ins.}$$

$$\rho = 0.3 \text{ lbs./in.}^3 \quad (\text{Steel})$$

$$h = 0.04 \text{ in.}$$

$$g = 12 \times 32.2 \text{ ins./sec.}^2$$

$$P_0 = 50 \text{ psi}$$

Then

$$T^2 = 5 \times 10^{-6} \text{ sec.}^2$$

$$T = 2.2 \text{ ms}$$

This is the valve closure time for this particular piston plate. This time is less than the required closure time of 4.16 ms. which suggests that this aspect of the design is satisfactory.

Remarks: If the blast pressure is larger, then both the required and actual closure time are reduced. Since the exact pressure-time distributions throughout the valve are almost impossible to predict, accurate values for closure times cannot be determined. However, the above calculations, which are on the conservative side, do indicate the feasibility of a successful mechanism.

If  $h = .125$ ", with all other parameters the same, then

$$T = 3.9 \text{ ms.}$$

#### 4. Impact Velocity

From the previous section we have the impulse-momentum relation

$$\int_0^t P dt_1 = mx$$

To obtain the velocity of a typical segment of the piston plate just before impact, let  $t = T$ , the closure time. Then, assuming the worst case occurs at the center of the plate,

$$\int_0^t P dt_1 = mv$$

where  $v$  is the impact velocity. If  $P$  is constant ( $P_0$ ) and  $m = \frac{\rho h}{g}$ , then

$$v = P_0 T \frac{g}{\rho h}$$

But

$$T = \left( \frac{2\rho h X}{P_0 g} \right)^{1/2}$$

Thus

$$v = \left( \frac{2P_0 g X}{\rho h} \right)^{1/2}$$

With

$$X = 4 \text{ in.}$$

$$P_0 = 50 \text{ psi}$$

$$g = 12 \times 32.2 \text{ in./sec.}^2$$

$$\rho = 0.3 \text{ lbs./in.}^3$$

$$h = 0.04 \text{ in.}$$

$$\begin{aligned}
v &= \left[ 2 \times 50 \frac{\text{lb.}}{\text{in.}^2} \times 12 \times 32.2 \frac{\text{in.}}{\text{sec.}^2} \times \frac{4 \text{ in.}}{0.3 \frac{\text{lb.}}{\text{in.}^3} \times 0.04 \text{ in.}} \right]^{1/2} \\
&= (40 \times 32.2)^{1/2} \text{ in./sec. (100)} \\
&= (4 \times 3.22)^{1/2} \times 1000 \text{ in./sec.} \\
&= 3,600 \text{ in./sec.}
\end{aligned}$$

Hence,

$$v = 300 \text{ ft./sec. for } \begin{bmatrix} P_o = 50 \text{ psi} \\ h = 0.04 \text{ in.} \end{bmatrix} \text{ or } \begin{bmatrix} P_o = 100 \text{ psi} \\ h = 0.08 \text{ in.} \end{bmatrix}$$

Other typical values would be

$$v = 210 \text{ ft./sec. for } \begin{matrix} P_o = 50 \text{ psi} \\ h = 0.08 \text{ in.} \end{matrix}$$

$$v = 425 \text{ ft./sec. for } \begin{matrix} P_o = 100 \text{ psi} \\ h = 0.04 \text{ in.} \end{matrix}$$

$$v = 735 \text{ ft./sec. for } \begin{matrix} P_o = 300 \text{ psi} \\ h = 0.04 \text{ in.} \end{matrix}$$

## 5. Static Stability

Under the free-flow or normal ventilation usage condition, the piston plate should not snap-through nor should there even be significant deformations if the cross-sectional area available for air passage is not to be reduced. The primary load acting on the piston plate in the open mode is that due to head loss between the two sides of the plate.

Each inch of water head loss contributes a pressure of

$$\begin{aligned}
\Delta H_1 &= 62.4 \text{ lbs./ft.}^3 \times \frac{1 \text{ in.}}{1728 \text{ in.}^3/\text{ft.}^3} \\
&= .036 \text{ psi}
\end{aligned}$$

The estimated head loss for this valve is two inches of water = .072 psi. It is therefore prudent to design the plate valve to withstand a maximum uniform pressure of 0.15 psi with an allowance for adjustment to about 0.05 psi.

The buckling pressure can be computed based on formulas derived in Reference (3).

For a geometric arch parameter

$$\lambda = \frac{2H}{h} \quad 25$$

where H is the rise, the buckling load of an arch is given by the formula

$$P_B = \left[ \frac{\pi^2 E h^3}{12R(R\beta)^2} \right] \quad (2.04)$$

For the plane strain case that we have here, E should be replaced with  $E/(1 - \nu^2)$  where  $\nu = \frac{1}{3}$  is Poisson's ratio. Using the following geometrical values:

$$R\beta = 16.75 \text{ in.}$$

$$R = 71 \text{ in.}$$

we can simplify the above formula to

$$P_B = \frac{5Eh^2}{(213)(16.75)^2}$$

If

$$E = 30 \times 10^6 \text{ psi} \quad (\text{Steel})$$

$$h = 0.04 \text{ in.}$$

then the static buckling pressure is

$$P_B = 0.16 \text{ psi}$$

which is the minimal acceptable value. If  $h = 0.125$  in., then

$$P_B = 4.9 \text{ psi}$$

Remarks:

It is immediately apparent that increasing the thickness will significantly increase the buckling load. However, one of the positive attributes of this valve is that it will close for shock waves with a relatively low peak overpressure. Thus, the maximum value of  $h$  would be limited by this requirement.

Relaxing the boundary conditions for the fixed-end conditions that were used in deriving the above formula will significantly reduce the buckling load. The optimal relationship between boundary conditions, plate thickness, and positive closure is extremely difficult to ascertain theoretically. For this reason, a considerable amount of flexibility in adjusting these conditions has been included in the prototype design so that various possibilities can be determined experimentally.

Because of the initial curvature of the plate, the prebuckling displacements of the plate with the ends rigidly fixed will be negligible. However, if the ends are free to move, no membrane force is developed and the piston plate could deform so as to seriously retard the air flow.

Depending upon the orientation of the valve, the weight of the plate itself could contribute to the static loading condition. This additional loading would be

$$P_a = \rho h \text{ psi}$$

For

$t = 0.04$  in. ,  $P_a = .012$  psi and for

$h = .125$  in. ,  $P_a = .048$  psi

Such a contribution is only of some significance (8% of buckling pressure) for the thinnest plate that is being considered. Due to the inability to accurately define the internal pressure distribution, this component of the loading can be ignored.

Following the above analysis, tests of pressure head loss practically eliminated the above considerations as a problem. The pressure head loss was found to be much smaller and this did not even cause a flat plate to buckle. The modified prototype valve is expected to use the flat plate arrangement with no more than 0.8 inches of water for 3300 cfm.

#### IV. BOLT AND STUD DESIGN

##### 1. General Comments

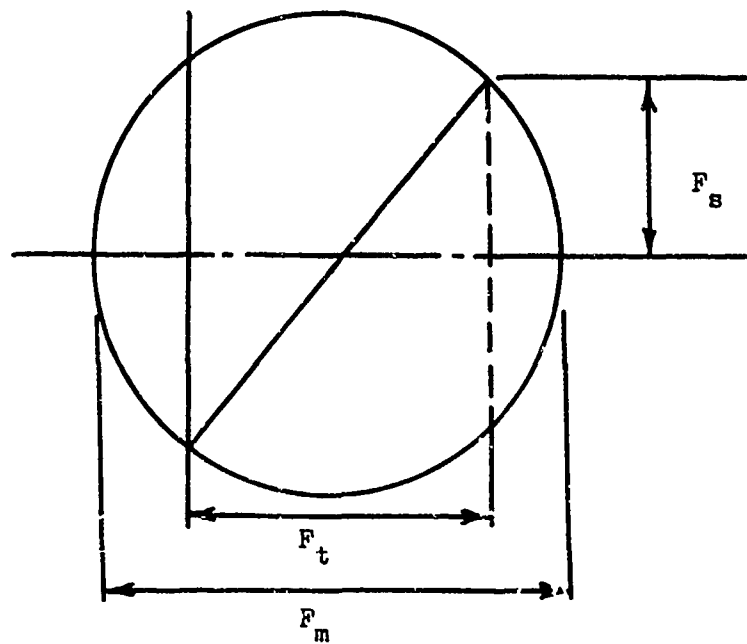
The large internal pressures for which the valve is designed requires the use of high strength bolts and studs. The bolts can be obtained commercially [Reference (4)] whereas the studs will be fabricated from 4340 steel rods which are heat treated to produce a minimum yield stress of 150 kipsi. Yield forces associated with these fasteners are summarized in the following table:

Diameter, Inches	Yield Force, Kips
$\frac{3}{4}$ (bolt)	56
1 (stud)	100
$1\frac{1}{4}$ (stud)	155

In general, a fastener is subjected to both an axial force and a shear force. It is conventional in bolt design [Reference (5)] to assume that the shear stress is uniform across the bolt, as is the tensile stress. For design purposes under combined stresses, a maximum shear stress criterion is used. Since the stresses are considered to be uniform, the Mohr's circle representation of the stress state can be expressed in terms of the resultant shear and axial forces. As the following figures indicates, this failure criterion is equivalent to stating that the diameter

of Mohr's circle must be less than the yield force. If  $F_s$ ,  $F_t$ , and  $F_y$  are the shear force, the tensile force and the yield force respectively, then this criterion can be expressed analytically by

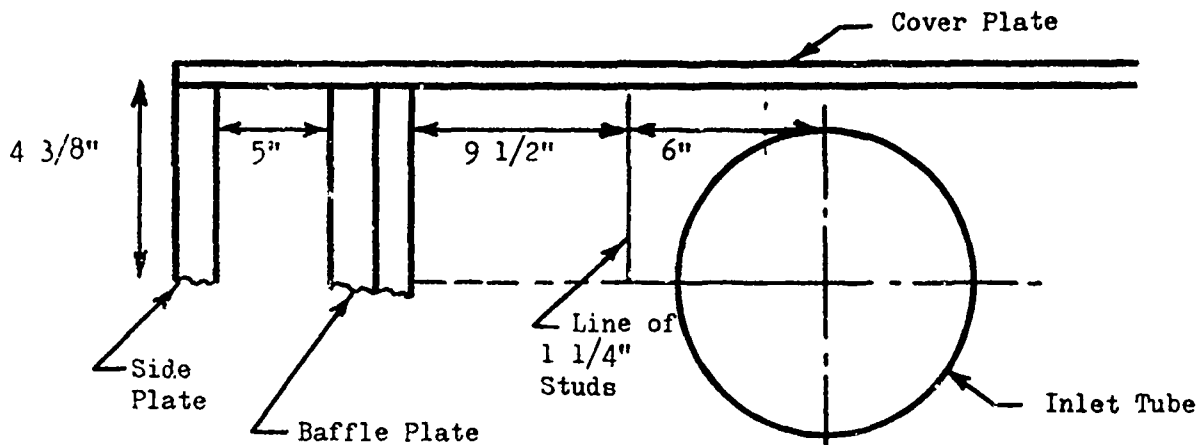
$$F_m = \left[ 4F_s^2 + F_t^2 \right]^{1/2} \leq F_y \quad (1)$$



## 2. General Analysis

Before performing a detailed analysis of the bolts and studs, it is appropriate to study a section of the valve that will yield valuable information concerning the forces on the fasteners.

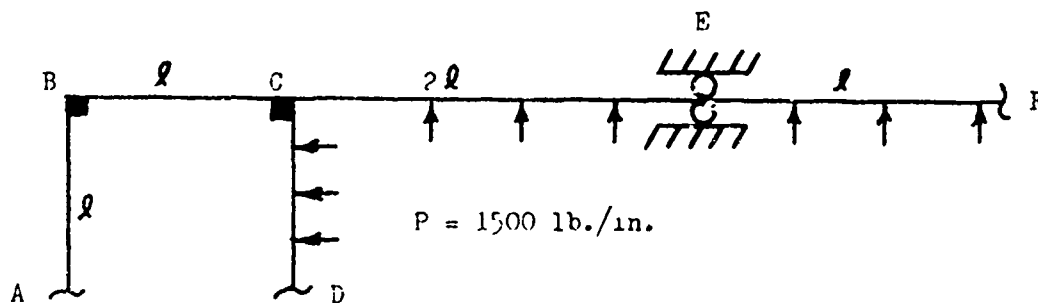
Suppose we cut a strip 1 inch wide through one-quarter of the valve in the vicinity of the inlet pipe. If end effects are ignored, then we have a system that is essentially a framework.



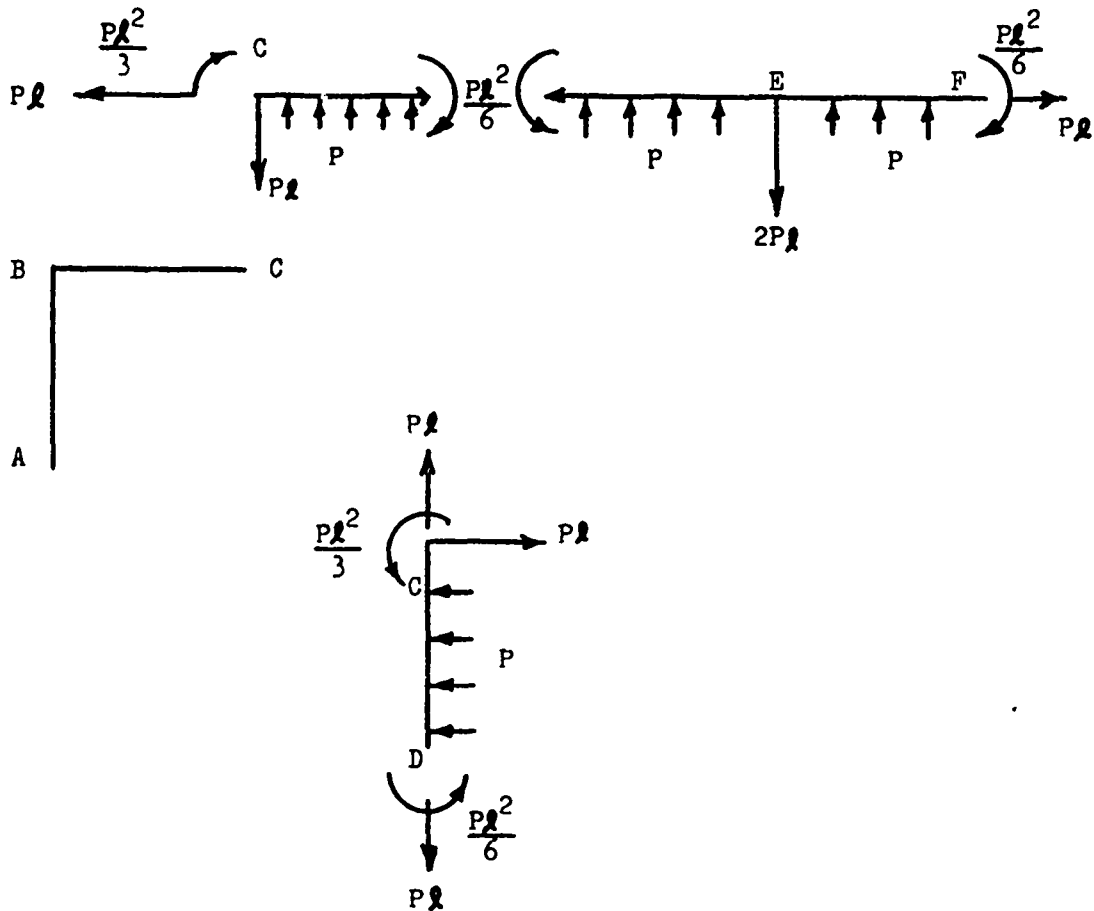
Framework Obtained by Considering a 1" Thick Portion of Valve.

We now consider two extreme loading cases that yield critical values for forces and moments.

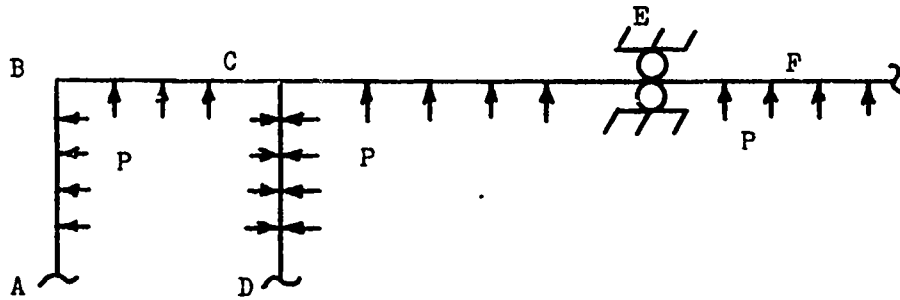
Case (1) Internal Pressure on One Side of Baffle Plate



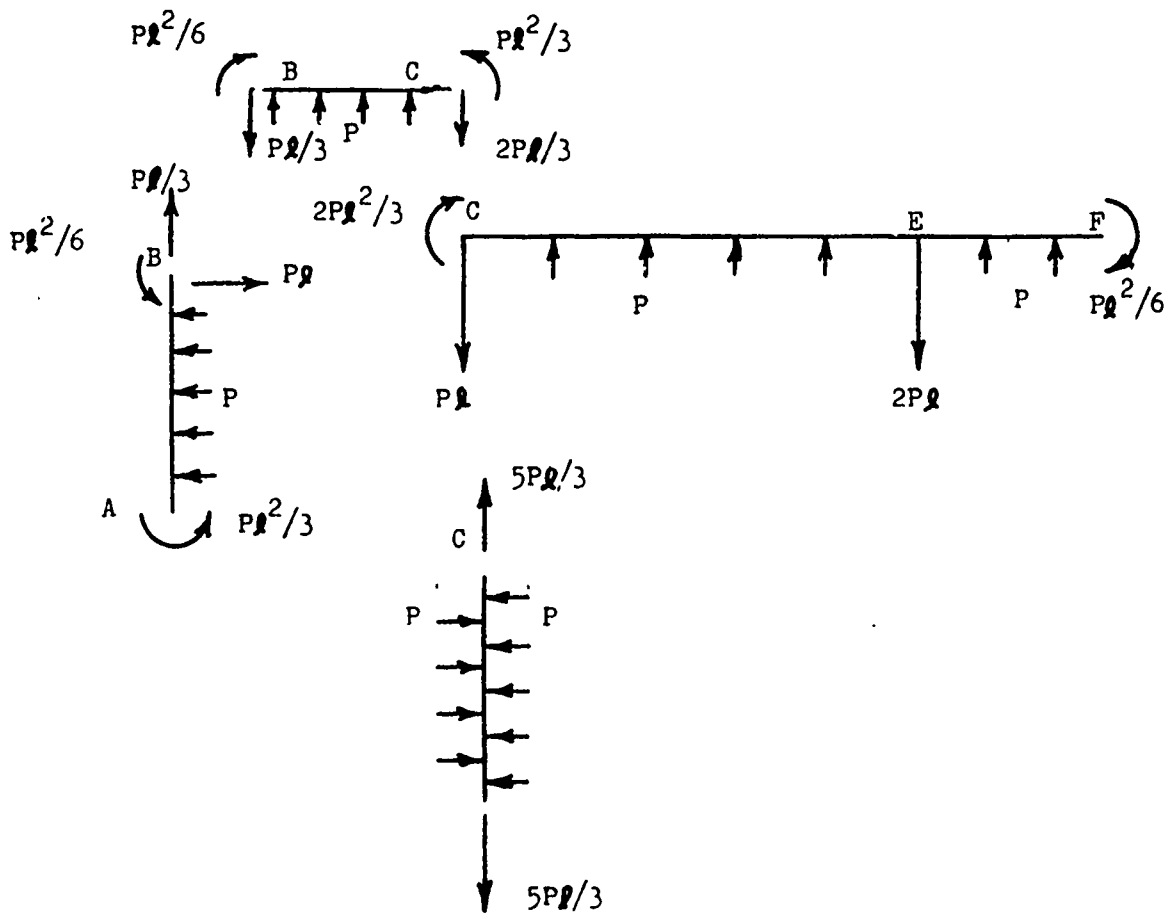
For convenience, replace the actual segment by the structure shown above where  $l$  is 5 inches. The deflections at points B, C, and E will be essentially zero and because of symmetry, the slope and shear force at points A, D, and F will be zero. This structure can be easily analyzed and the critical forces and moments are shown on the following free-body diagrams.



Case (2) Internal Pressure on Both Sides of Baffle Plate

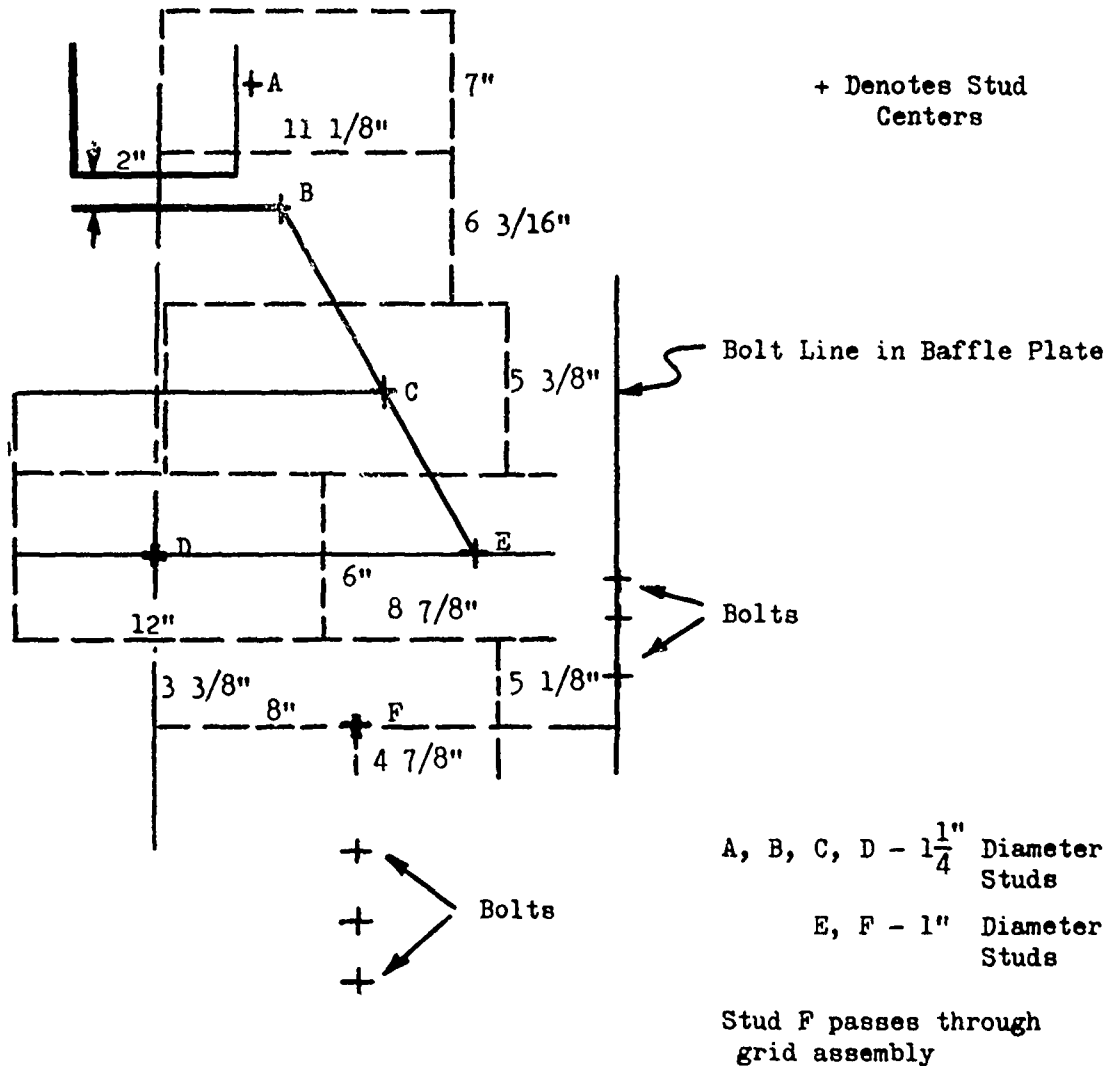


Again, we take the displacements of points B, C, and E to be zero and by symmetry the slope and shear force at points A, D, and F will be zero. An analysis of this structure yields the forces and moments shown on the following free-body diagrams:



### 3. Stud Selection

These studs should withstand a force equivalent to the maximum internal pressure acting on an area delineated by lines that bisect the distances to adjacent studs. For example, if we sketch the region near the end of the inlet tube, the studs should withstand the pressure on the surrounding plate to the extent of the dotted lines (See sketch in the section on the design of the cover plate, as well as the design drawing).



(a) Studs A, B, C, and D

Denote the forces in these studs by  $F_A$ ,  $F_B$ ,  $F_C$ , and  $F_D$ , respectively. Then

$$F_A = 1500 \times 7 \times 11\frac{1}{8} = 117 \text{ kips}$$

Note that this force agrees with that derived in the last section which gave a stud force of

$$F_A = (2P\ell)(7)$$

with approximately equal to 5 in.

Similarly,

$$F_B = 1500 \times 6\frac{3}{16} \times 11\frac{1}{8} = 104 \text{ kips}$$

$$F_C = 1500 \times 5\frac{3}{8} \times 13\frac{3}{8} = 108 \text{ kips}$$

$$F_D = 1500 \times 6 \times 12 = 108 \text{ kips}$$

Additional stresses due to bending and shear will be negligible. All of these stud forces are well under the yield force of 155 kips.

(b) Stud E

The force in stud E is

$$F_D = 1500 \times 6 \times 8\frac{7}{8} = 80 \text{ kips}$$

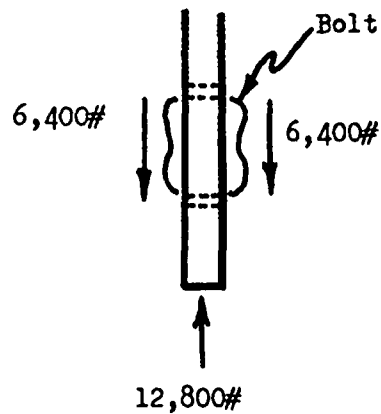
which is less than the yield force of 100 kips for a 1 inch diameter studs.

(c) Stud F

The axial force is

$$F_F = 1500 \times 8 \times 3\frac{3}{8} + 4\frac{7}{8} \times 5\frac{1}{8} = 78 \text{ kips}$$

The effect of the bending moment will be insignificant. However, from the analysis of a typical grid plate, it might be possible to have a shear force of 6,400 lbs. based on the following free-body diagram:



From the yield criterion

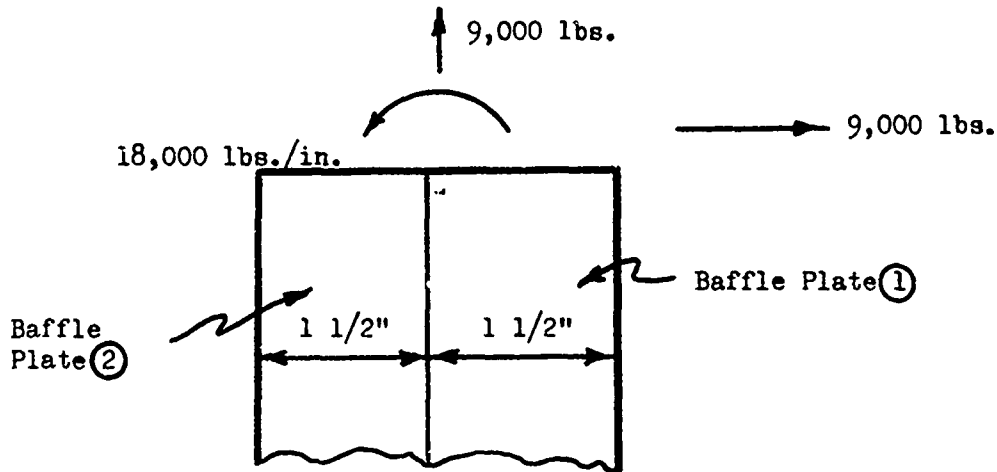
$$\begin{aligned}
 F_m &= \left[ 4F_s^2 + F_t^2 \right]^{1/2} \\
 &= \left[ 4(6.4)^2 + (78)^2 \right]^{1/2} \\
 &= 79 \text{ kips}
 \end{aligned}$$

which is less than  $F_y$  for a 1 inch stud.

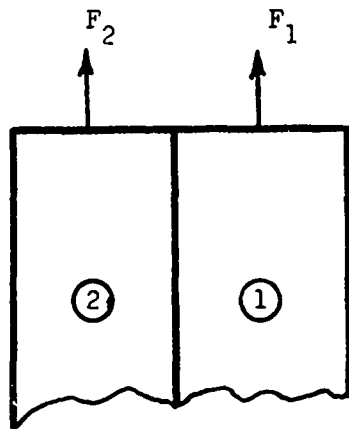
4. Bolt Spacing

(a) Bolts in the Baffle Plates

Consider the forces in the bolts that attach the cover plate to the baffle plate. According to the analysis performed for Case (1) in part 2, this particular connection may have to transmit a shear force  $P\ell$ , an axial force  $P\ell$  and a moment  $\frac{P\ell^2}{3}$ , per inch along the baffle. If we choose  $\ell = 6$  ins. (conservatively), then the free-body diagram of the edge of the baffle plate becomes



Assume these edge loadings are transmitted to the baffle plates by bolt forces  $F_1$  and  $F_2$  per unit length as follows:



Then, to transmit the axial force and moment we must have

$$F_1 + F_2 = 9,000$$

$$(F_1 - F_2) \frac{3}{2} = 18,000$$

Solving for  $F_1$  and  $F_2$ , we get

$$F_1 = 10,500 \text{ lbs.}$$

$$F_2 = -1,500 \text{ lbs.}$$

Actually, the compressive force would be taken up by contact forces between the plates.

The maximum allowable spacing  $\delta$  in baffle (1), based on a yield force of 56,000 lbs. for a  $\frac{3}{4}$  inch bolt, is

$$\delta = \frac{56,000}{10,500} = 5 \text{ in.}$$

The actual spacing of 3 in. leads to a tensile force of

$$F_t = 31,500 \text{ lbs.}$$

in each bolt. If we assume that these bolts take two-thirds of the shear force (since there are twice as many of these bolts as there are bolts in plate (2), then the shear force in each bolt is

$$F_s = \frac{2}{3} \times 3 \times 9000 = 18,000 \text{ lbs.}$$

Thus

$$F_m = \left[ 4F_s^2 + F_t^2 \right]^{1/2}$$
$$= 45 \text{ kips}$$

which is less than  $F_y$ .

For Case (2) in Part 2, these bolts have to withstand an axial force of  $\frac{5}{3} P\ell$  per unit length with no moment. This yields a maximum tensile force of approximately ( $\ell = 5.8''$ )

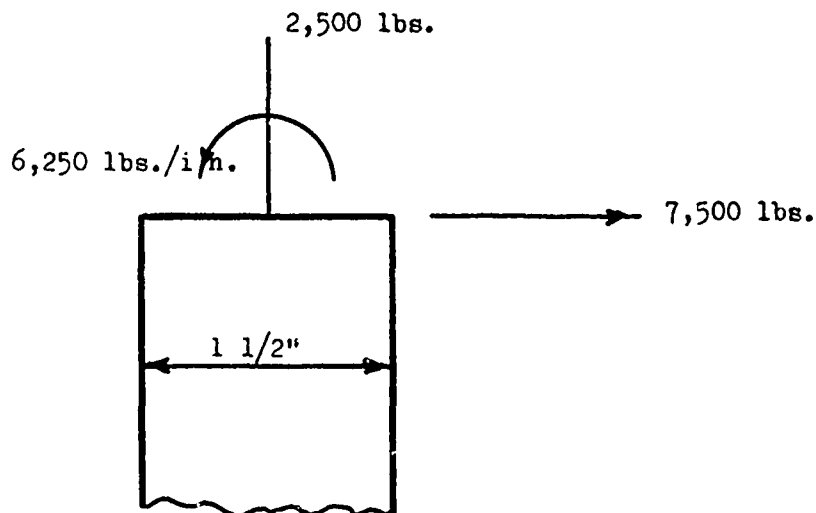
$$F_t = 50 \text{ kips}$$

in each bolt in baffle ② which is below the yield force.

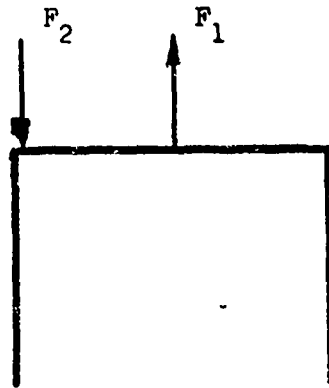
For the length of baffle plate in the general vicinity of the piston plate, the loading situation is very similar to that on the edge plate which is handled next.

(b) Bolts in the Side Plates

According to Case (2) of Part 2, the forces and moments per inch transmitted to the edge of the side plate are those shown on the following free-body diagram (here  $\ell = 5$  in.):



The normal forces per unit inch on the side can be approximated by



where  $F_1$  is the bolt force per unit length and  $F_2$  is a compressive "reaction" force. We have

$$F_1 - F_2 = 2,500$$

$$(F_1 + F_2) \frac{3}{8} = 6,250$$

which yields

$$F_1 = 9,600 \text{ lbs./in.}$$

From the yield criterion, the maximum bolt force per inch is

$$F_m^1 = \left[ 4(7.5)^2 + (9.6)^2 \right]^{1/2}$$

$$= 17.8 \text{ kips/in.}$$

The maximum spacing allowed would be

$$= \frac{55}{17.8} = 3.1 \text{ ins.}$$

Thus the 3 in. spacing given in the design specifications meets this requirement.

(c) Remaining Bolts

The bolts in the end plates and the plates that support the grid assembly must meet a load requirement that is very similar to that for the side plates. Thus, the analysis of this section essentially completes the design analysis of the model blast valve.

## V. DESIGN ANALYSIS OF PROTOTYPE

### 1. Introduction

The format followed for the analysis of prototype components is similar to that used for the model. Critical loading cases are utilized and under these conditions, the analysis shows that each component will remain elastic.

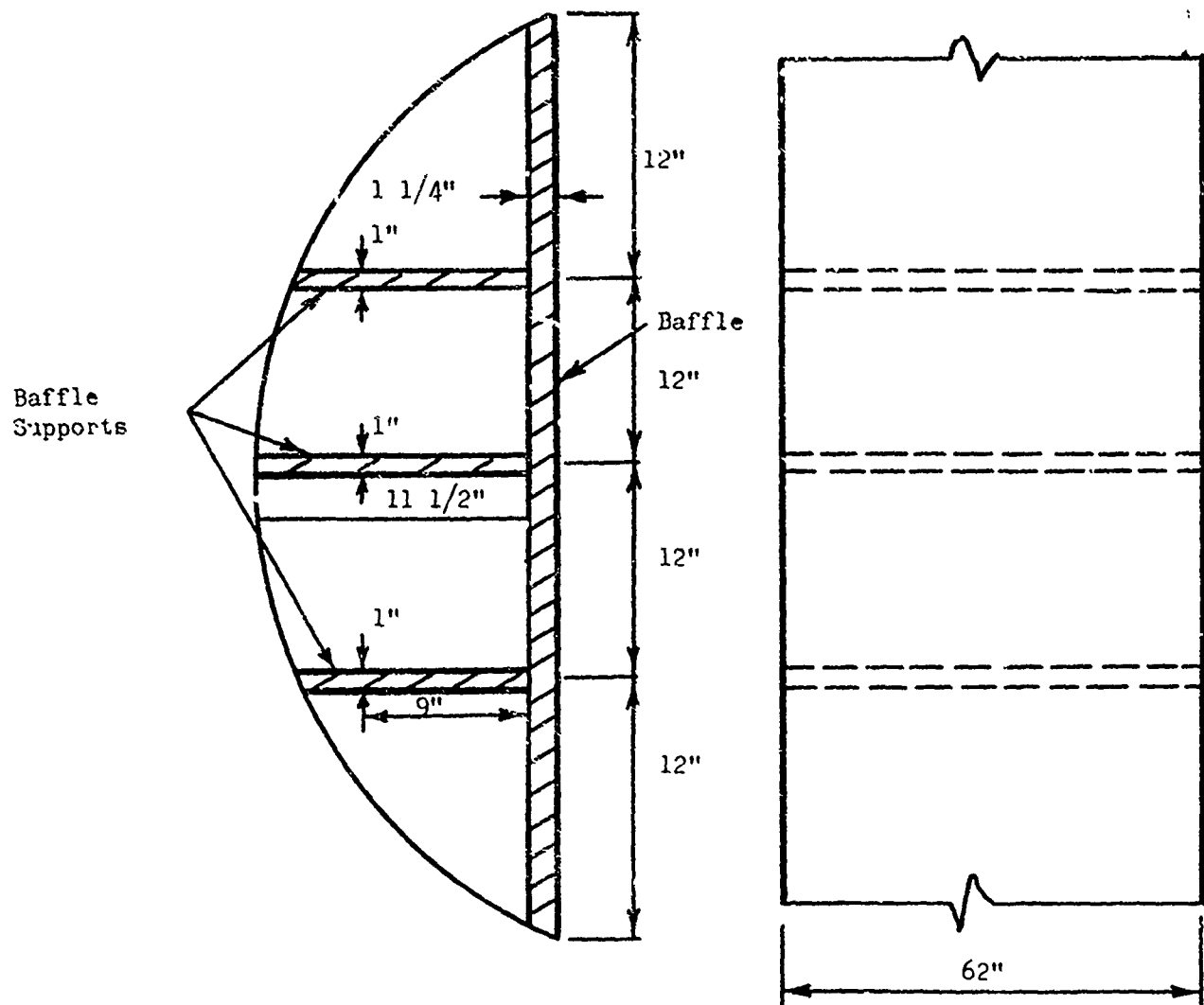
Since experimental tests with the model may indicate that some alterations in the basic design are necessary, neither a detailed analysis nor design drawings are specified for the prototype. Instead, the analysis that is given is intended to show that the basic dimensions are feasible and the resulting valve is illustrated on the conceptual drawings.

Some of the analysis is completely analogous to that given for the model. In particular, the basic dimensions associated with the free flow path length, piston plate, and grid assembly are essentially unchanged so there is no need to repeat the design analysis of these aspects of the prototype.

The following sections consider the major components of the prototype under the design load. Sketches are given, but for an accurate presentation of dimensions and relative positions of components, the conceptual drawings should be used.

## 2. Baffle and Daffle Support Plates

### a. Geometry



### b. Material

USS T1 Steel

$$\sigma_y = 100,000 \text{ psi}$$

$$\sigma_u = 115,000 \text{ psi}$$

c. Design Load

(1) Baffle

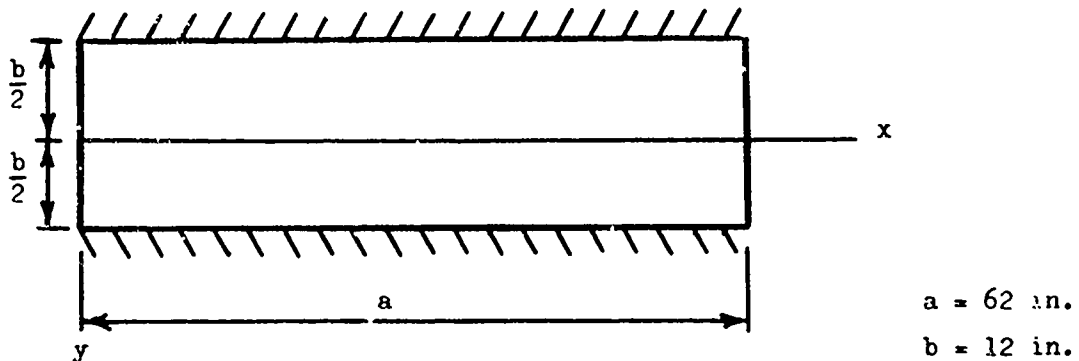
The baffle can be considered as a combination of four plates, each of which are 12 in. by 62 in. and are rigidly supported on the two longest sides and free on the other two sides. The design load is 1500 psi pressure on one side.

(2) Baffle Supports

For all practical purposes, the baffle will not have to withstand a lateral pressure loading since the pressure will be acting on both sides of the plate. Thus, we need consider only an edge loading of  $1500 \times 12 = 18,000$  lbs./in. and investigate the possibility of loss of stability. For this analysis, the critical plate is the one  $11\frac{1}{2}$  in. wide.

d. Analysis

(1) Baffle



The edges  $y = \pm \frac{b}{2}$  are built in. The conditions at  $x = \frac{a}{2}$  will not be affected by the boundary conditions at  $x = 0$  and  $x = a$ , so we can take these edges to be simply supported.

Then, according to Reference (1), page 187, the maximum moment occurs at  $x = \frac{a}{2}$ ,  $y = \frac{b}{2}$ , and is given by

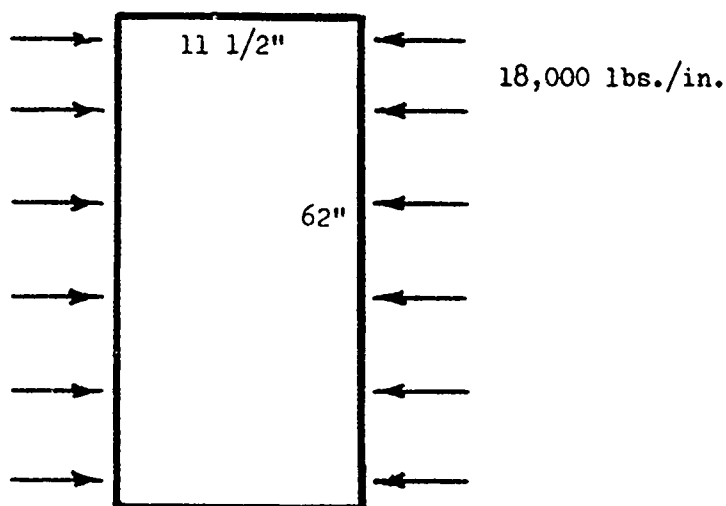
$$M_y = -0.0833qb^2$$

The maximum bending stress is

$$\begin{aligned}(\sigma)_{\max} &= \frac{6(M)_{\max}}{h^2} \\ &= \frac{6}{(5/4)^2} (0.0833) (1500) (12)^2 \\ &= 69,000 \text{ psi}\end{aligned}$$

which is less than the yield stress.

(2) Baffle Support



A lower bound to the buckling load can be obtained by considering a unit strip and by assuming it acts as a simply

supported column. The Euler buckling load for this case is

$$P_B = \frac{\pi^2 EI}{l^2}$$

$$E = 30 \times 10^6 \text{ psi}$$

$$I = \frac{1}{12} bh^3 = \frac{1}{12} \text{ in.}^4$$

$$l = 12 \text{ in.}$$

Thus,  $P_B = 174,000$  lbs. which is more than the yield load.

The 18,000 lbs./in. load that we have is well below the buckling load and yield load of the material.

e. Remarks

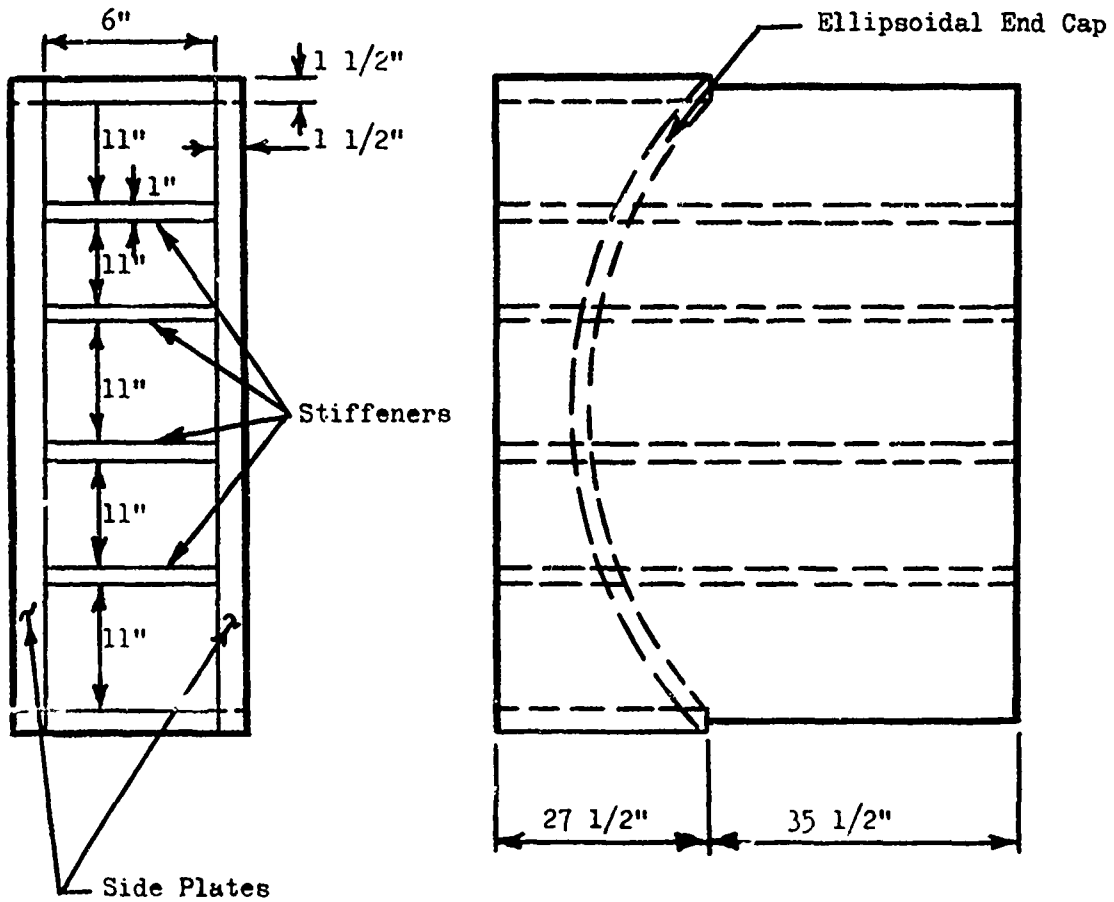
For the case of internal pressure on just one side of the baffle, a considerable edge moment will be transmitted to the cylindrical wall. The maximum value of this moment will be that given in the above analysis, namely (with the minus sign discarded),

$$\begin{aligned} M_y &= 0.0833qb^2 \\ &= (0.0833) (1500) (12)^2 \\ &= 18,000 \text{ lb.ins./in.} \end{aligned}$$

If the flexibility of the cylindrical wall is taken into account, the transmitted moment will be somewhat less than this value (See analysis of cylindrical wall).

### 3. Inlet Side Plates and Stiffeners

#### a. Geometry



#### b. Material

USS T1 Steel

$$\sigma_y = 100,000 \text{ psi}$$

$$\sigma_u = 115,000 \text{ psi}$$

c. Design Load

(1) Side Plate

The side plate should withstand an internal pressure of 1500 psi. The case of pressure on both sides of the side plate will be much less severe.

(2) Stiffener

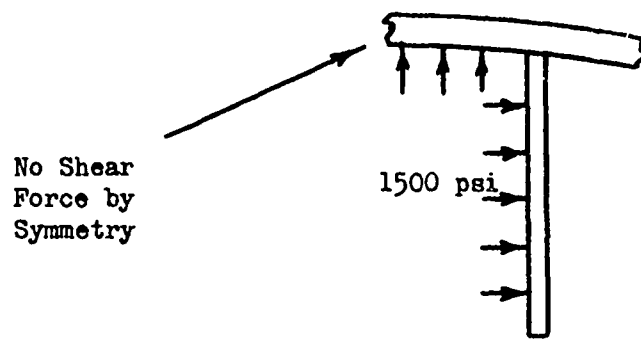
The stiffener will have to withstand a pressure differential that is primarily due to the change in the shock wave as it passes along the inlet. This differential can be ignored. Thus, the only force will be that due to the effects of the side plates. Thus, the stiffener will have to withstand a membrane force of  $1500 \times 11 = 16,500$  lbs./in.

d. Analysis

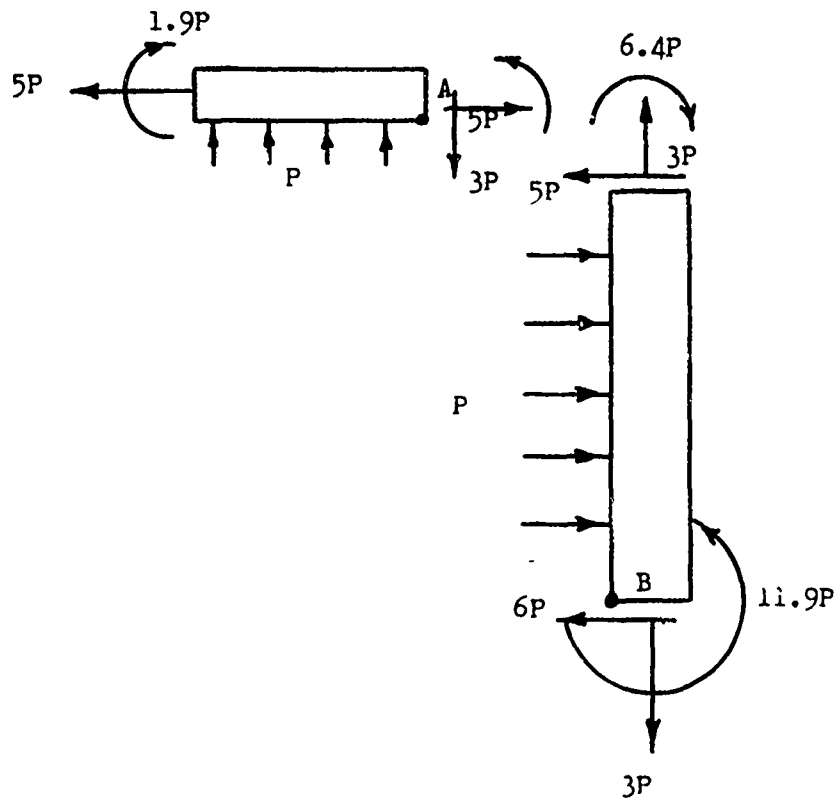
The analysis is very similar to that performed for the baffle and baffle support plates. For an interior section, the side plate can be considered composed of segments that are 63 in. by 11 in. with rigid supports on the two longest sides. From the analysis for the baffle plate, the maximum stress is

$$\begin{aligned}(\sigma)_{\max} &= \frac{6(M)_{\max}}{h^2} \\ &= \frac{6}{(5/4)^2} (0.0833) (1500) (11)^2 \\ &= 58,000 \text{ psi}\end{aligned}$$

For the portion of the inlet that includes the cylindrical wall, the following situation holds:



Consider a segment of unit width. Then from structural analysis, an approximation for the forces and moments acting on this segment would be the following:



$$P = 1500 \text{ lbs./in.}$$

The critical point in the cylindrical panel is Point A

where

$$\begin{aligned}(\sigma)_{\max} &= \frac{N}{A} + \frac{Mc}{I} \\ &= \frac{5 \times 1500}{(3/2)} + \frac{6.4 \times 1500}{\frac{1}{12}(1)(3/2)^3} \times \frac{3}{4} \\ &= 5,100 + 25,600 \\ &= 31,000 \text{ psi}\end{aligned}$$

For the side plate, the stress at point B governs. There we have

$$\begin{aligned}(\sigma)_{\max} &= \frac{N}{A} + \frac{Mc}{I} \\ &= \frac{3 \times 1500}{(3/2)} + \frac{11.9 \times 1500}{\frac{1}{12}(1)(3/2)^3} \times \frac{3}{4} \\ &= 3,000 + 48,000 \\ &= 51,000 \text{ psi}\end{aligned}$$

Both of these stresses are well below the yield stress (See analysis of cylindrical wall).

Because of the uniform loading on the side plate panels, relatively little bending moment will be introduced into the stiffeners which can easily withstand the direct tensile stress of 16,500 psi.

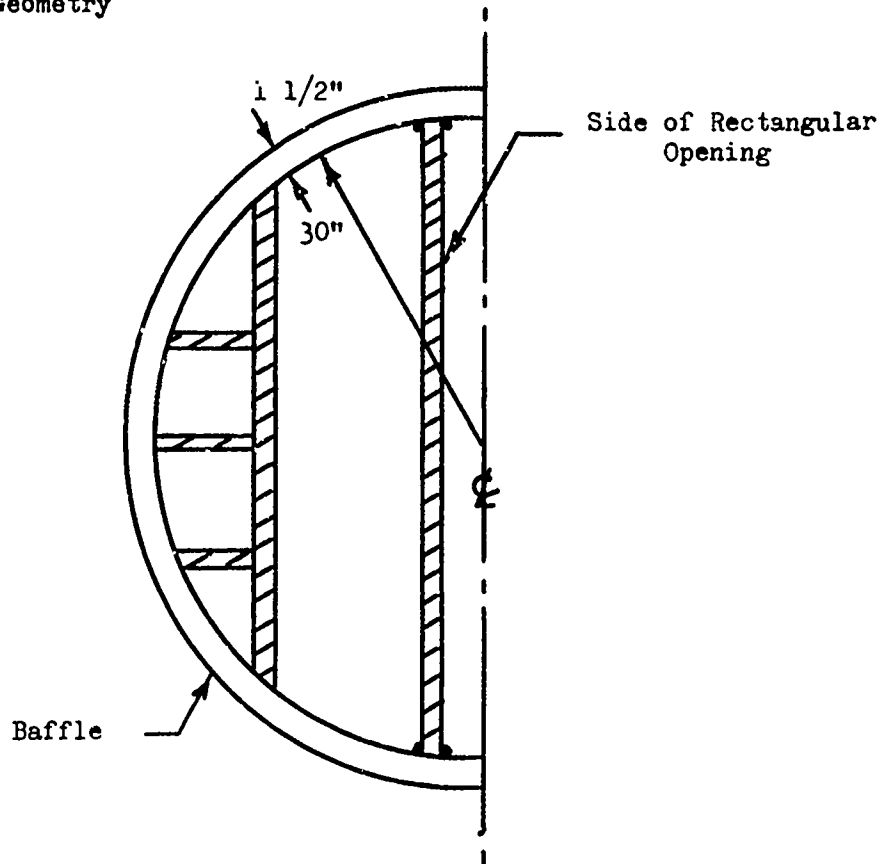
e. Remarks

Two areas of concern involve the positive closure mechanism and the region where the rectangular inlet is welded to the ellipsoidal end. For the material surrounding the positive closure device, an analysis at this time would be premature. It would be preferable to wait until the proposed device be approved before proceeding further with the analysis.

An analysis of the stresses in the neighborhood of the weld line along the ellipsoidal end would require a much more sophisticated approach than is feasible here. However, from the above analysis, it would seem that no major problems should arise for expected increases in maximum stresses.

4. Cylindrical Wall

a. Geometry



Length of Cylindrical Wall = 62 in.

b. Material

USS T1 Steel

$$\sigma_y = 100,000 \text{ psi}$$

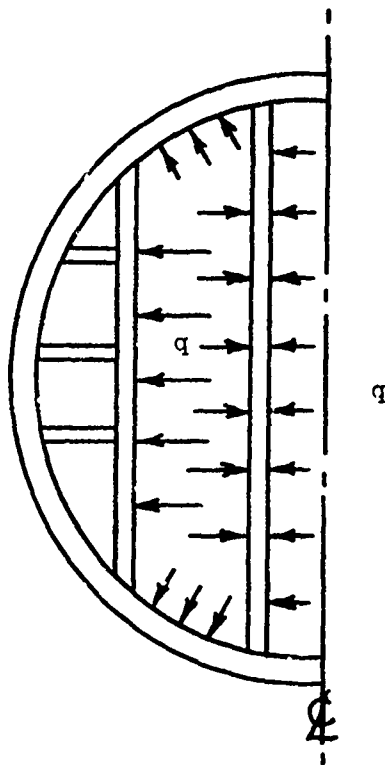
$$\sigma_u = 115,000 \text{ psi}$$

c. Design Load

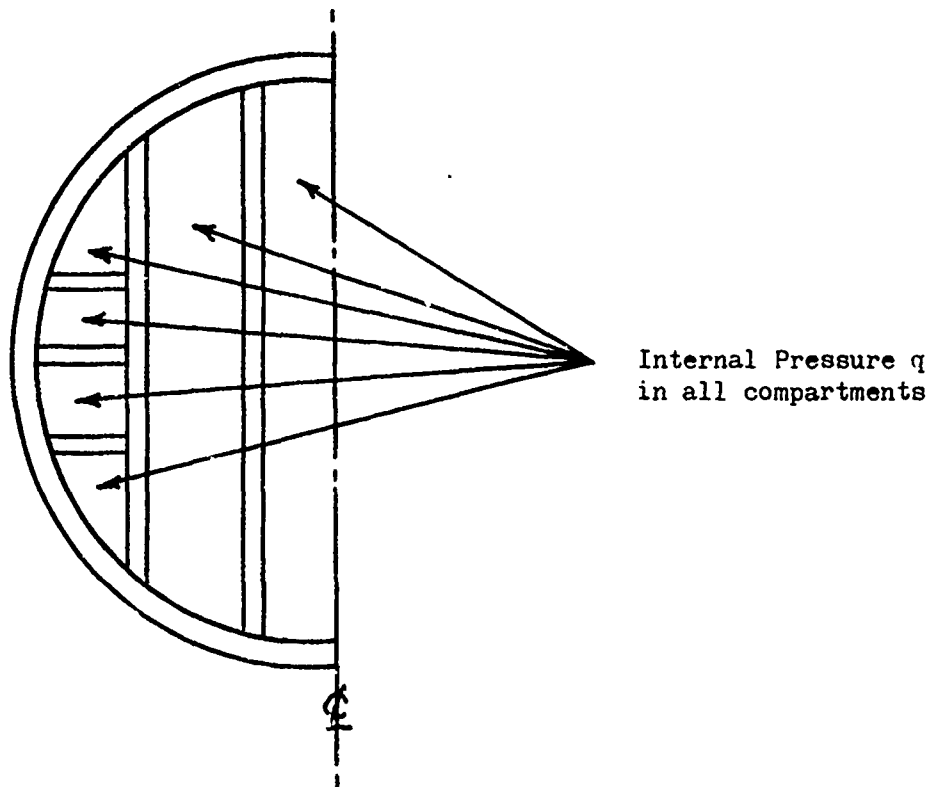
Case (1) Pressure Inside the Rectangular Inlet

This case has been handled in connection with the analysis of the inlet.

Case (2) Pressure on the Internal Side of the Baffle



Case (3) Pressure on Both Sides of the Baffle



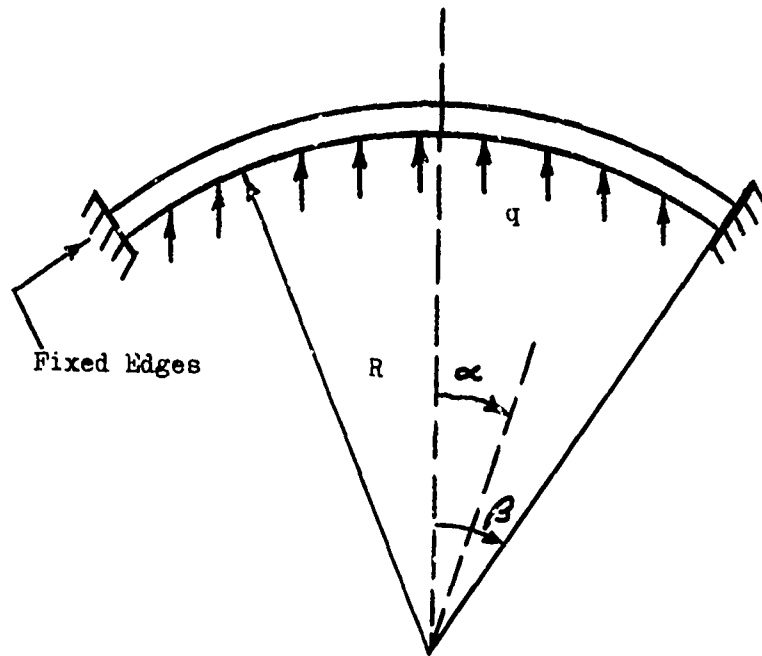
Case (4) Stresses in the Vicinity of End Joints

Because of the welded joint on the inlet end and the flange joint on the exit end, bending stresses will be introduced. These stresses may be a critical factor in the design.

d. Analysis

Cases (2) and (3)

Both of these cases can be handled by considering a segment of unit width under the following load and boundary conditions:



The angle  $\beta$  is chosen to fit the arc length of concern; for example, baffle plate to inlet side plate, baffle support plate to baffle plate, etc. The action of these plates on the cylindrical wall can be conservatively taken into account by the fixed end boundary conditions shown above.

The maximum moment and stress resultant occur at  $\alpha = \beta$  where, to a first approximation,

$$M = \frac{R^2 \beta^2 q}{3}$$

$$N = \frac{R \beta^2 q}{3}$$

The arc between the side inlet plate and the baffle yields the largest value of  $\beta$  so this will be the governing case. The span is  $31^\circ$  or

$$\beta = \frac{1}{2} \left( \frac{31}{57.3} \right) = 0.27 \text{ rad.}$$

Then

$$R = 8.12 \text{ in.}$$

$$M = \frac{(8.12)^2(1500)}{3} = 33,000 \text{ in.lbs./in.}$$

$$N = 1100 \text{ lbs./in.}$$

and the maximum stress is

$$\begin{aligned}(\sigma)_{\max} &= \frac{N}{h} + \frac{6M}{h^2} \\ &= 89,000 \text{ psi}\end{aligned}$$

#### Case (4)

The stresses in the neighborhood of a joint between a cylinder and an ellipsoidal end subjected to internal pressure are considered on page 484 of Reference (1). For the type of ellipsoidal head that we have here ( $b/a = 2$ ), the maximum longitudinal and hoop stresses become

$$(\sigma_l)_{\max} = 2.172 \frac{qr}{2h}$$

$$(\sigma_h)_{\max} = 1.128 \frac{qr}{h}$$

respectively. Since  $(\sigma_h)_{\max}$  is the larger of the two, it is the determining factor. For our design specification

$$\begin{aligned}(\sigma_h)_{\max} &= 1.128 (1500) \frac{(30)}{(3/2)} \\ &= 34,000 \text{ psi}\end{aligned}$$

For the exit end, the flange itself serves as a reinforcing element. On the inlet end where the ellipsoidal end and the cylindrical tank are welded together, a reinforcing ring could be used to ensure that the maximum bending stresses are well below yield (not shown on conceptual drawing).

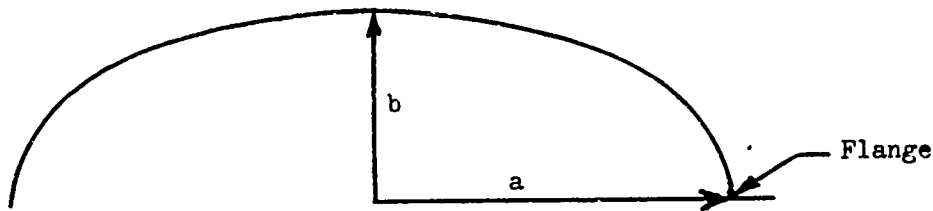
## 5. Semi-elliptical Head

### a. Geometry

Major radius  $a = 30$  in.

Minor radius  $b = 15$  in.

Thickness =  $1\frac{1}{2}$  in.



### b. Material

USS T1 Steel

$$\sigma_y = 100,000 \text{ psi}$$

$$\sigma_u = 115,000 \text{ psi}$$

### c. Design Load

#### Case (1)

For points sufficiently far from the edges, membrane theory can be applied to find the stresses due to an internal pressure of 1500 psi.

#### Case (2)

The rectangular inlet, rigidly fastened to the head, will cause bending stresses to arise. This possibility should be considered.

d. Analysis

Case (1)

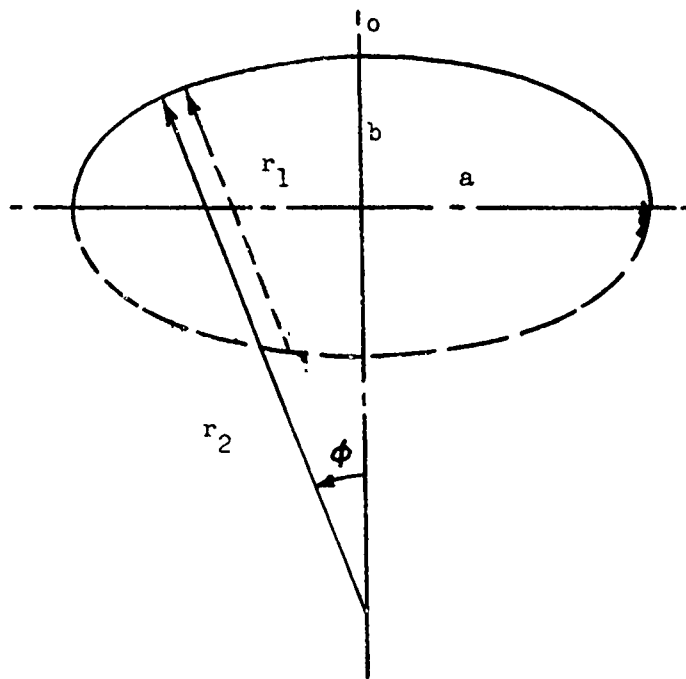
According to Reference (1), page 440, the membrane stress resultants are

$$N_{\phi} = \frac{qr_2}{2}$$
$$N_{\theta} = qr_2 \left\{ 1 - \frac{r_2}{2r_1} \right\}$$

where

$$r_1 = \frac{a^2 b^2}{(a^2 \sin^2 \phi + b^2 \cos^2 \phi)^{3/2}}$$

$$r_2 = \frac{1}{(a^2 \sin^2 \phi + b^2 \cos^2 \phi)^{1/2}}$$



At the crown of the shell (point o),  $\phi = 0$  and

$$r_1 = r_2 = \frac{a^2}{b}$$

which means that

$$N_\phi = N_\theta = \frac{qa^2}{2b}$$

With a thickness of  $h = 1\frac{1}{2}$  in., the stresses are

$$\begin{aligned}\sigma_\phi = \sigma_\theta &= \frac{qa^2}{2bh} \\ &= \frac{(1500)(30)^2}{2(15)(3/2)} \\ &= 30,000 \text{ psi}\end{aligned}$$

At the equator (or the flange area),  $\phi = \frac{\pi}{2}$ , and

$$r_1 = \frac{b^2}{a}$$

$$r_2 = a$$

so that

$$N_\phi = \frac{qa}{2}$$

$$N_\theta = qa \left( 1 - \frac{a^2}{2b^2} \right)$$

This yields the following membrane stresses:

$$\sigma_\phi = 15,000 \text{ psi}$$

$$\sigma_\theta = -30,000 \text{ psi}$$

The maximum difference in principal stresses is

$$\sigma_\phi - \sigma_\theta = 45,000 \text{ psi}$$

which is less than the yield stress.

Case (2)

A study of the interaction of the rectangular inlet with the ellipsoidal end is unwarranted at this time. Such an analysis could be easily handled by existing computer codes but before this task is undertaken, all of the other aspects of the valve should be approved.

e. Remarks

A discussion of the effect of bending stresses introduced by the connection to the cylindrical shell is discussed in the previous section on the cylindrical wall. Localized bending stresses will be introduced, but the presence of the flange will greatly alleviate these stresses as far as the end is concerned.

It should be noted that if the ellipsoidal end was continuous, the given thickness would satisfy the ASME-8 Unified Pressure Vessel Code which specifies a thickness  $t_h$  for this case as follows:

$$t_h = \frac{qd_i}{2(\sigma_a e - 0.1q)}$$

where

$q$  = pressure, psi

$d_i$  = internal diameter

$\sigma_a$  = allowable stress, psi, and

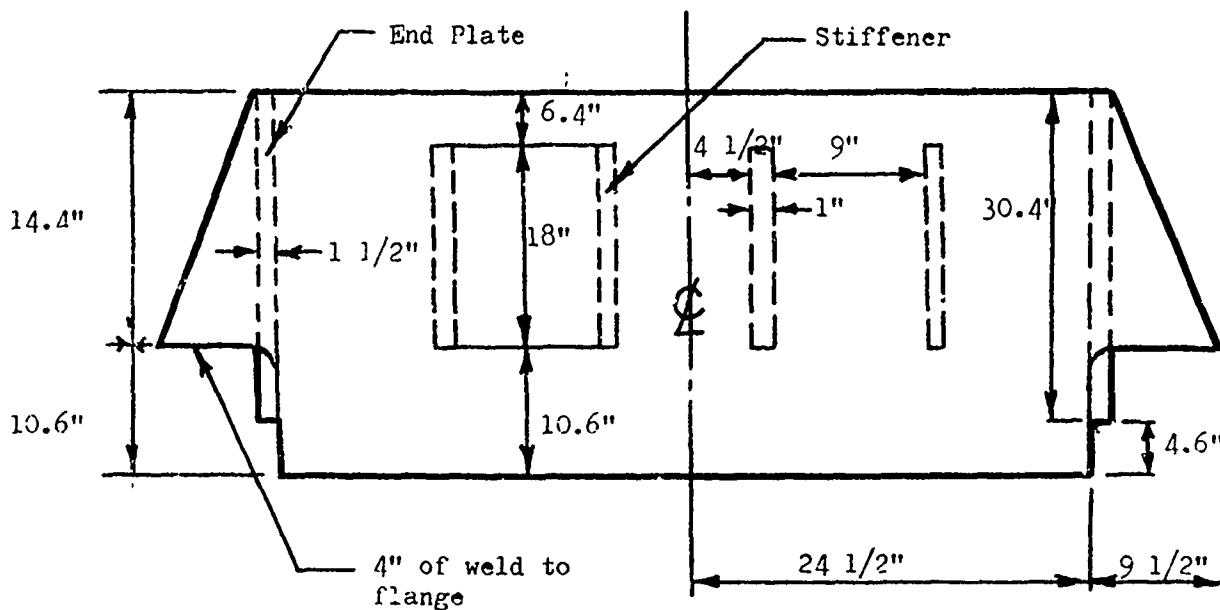
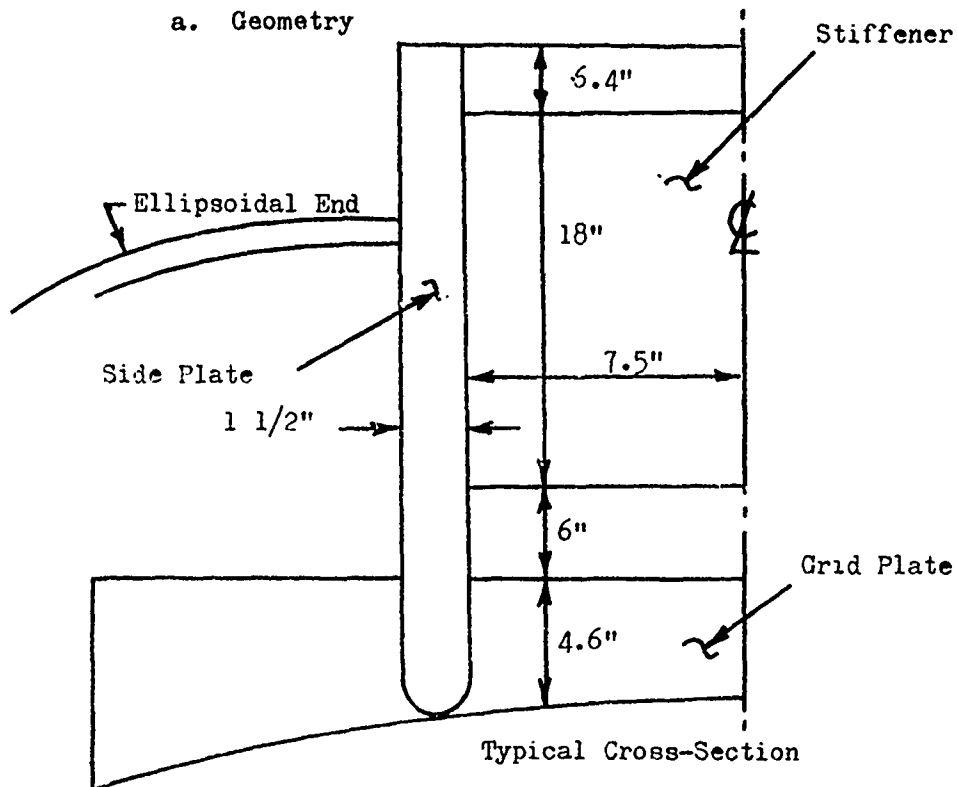
$e$  = welded joint efficiency

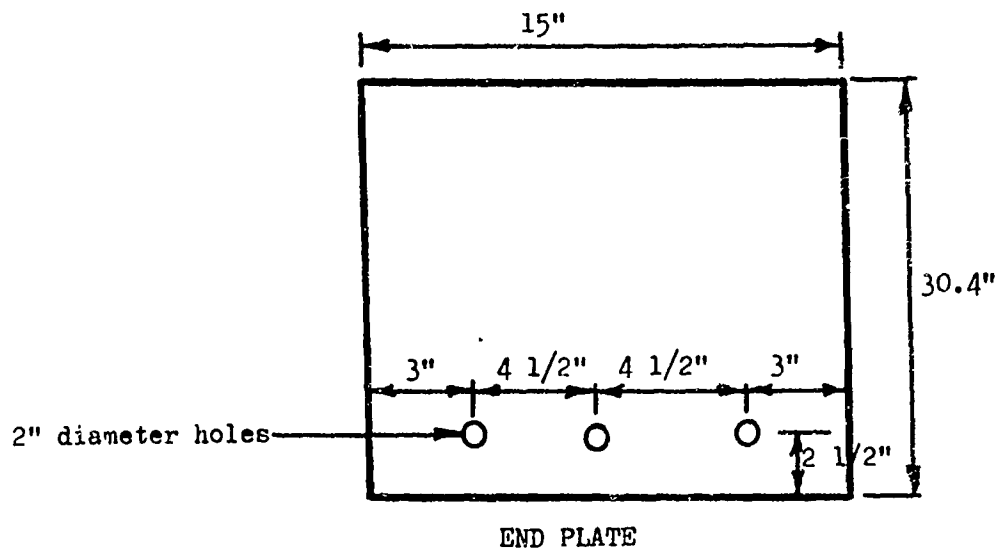
When a high strength, low hydrogen rod such as class E11018 electrode is used,  $e = 1$ . Then

$$t_h = \frac{1500(60)}{2[100,000(1) - (0.1)(1500)]}$$
$$= 0.45 \text{ in.}$$

6. Exit: Side and End Plates, and Stiffeners

a. Geometry





b. Material

USS T1 Steel

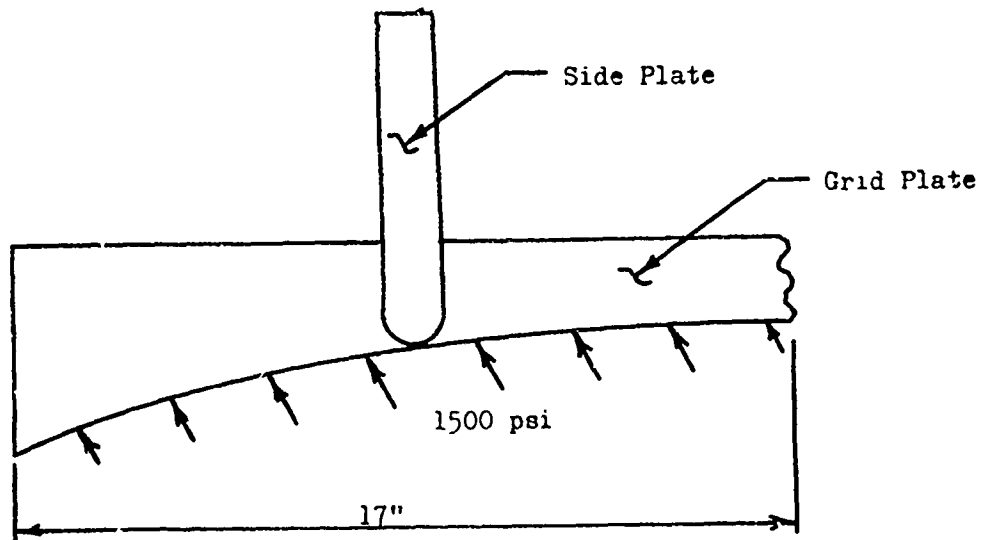
$$\sigma_y = 100,000 \text{ psi}$$

$$\sigma_u = 115,000 \text{ psi}$$

c. Design Load

Case (1)

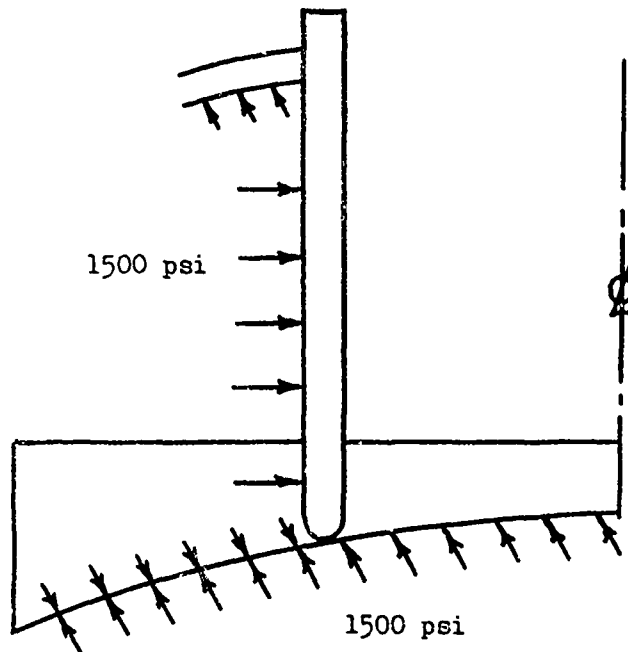
When the shock front first reaches the grid plate,  
we could have the following load:



Assume the side plate is simply supported at the ends and that it supports a load of  $1500 \times 17 = 25,500$  lbs./in.

Case (2)

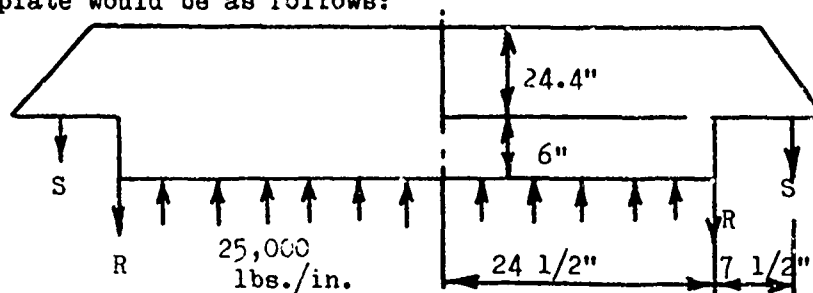
When the blast valve has filled, the following situation could exist:



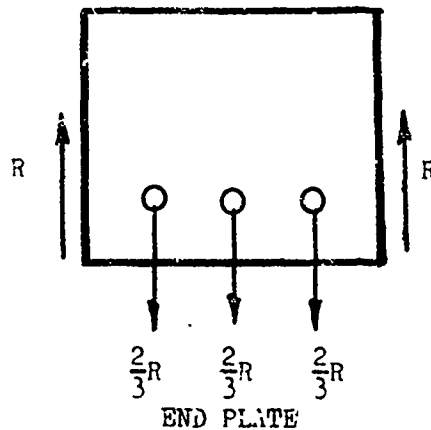
d. Analysis

Case (1)

Simplified free body diagrams of a side plate and an end plate would be as follows:



SIDE PLATE



R - reaction force transmitted to end plate

S - reaction force transmitted to the flange

Assume the resultant force on the end plate is equally distributed to the three bolts as shown. The primary function of the stiffeners and ellipsoidal end in this situation is to prevent the side plate from buckling.

In considering the side plate, we further assume that because of the large depth, the plate acts like a rigid beam. To make the problem statically determinant, assume that because of the bolt holes, slippage between the end plate and the supporting frame will occur. This would allow the reactive forces to be equal, that is,  $R = S$ . By equilibrium then

$$2R = 24\frac{1}{2} \times 25,500$$

$$= 625,000 \text{ lbs.}$$

or

$$R = 313,000 \text{ lbs.}$$

A  $2-4\frac{1}{2}$  UNC high strength bolt can sustain a shear force of 250,000 lbs. which is larger than  $\frac{2}{3}R = 208,000$  lbs.

The maximum force  $F_w$  that could be carried by the weld is the yield stress of the material times the contact area, i.e.,

$$\begin{aligned} F_w &= 100,000 \times \left(4 \times 1\frac{1}{2}\right) \\ &= 600,000 \text{ lbs.} \end{aligned}$$

which is almost twice the design load of 313,000 lbs.

To obtain an approximation for the maximum bending stress in the side plate, assume the ends are simply supported at a distance  $l = 24.5 + 4 = 28.5$  in. from the center. The maximum moment would then occur at the center and be equal to

$$\begin{aligned} (M)_{\max} &= \frac{Pl^2}{2} \\ &= \frac{25,500}{2} (28.5)^2 \\ &= 104 \times 10^5 \text{ lbs./in.} \end{aligned}$$

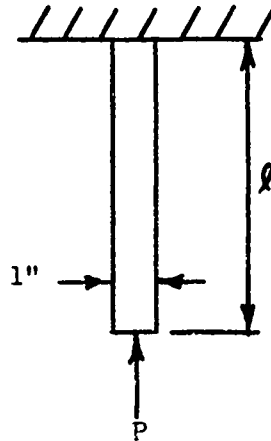
The maximum bending stress is

$$\begin{aligned} (\sigma)_{\max} &= (M)_{\max} \frac{c}{I} \\ &= 104 \times 10^5 \times \frac{15}{\frac{1}{12} \times \frac{3}{2} \times (30)^3} \\ &= 46,000 \text{ psi} \end{aligned}$$

Since there is a considerable amount of fixity at the ends, the maximum bending stress will be below this value.

Of some concern in this case is the possibility of buckling. Because of the stiffeners, the boundary conditions

are difficult to specify accurately. However, a reasonable approximation to the buckling force can be obtained by assuming that a segment 1 in. long will behave as a column. The governing situation can be modelled as follows:



Because of the stiffeners, the maximum effective length would be

$$l \approx 6 + \frac{11}{2} \approx 12 \text{ in.}$$

The buckling load is given by

$$P = \frac{\pi^2 EI}{4l^2} = \frac{\pi^2 \times 30 \times 10^6}{4(12)^2} \times \frac{1}{12} (1) \left(\frac{3}{2}\right)^3$$

$$= 147,000 \text{ lbs.}$$

which is considerably above the edge force of 25,500 lbs./in.

#### Case (2)

Again, because of the stiffeners, it is very difficult to present an accurate but elementary analysis. However, it is conceivable that the critical point as far as the side

plate is concerned would be one that is next to the grid. From the analysis of the model, the edge force is 12,000 lbs./in. and the edge moment is 32,000 in.lbs./in. This produces a maximum stress of

$$\begin{aligned}(\sigma)_{\max} &= \frac{N}{A} + \frac{Mc}{I} \\ &= \frac{12,000}{\frac{3}{2}} + \frac{32,000}{\frac{1}{12} (1) \left(\frac{3}{2}\right)^3} \times \frac{3}{4} \\ &= 93,000 \text{ psi}\end{aligned}$$

The resultant edge forces on the end plates and the stiffeners will be the order  $1500 \times 12 = 18,000$  lbs./in. compression with very small edge moments. Thus, the resulting stresses will be insignificant.

## 7. Concluding Remarks

The preceding sections indicate that the specifications for the prototype are adequate for a maximum static pressure of 1500 psi. No analysis of the ellipsoidal head on the exit end is given since the geometry and loads are similar to that at the inlet end. A detailed analysis in the vicinity of the intersection of the rectangular inlets and the ellipsoidal heads at both ends was not attempted because of the involved geometry. However, an adequate reserve strength was allowed to more than compensate for any stress concentrations that might arise because of these connections.

More detailed information of the stress distribution in all components of the blast valve could be obtained with the use of a finite element code. In fact, with the use of a more accurate description of the possible dynamic loads, such a code could be used to analyze the complete structure. It is highly probable that the suggested prototype is considerably overdesigned and that a more accurate analysis could lead to significant reductions in the thicknesses of many components. However, this study does show that the suggested valve is feasible and that additional testing and evaluation are warranted.

## VI. VALVE CONSTRUCTION AND ANALYSIS OF FIRST TEST SERIES

### 1. Construction of Sectional Test Valve and its Modification

With the government acceptance and approval of the design and stress analysis of the prototype and the sectional test valve, the project continued with the construction of the test valve.

Except for a problem in obtaining fully tempered spring steel diaphragms for the first series of tests, there was no difficulty in constructing the test valve.

The reason for the temper problem was that the first test series required curved and bent diaphragms of tempered spring material, so that factory tempered material could not be used. Even with heat plates to maintain temperature during transfer to quench, only about sixty percent of full temper could be achieved in local machine shops. However, this turned out not to be a serious problem because all of the conclusions would have been exactly the same even if the fully tempered diaphragms were available. The main lesson learned regarding temper was that factory tempered spring material should be used. Therefore, in the second test series, the valve modification would adapt to flat diaphragms, so that the factory tempered material could be used.

Also, the modification to insert in the valve for use in the second series of tests was fabricated as shown in the shop drawings, Figure 15.

## 2. First Test Series

The first test series on this valve was done primarily to observe the principle of operation of using the thin plate in conjunction with a short delay path to produce an operational valve. There was little doubt that impact effects would be likely to present problems. The possibility of excess backpressure across the ends of the diaphragm was known, but exactly how this would affect the performance of the valve was not known. Therefore, the test valve was designed so that diaphragms and the closure mechanism could easily be modified.

Spring steel diaphragms were made so that their ends could be free or clamped, as shown in Figures 16 and 17. Pressure-time gages were mounted at positions shown in Figure 16 to measure the applied shock wave pressure, the pressure on the diaphragm, pressure at the end of the delay path, and the transmitted pressure through the valve.

The tentative test plan was set up with the assumption that there would be no serious failures. When the rather serious impact yield and reopening of the valve was discovered early in the tests, it was realized that the remaining tests would have to be directed to examining these problem areas more thoroughly. Therefore, diaphragms without their ends bent and clamped, and the use of a Neoprene layer attached to the impact surface would be studied in the remaining tests of this test series.

Figure 17 shows how the excess backpressure acted to reopen the valve, and Figures 18 and 19 show the measured pressure-time responsible for developing the excess backpressure, and also shows the transmitted pressure caused by reopening.

### 3. Evaluation of First Test Series

This evaluation is based on the results of the first test series.

The important conclusions derived from the first series of tests were remedies to correct faults or malfunctions in three main areas described in the following.

There was a need to find better constituent materials for diaphragms to withstand the high impact forces which occurred when the valve was closed with high pressure shock. These constituent materials include the thin spring base plate, the elastic layer, and the adhesive for bonding the two together to compose diaphragms. The preferred materials could be determined by actual tests in the valve of a variety of these types of materials.

When the entering shock wave or rapid compressional front arrives at the end of the delay paths, the path had been closed, and the wave reflected to higher pressure. This higher pressure is the reflected backpressure that exceeded the pressure holding the valve closed from the opposite side. This excess reflected backpressure was about 30 psi for the nominal 176 applied shock pressure to the clamped end diaphragm. It forced the end quarters

of the diaphragm to move backward, away from the grid, and to lift the sides of the center portion of the diaphragm and let high pressure air pass through the valve. This process is caused by the pressure difference above and below the diaphragm as expressed by Figure 17. Note also, the resulting transmitted pressure in Figure 19 shows the same process when the ends of the diaphragm were not clamped for the 155 psi applied shock pressure.

When the reflected excess backpressure caused the end quarters of the diaphragm to move away from the grid, the motion was so vigorous that it bent the diaphragm, whether clamped or unclamped. In the case of the free end diaphragm, the ends were forced back against and partly around support bolts in the valve with sufficient force to wrap partially around the bolts.

The free end arrangement was somewhat effective in venting the reflected backpressure, in that the transmitted pressure caused by reopening was reduced to about one-third when diaphragm ends were unclamped. This free end system could be a useful technique for backpressure relief without damage, if the magnitude of excess backpressure could be substantially reduced.

It was realized that a more positive method was available for preventing reopening of the valve by excess backpressure, regardless of its magnitude. This method depends on a double diaphragm arrangement in which slots are cut through the end sections of the lower diaphragm, coinciding with slots in the grid on which it impacts. When any excess backpressure develops, it does not disturb

the lower diaphragm as it is seated against the grid, and therefore, does not reopen the valve. With this arrangement, the reflected backpressure acts through the slots to move the back diaphragm away from contact with the slotted diaphragm. Therefore, with this double diaphragm arrangement, a backup grid is needed to distribute the forces and stop the backward movement of the back diaphragm.

Also, it was realized that waves can reflect to pressures higher than their stagnation pressures only in a non-steady process. Thus, if the non-steady portion of the reflection at the end of the delay paths is absorbed by a volume, then effectively quasi-steady conditions will determine the maximum pressure which will not exceed the stagnation pressure at the time a maximum pressure is reached in the volume.

If a discontinuous jump in pressure occurred at the entrance of the delay path, we would have seen even higher reflected pressures, and the increase in volume necessary to absorb this reflected pressure would need to be about 1.5 times the volume of the delay path.<sup>7</sup> However, the entrance chamber causes a gradual pressure increase of 2 to 3 milliseconds to maximum to be applied to the delay path entrance. This may not seem like much, but when it compares to the travel time in the delay path, or to the filling time of a chamber at the end of the delay path, it is very significant. Therefore, in this case, the volume at the end of the delay paths can be increased to approximately the volume of the delay path to prevent excess reflected backpressure.

This volume adjustment could not easily be made in the test valve. Therefore, it was decided that the double diaphragm arrangement with the backup grid modification should be tested, realizing that if this tested successfully with the high reflected backpressure, it would certainly be successful when the backpressure is reduced by the volume adjustment.

Pressure head loss was measured and the theory previously developed shows<sup>n</sup> the following.

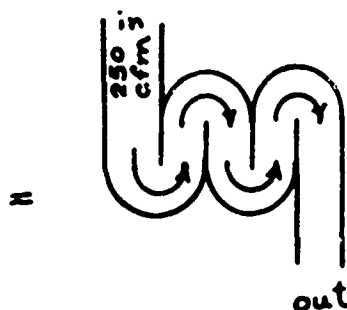
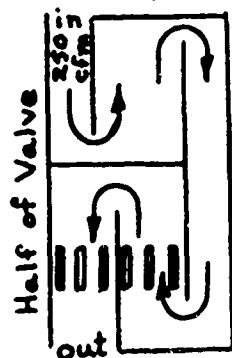
#### 4. Pressure Head Loss

The path of normal ventilation flow through the valve involves changes in cross sectional area and shape, sharp 180 degree turns, and a grid plate, all of which do not resemble a conventional duct system subjectable to conventional engineering head loss calculations. However, conservative conditions can be imposed on this system to make it resemble a conventional system so that a conservative head loss can be calculated as follows:

##### (a) Head Loss by Turns and Lengths

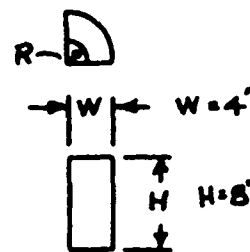
Assume the following diagram analogy for half of the

valve model:



4 each 180° turns  
or 8 each 90° turns

Where.



$$\frac{R}{W} = 0.5 \quad \frac{H}{W} = 2$$

According to Reference 8, the equivalent loss-distance-to-width-radius  $L/W$  per 90 degree turn is 65, so the length is 21 feet. Therefore, the total loss length equivalent for the 8 turns is 168 feet.

The actual length through the valve is approximately 15 feet for a total length equivalent of 183 feet.

$$L = 183 \text{ feet}$$

(b) Head Loss by Grid Plate

From the pipe flow equation

$$\Delta P = \frac{f L \rho \bar{u}^2}{2 D}$$

different ducts have the same loss when  $P/\rho \bar{u}^2$  can be equated, or when

$$\frac{L_1}{D_1^2} = \frac{L_2}{D_2^2}$$

Assume an element of the grid cross section to be  $1/4'' \times 2''$  and a length of 12".

Reference 8 shows this duct to be equivalent to a circular duct of 0.69" diameter. Similarly, the 4" x 8" duct diameter equivalent is 6.1". Therefore, the equivalent loss length in the small duct can be related to loss length in the 6.1" duct. This was necessary because the available air friction flow charts were not given for diameters below 1.5", so that

$$L_1 = 12 \left( \frac{6.1}{0.69} \right)^2$$

$$= 940'' \text{ or } 78 \text{ feet}$$

(c) Total Head Loss

Combining the three sources of head loss for a total equivalent length of 261 feet. Since the equivalent duct diameter is 6.1", according to Reference 8, the total head loss for 250 cfm is 0.45 inches of water per 100 ft. equivalent is therefore

$$\Delta H = 261 \left( \frac{0.45}{100} \right) = 1.17 \text{ inches of water}$$

This theoretical determination of the pressure head loss was made it to be conservative because the method used, Reference 8, was based on axially symmetric changes on cross sectional area and 180 degree turns without increased cross sectional areas. In the valve, most of the turns have at least a 30 percent area increase relative to the entrance area.

(d) Experimental Measurements of Pressure Head Loss

When the valve was mounted in the shock tube, the pressure head loss was measured for flow in both directions, and also with the grid modification in place. Figure 20 shows these measurements.

From these measurements and with the theory relating pressure head loss,  $\Delta P$ , to the volume rate of flow,  $\Delta V/\Delta t$ , it is possible to calculate accurately how a new cross sectional area modification will affect the normal ventilation flow.

From the theory

$$\Delta P = c \frac{(\Delta V)^2}{A \Delta t} \quad (1)$$

where the constant  $C$  has the dimension of density, and contains dimensionless conversion factors, and  $A$  is the cross sectional area.

Since the individual losses in the valve are additive to get the total loss, any individual loss element can be examined separately. The impact grid is an element that is to be changed in the prototype and needs to be examined separately, so that

$$\Delta P_{(\text{total})} = \sum \Delta P + \Delta P_{(\text{grid})} \quad (2)$$

from eq.(1)

$$\Delta P_{(\text{total})} = \sum \Delta P + C \left( \frac{1}{A} \frac{V}{t} \right)^2 \quad (3)$$

Measurements were made at  $\Delta V / \Delta t = 500$  cfm for  $A = 56$  sq. in. and for  $A = 23$  sq. in., to get respectively,

$$\Delta P_{(\text{total})} = 0.45 \text{ inches of water}$$

$$\Delta P_{(\text{total})} = 1.78 \text{ inches of water}$$

and calculate from eq.(3)

$$\sum \Delta P = 0.18 \text{ and } C = 3.39 \times 10^{-3}$$

so that

$$\Delta P_{(\text{total})} = 0.18 + 3.39 \times 10^{-3} \left( \frac{500}{A} \right)^2 \quad (4)$$

Reference to Section VIII shows that 3/8 inch grids will separate 1/4 inch slots as recommended prototype modifications. Were this modification applied to the test valve, then  $A$  is 38 sq. in., and the resulting pressure head loss versus the volume rate of flow is shown on the figure. Note the 12 percent increase for exhaust flow.

In the real ventilation system, two valves would be required

for intake and exhaust flow, so the total pressure head loss would be the sum  $0.82 + 0.73 = 1.55$  inches of water. Also, in the real prototype system, the corresponding volume rate of flow would be approximately 3.330 cfm, corresponding to 500 cfm in the test valve for the same pressure head loss.

## VII. SECOND TEST SERIES

### 1. Discussion

The instrumentation, the mounting of the valve to the shock tube, and other test procedures were essentially the same as those in the first test series.

Tests on the elastic layer were done under conditions that would be harsh enough to be likely to cause some impact damage in every test. This was accomplished by not using the backup grid modification and applying 147 psi incident shock pressure. The various materials collected for these tests are shown in the following "List of Materials", with information provided by suppliers or manufacturers.

#### LIST OF MATERIALS

##### SPRING BASE AND BACK DIAPHRAGM MATERIALS

Spring Steel 1095	Temp. C35	0.032 in. thick
Spring Steel 1055	Temp. C37	0.025 in. thick
Spring Steel 1055	Temp. C37	0.050 in. thick
Spring Steel 1074	Temp. C40	0.025 in. thick
Spring Steel 1074	Temp. C40	0.050 in. thick
Stainless Spring Steel 410	Temp. Spring	0.025 in. thick
Stainless Spring Steel 410	Temp. CR	0.042 in. thick
Stainless Steel 301	Temp. FH	0.050 in. thick
Stainless Steel 302	Temp. FH	0.032 in. thick
Titanium-6Al-4V	Temp. Heat K-3829	0.032 in. thick

### SPRING BASE AND BACK DIAPHRAGM MATERIALS

(continued)

Phospho-bronz Spring	Temp. Spring	0.032 in. thick
Monel	Temp. CR	0.040 in. thick
Scotchply 1002 (fiberglass)		0.070 in. thick
Scotchply 1002 (fiberglass)		0.100 in. thick

### ELASTOMER LAYER MATERIALS

Natural Rubber	Style 606	0.125 in. thick
Natural Rubber	Style 606	0.250 in. thick
Synthetic Rubber	MIL-R-6855-CR40	0.125 in. thick
Hypalon Rubber		0.125 in. thick
Hypalon Rubber		0.250 in. thick
Pylon Rubber		0.250 in. thick
Silicone Rubber	CHR9050	0.125 in. thick

### ADHESIVES

Aron Alpha  
Resiweld - H. B. Fuller Co., 7004  
Weldwood Contact Cement, U. S. Plywood  
Scotch-Grip Contact Cement 2210  
Scotch-Weld Structural Adhesive  
Eccobond 87H Contact Cement  
Silicone Adhesive, Dow Corning 96-083  
Coast Pro-Seal 830

## 2. Evaluation of Second Test Series

This evaluation is based on results of the second test series, Reference 9, which should be referred to if more details not covered in this report are desired.

Of the materials tested, the following was determined.

The Aron Alpha was the best adhesive tested and was used for all double diaphragm construction. The Coast Pro-Seal 890 bonded well to the metal, but not to the natural rubber. This adhesive may be good if the rubber surface is well roughened.

The fiberglass, Scotchply, was the best spring-base material tested, mainly because it did not become deformed as metal diaphragms did under the same conditions. Of the metal diaphragms tested, the titanium alloy and the spring stainless steel 410 were the best because they showed the least yield of the metals tested under the same conditions. In these cases, the impact damage could be controlled by thicker elastic protection, but backpressure damage could only be controlled by reduced backpressure.

The natural rubber and synthetic rubber seemed to afford the best protection to the base metals and suffered the least impact damage themselves.

In all cases, the double diaphragm was completely effective in preventing reopening of the valve by reflected backpressure. This was verified by the absence of excess pressure surges transmitted after the valve had closed.

The unbalanced distribution of pressure caused by reflected

backpressure on the ends of the back diaphragm caused a hump distortion at the center of all metal back diaphragms tested, but not to Scotchply diaphragms.

The backup grid modification served its intended function to receive the back diaphragm without causing damage. It also served to reduce the closing pressure since about 78 percent of the cross section was closed by this backup grid. This caused the valve to close more slowly and thereby, to sustain less impact force. Pressure measurements were not made under the backup grid, so the real closing pressure is not known. As expected, this reduced closing pressure seriously affected the closure time at low applied shock pressures, so that some pressure did pass through the delay paths before closure was complete. However, this bypassed pressure was only about one-fifth of the applied low shock pressure.

The only damage sustained by the elastic layer was surface damage where it contacted edges of the impact grid slots, which seemed to be caused by a sliding of the surface parallel to these edges. This surface damage was quite shallow and was not found to be serious, as repeated high pressure tests did not increase the extent or depth of the damage. However, this surface damage should be eliminated if possible, because higher closure pressures will be expected if a more open backup grid is recommended to facilitate low pressure closure.

The most important of the pressure-time measurements made was the transmitted pressure wave. The transmitted pressure-time record shows four important points. It will be worthwhile

discussing these points in some detail.

For the nominal 176 psi applied shock pressure, a very thin pressure spike was the first disturbance transmitted through the valve. This spike attenuated from 20 psi at station 5 to 13 psi at station 6, Figure 16, which is 1.6 feet further downstream, for an attenuation rate of 4 psi per foot of travel. This is approximately the attenuation rate of a pressure spike having a base duration of  $1/4$  millisecond, and this is approximately the measured base duration of the recorded spike. From this, it can be shown that the spike will reach about 7 psi in the next 1.5 feet of travel.<sup>10</sup>

The second important point is that at 7 psi, the negative slope of the spike suddenly increases to a base of about one millisecond. This will slow the attenuation of the peak pressure to about 0.5 psi per foot of travel. This means that the peak transmitted shock pressure would be approximately 2 psi at 10 feet further down stream in a uniform cross sectional duct. Lateral expansion will produce the 2 psi in less than 10 feet.

Considering the source of this spike, since it is the first disturbance to get through the valve, it must be produced directly from the entering shock front that passes the edges of the diaphragm. The piston action of the diaphragm could not possibly generate a spike of such high pressure and short duration.

This initial spike is followed by two successive weaker spikes that are probably diffracted or reflected from the first spike that originates from edges of the diaphragm and passes through the grid.

The fourth point is the long duration of very low overpressure following these spikes and continuing after the valve had closed. This represents low pressure flow and since there is no surge, it represents rather steady flow which must be caused by a continuous leak from the high pressure region of the valve. The unsealed interface between the modification and where this modification seats on the original valve grid probably allows enough high pressure leakage to account for this low pressure transmitted flow. Of course, this would not occur for the modification built into a valve.

One double diaphragm arrangement was used in seven test runs, including one applied shock at 250 psi incident pressure, or 1,640 psi reflected pressure. This arrangement sustained only superficial damage that did not increase with successive runs and did not alter its performance. This arrangement was composed of Scotchply 1002 with surface fibers aligned perpendicular to the grid slots. Both front and back diaphragms were of this material 0.1 inch thick. A 1/8-inch thick natural rubber layer was bonded to the impact surface. On the back of impact diaphragm were strips of 1/8-inch thick natural rubber running from end to end to provide 8 each 1/2-inch channels so that reflected backpressure could be conducted between both diaphragms to their center portion. Tests showed that this channel system was not successful as a means to prevent the hump distortion of metal back diaphragms.

It appeared that more and even higher pressure shocks could have been applied to this 0.1 inch thick Scotchply double diaphragm arrangement without sustaining further damage.

All of the surface damage to rubber appeared to be caused by sliding along edges of grid slots and not by impact. The reason for the sliding hypothesis is that wherever surface cutting occurred, rub marks also occurred in the same vicinity, running perpendicular to the cuts where the rubber contacted a surface and that no surface damage occurred in the center portion of the impact surface. This sort of friction could develop when the center portion of the diaphragm moves into contact with the grid and draws the tightly contacted ends toward the center.

## VIII. RECOMMENDED MODIFICATIONS OF THE VALVE

The tests showed which of a large number of constituent diaphragm materials tested had the best tolerance to impact. The tests also showed how to correct malfunctions caused by backpressure. It should be obvious that there is considerable dependence between some of the important functions of the closure mechanism actuated by shock, so most of the recommendations are associated as a set. In the following, each distinguishable area where modifications are recommended is discussed individually.

### 1. Reflected Backpressure

The only serious effect of reflected backpressure when the double diaphragm arrangement was used was the strong unbalanced pressure distribution between the top center and the bottom ends of the back diaphragm that caused the hump deformation in metal diaphragms. The reflected backpressure did not cause reopening of the valve, so it is recommended that the double diaphragm arrangement be used in the prototype valve. The Scotchply back diaphragm was not deformed as the metal diaphragms were. However, the Scotchply did show that stretching did occur as the surface fibers were separated where the apex of the hump would have occurred in metal diaphragms. This stretching separation would perhaps be avoided if the surface fibers in the Scotchply were aligned from end to end, instead of from side to side.

Even though the reflected backpressure is not a problem where

Scotchply diaphragms are used, it is recommended that this back-pressure be reduced as much as possible.

The process whereby reflected shock pressure can be developed in a chamber are described in Reference 7. Essentially, supersonic flow does not allow a backup of pressure from the chamber until an upstream facing shock front of sufficient velocity develops and moves against the incoming supersonic flow. The theory of this process is born out by experiment when the process begins as a discontinuous pressure wave. However, in the case of the valve in which the theory is to be applied in order to find a proper volume at the end of the delay path that will prevent reflected pressure from developing, the driver pressure entering the delay paths showed a rise time of 2 to 3 milliseconds, and not a discontinuous front. This makes a precise theoretical determination of a chamber pressure curve difficult, especially when the rise time is comparable to the travel time in the delay path. However, it is not necessary to accomplish a precise determination, since the important thing is to realize that the discontinuous driver allows development of the reflected pressure in the chamber earlier than any other kind of wave front. Therefore, a correction for shock wave filling of a chamber to avoid reflected pressure will be an overcorrection for the compressional wave acting in the valve.

In the entrance chamber of the test valve, 2 to 3 milliseconds were required for maximum pressure to be reached. This 2 to 3 millisecond rise time is the driver pressure time that determines the rise time of the transmitted wave in the delay paths. Because

of this slow rise time, the reflected pressure at the end of the delay paths was only 130 psi instead of the theoretical maximum of 200 psi for the nominal 176 psi applied shock pressure. It is desired that this 130 psi be further reduced to approximately 100 psi and close to the pressure acting in the opposite direction through the diaphragm. This sort of reduction in pressure at the end of the delay path can be achieved by providing a volume increase to further delay the pressure-fill-time. Theoretically, this would be satisfied by a chamber having a volume of about 1.5 times that of the entrance duct (delay path) when a driver pressure is discontinuous at 160 psi. In the prototype valve, a volume exists at the end of the delay paths which only requires a slight increase to match the volumes of the delay paths. Since the delay paths in the prototype valve are now 5 feet long, and a natural volume increase of about 3 feet now exists at the end of the delay paths in the prototype, it is recommended that the grid-diaphragm system in the prototype be moved one foot further into the valve, thereby increasing the volume at the end of the delay paths and decreasing the volume of the delay paths to be approximately equal. The decrease in the delay path length and the shock travel time therein caused by this adjustment is negligible, as it is outweighed by the advantages of not having to use a thicker back diaphragm to contain high backpressure.

## 2. Impact Grid

The backup grid modification included a modified impact grid, Figures 7 and 15. This rather substantial reduction in the number of openings in the impact grid had no basic advantage with regard to impact damage and backpressure effects. It greatly increased the pressure head loss from 0.45 to 1.78 inches of water at 500 cfm, Figure 20. The 3/4-inch surfaces between 1/4-inch slots provided a wider surface for attaching elastic strips. For convenience in attaching elastic strips, the impact grid should be composed of 3/8-inch separations between the 1/4-inch slots. It is calculated that this recommended grid spacing will increase the pressure head loss to about 0.73 inches of water at 500 cfm.

The only damage done to the elastic layer by impact was thought to be caused by the sliding of the elastic layer along the edges of grid slots while in tight contact with those edges. The sliding action is believed to occur when most of the baseplate has made contact with the grid, but a few inches at the center still has to move into contact. Under high pressure, this center is forced into contact, thus drawing the rest of the surface toward the center. Since the rest of the surface is pressed against the grid, limited shearing occurs.

It is believed that most of this shearing can be eliminated if the central half of the impact grid is flat and the ends turned up as required to get the normally opened space. Also, it is recommended that all edges of the grid be rounded to about 1/64-inch radius. This also includes the bottom edges that are not involved

in the impact, so as to minimize pressure head loss. There is a possibility that the impact grid would be covered with elastic strips instead of the impact diaphragm. This would also eliminate shearing at edges, since in this case, the edges would be the elastic material. This variation would also remove the mass of the elastic layer on the closure mechanism and allow the closure to be faster.

The turned up ends of the impact grid serve to provide the normally open space between the center portion of the impact grid and the base plate. This space should be no less than 2 inches.

### 3. Double Diaphragm Arrangement and Triple Diaphragm

Even though the backpressure can be reduced by the volume adjustment, the double diaphragm arrangement is recommended for use in the prototype.

The optimum thickness of the diaphragms is based on increased thickness for favorable impact strength and decreased thickness for favorable short closing time and perhaps less impact inertia. It is not possible to arrive at an optimum set of design specifications without a large number of tests, and it is probably not essential. What is essential is that we know that damage does not occur for at least the 176 psi applied shock pressure and that closure is sufficiently fast to block low pressure effectively. From experience of these tests, some judgment of materials and thicknesses can be made.

For the prototype valve, it is recommended that the baseplate be 0.10 inch thick Scotchply and the backplate be 0.050 inch thick

Scotchply. The baseplate also may be made of titanium alloy approximately 0.040 inch thick. With a slightly thicker elastic layer, 1/4-inch thick, the titanium baseplate should not experience impact damage even with a larger backup grid opening area.

Another possibility as an outgrowth of the double diaphragm arrangement and made possible by the backup grid, is the use of a triple diaphragm in which two of the back diaphragms are plane and unslotted. The reason for this triple diaphragm is that an air inlet can be arranged to let air between these two diaphragms to force them apart and to close the valve. This air inlet can be sensory or manually actuated as a pneumatic closure that can act very fast and can probably close the valve within 50 milliseconds. This pneumatic closure will eliminate the mechanical closure, utilizing the half cylinders shown in Figures 1 and 3. This will give the entire valve the same insensitivity to ground shock. Since this triple diaphragm eliminates need for the original slot entrance, the new entrance should be a 19 inch diameter opening. Also, the total combined thickness of the triple diaphragm arrangement does not need to be increased since their impact support is nearly additive. Therefore, it is a recommendation that the triple diaphragm arrangement be used in the prototype with each of the back diaphragms being about 0.030 inch thick Scotchply. It is also recommended that the entrance orifice be a 19 inch diameter opening that ends at least 3 feet above the backup grid to insure even shock loading distribution on the closure surface.

#### 4. Backup Grid

The backup grid used in the modified valve tests accomplished two things. It received and distributed the force caused by the backward movement of the backplate by reflected backpressure, and it reduced the closure pressure by covering 78 percent of the diaphragm area with a grid.

The reduction in closure pressure was not a problem except at low applied shock pressure where the closing was much too slow for good low pressure performance.

With the reduction of reflected backpressure, the backup grid can have a much larger open area and significantly reduce the low pressure closing time.

It is recommended that the backup grid leave at least 50 percent of its surface open. To facilitate the structural design, the backup grid should be integrated with the impact grid, both of which can be removed from the valve housing as a unit.

#### 5. Elastic Impact Layer

The elastic layer attached to the impact surface prevents damage to the baseplate when it impacts against the grid.

The 1/8-inch thick natural rubber prevented yield of metal diaphragms from impact when the backup grid was used, but not when the backup grid was not used. No damage was done to metal diaphragms when 1/4-inch thick natural rubber covered the impact surface without the backup grid, thereby indicating that the thickness of the

natural rubber has a lot to do with impact yield of the metal.

If the pickup grid open area is increased from that of the tests, a thicker natural rubber layer should be used, especially with the metal baseplate. With Scotchply diaphragms, 3/16-inch thick natural rubber should be adequate, and with titanium alloy or spring stainless steel, 1/4-inch thick natural rubber should be adequate.

The elastic layer should cover the end portions of the impact diaphragm between slots, as well as the center portion. The natural rubber should be bonded to the plate with Aron Alpha adhesive or other cyanoacrylate cements.

The use of the elastic layer attached to the impact grid, instead of to the diaphragm, should be considered for future tests and possibly for the prototype.

## IX. CONCLUSIONS AND RECOMMENDATIONS

A pre-test valve design was shown in drawings and the features of its expected performance was discussed. This valve was tentatively designed to be shock pressure actuated, or with a remote or manual actuation capability. In a typical air entrainment system of a blast hardened facility, it was presumed that less than 2 psi would be allowed through the valve for shock pressures on the ground surface up to 1,000 psi, and normal ventilation of a unit valve would be 3,330 cfm, with a pressure head loss of less than 1.5 inches of water. Tests showed that the 2 psi condition could be expected within 10 feet of the protected exit of the valve for much higher surface pressures, and the pressure head loss would be about half of the theoretical estimate.

One dimension of the valve that is independent of scaling properties of the closure process was decreased to design a test valve which would be adaptable to a shock tube. This test valve was constructed and tested in a high pressure shock tube. The first series of tests showed three performance faults and indicated methods of correcting these faults. A second series of tests were conducted to prove whether or not the indicated methods would correct the faults. The results were all positive and a set of recommended modifications to apply to the prototype were given.

The main conclusions on the expected performance of the modified prototype are as follows:

1. That the air shock reaching the valve from at least 2,000 psi on the ground surface can be handled by the valve;
2. That the valve is so insensitive to ground shock that even some permanent distortion of the valve housing can be tolerated without impairing its performance;
3. That pressure head loss of about 75 inches of water will let one unit valve deliver 3,330 cfm.

The modified prototype valve is expected to satisfy, or better than satisfy, all government requirements and specifications of this valve.

It is recommended that this prototype valve be constructed for a field test in a simulated blast hardened facility. Also, it is suggested that the prototype valve and the facility be designed to conduct further tests by using high explosives in the entrance shaft in a semi-shock tube situation. This would allow a great variety of blast conditions to be tested which could not be accomplished in the conventional field test.

#### REFERENCES

1. Tomoshenko, S. and Woinowsky-Krieger, S., Theory of Plates and Shells, McGraw-Hill, 1959.
2. Kraus, H., Thin Elastic Shells, J. Wiley & Sons, Inc., 1967.
3. Schreyer, H. L., and Masur, E. F., Buckling of Shallow Arches, J. of Engineering Mechanics Division, Proceedings of ASCE, Volume 92, No. EM4, August, 1966.
4. The Allen Manufacturing Co., Allen Hex-Socket Screw Handbook, 1964.
5. Bresler, B., and Li., T. Y., Design of Steel Structures, J. Wiley & Sons. Inc., 1960.
6. Clark, R. O., and McMurtry, W. M., Test of Piston Plate Airblast Valve, Letter Report of CERF-AFWL to NCEL.
7. Clark, R. O., and McMurtry, W. M., Shock Wave Filling of Chambers, AFWL-TR-70-73, September, 1970.
8. ASHRAE, 1960 Guide and Data Book.
9. Clark, R. O., and McMurtry, W. M., Tests on Modified Piston Plate Airblast Valve (Second Test Series), Letter Report of CERF-AFWL to NCEL, February, 1972.
10. Clark, R. O., Theory for Viscous Shock Attenuation in Ducts Based on the Kinetic Theory of Gases Experimentally Verified to a Shock Strength of 68, AFWL-TR-65-204, July, 1966.

ALL

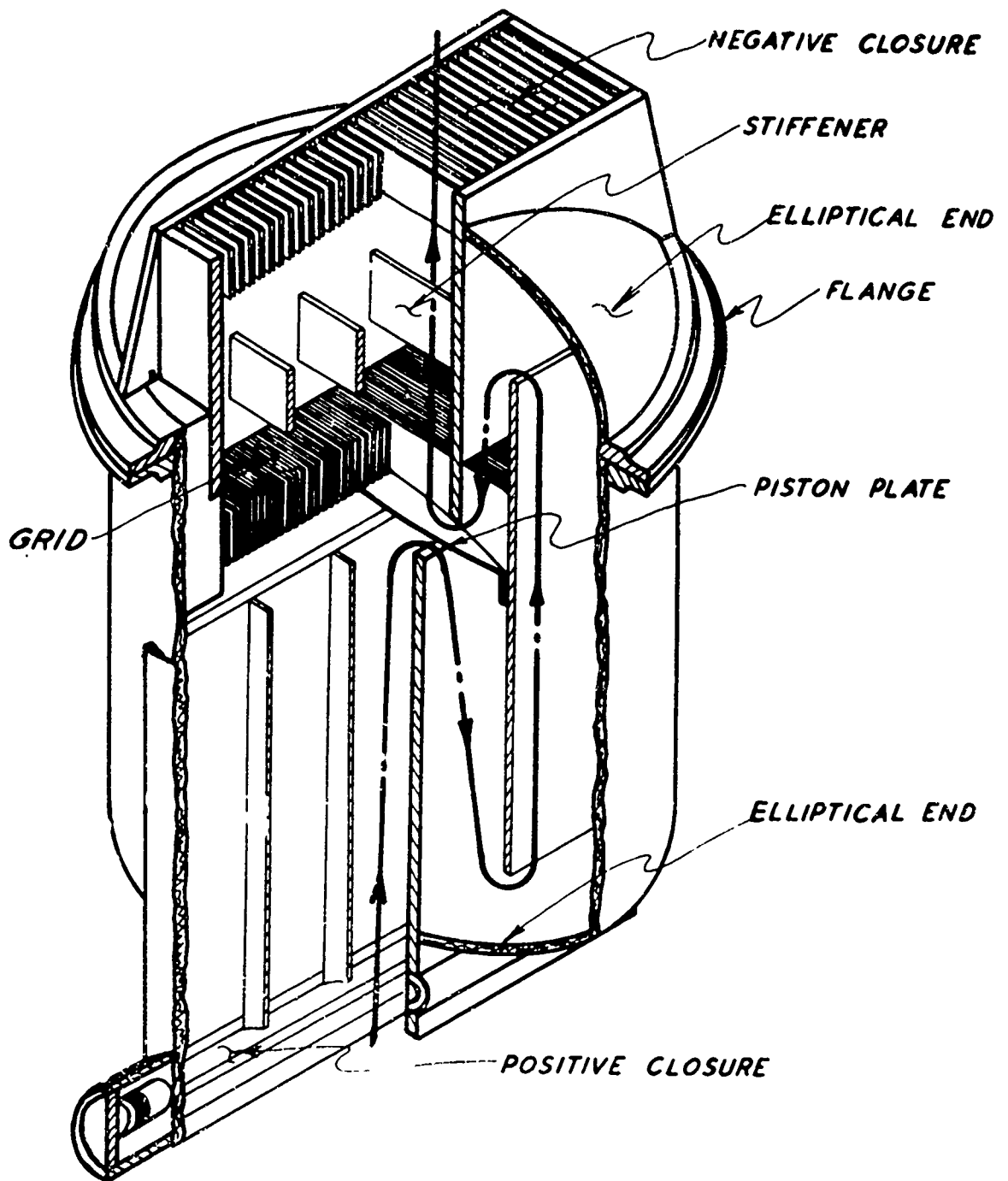


Figure 1 Pre-Test Sectional  
View of Original Prototype Valve

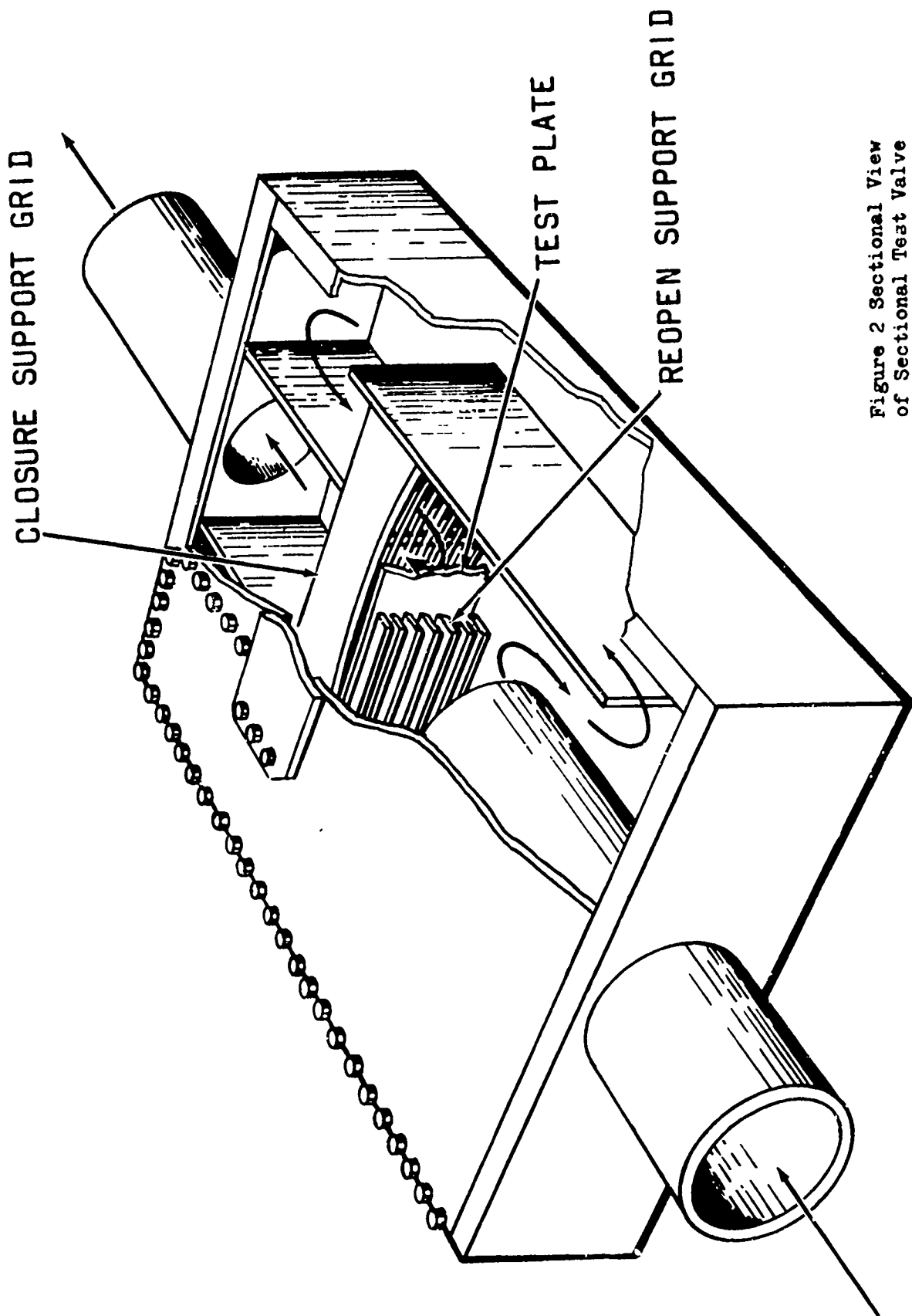
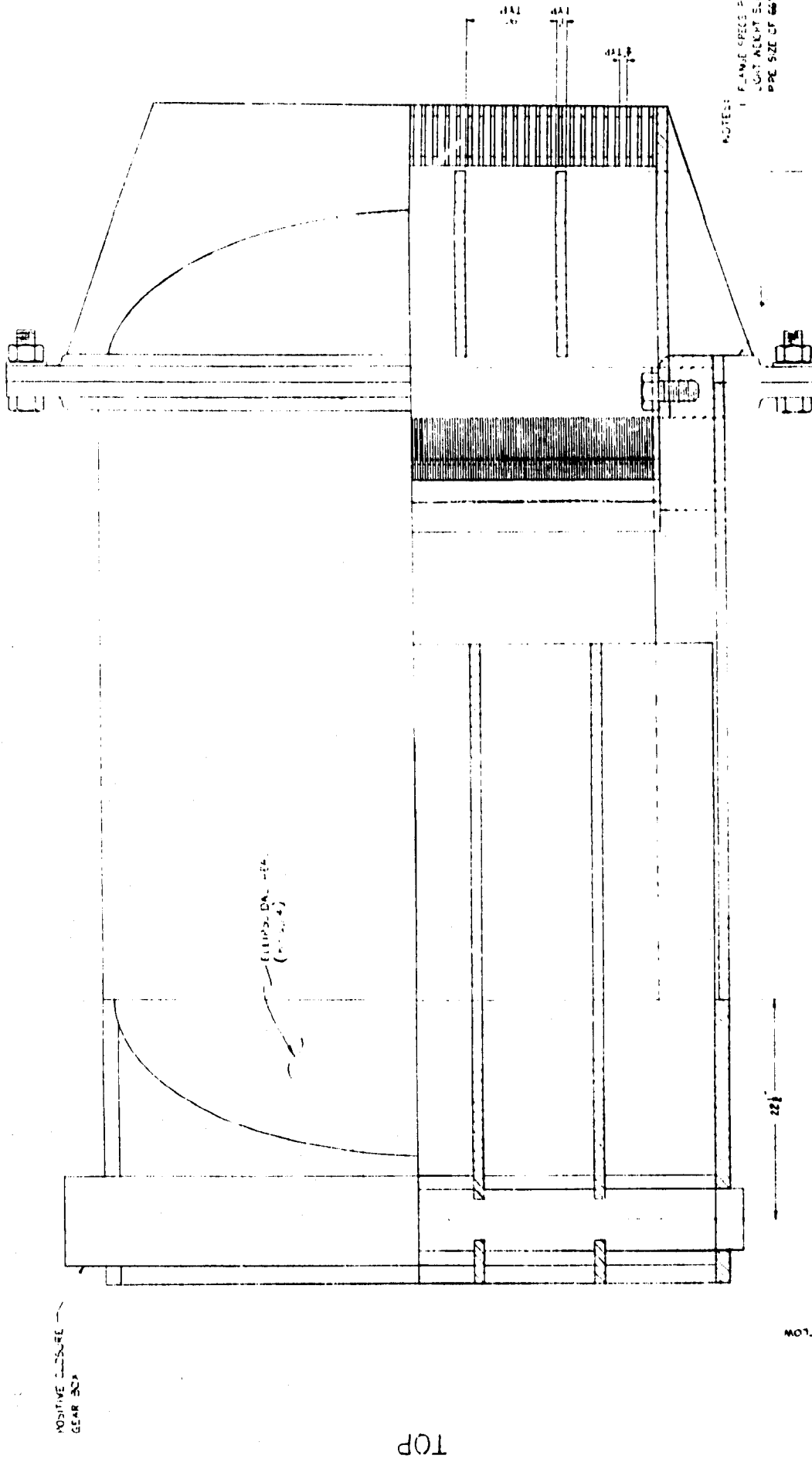


Figure 2 Sectional View  
of Sectional Test Valve



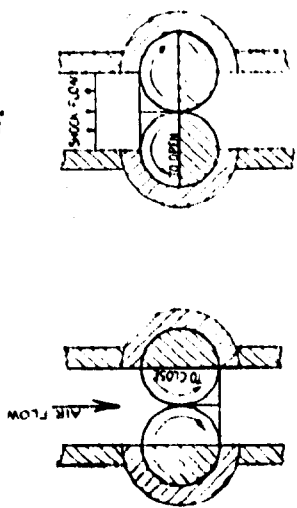
POSITIVE MEASURE  
GEAR BOX

TOP

ELLIPSOIDAL GEAR  
(P. 100)

NOTES:

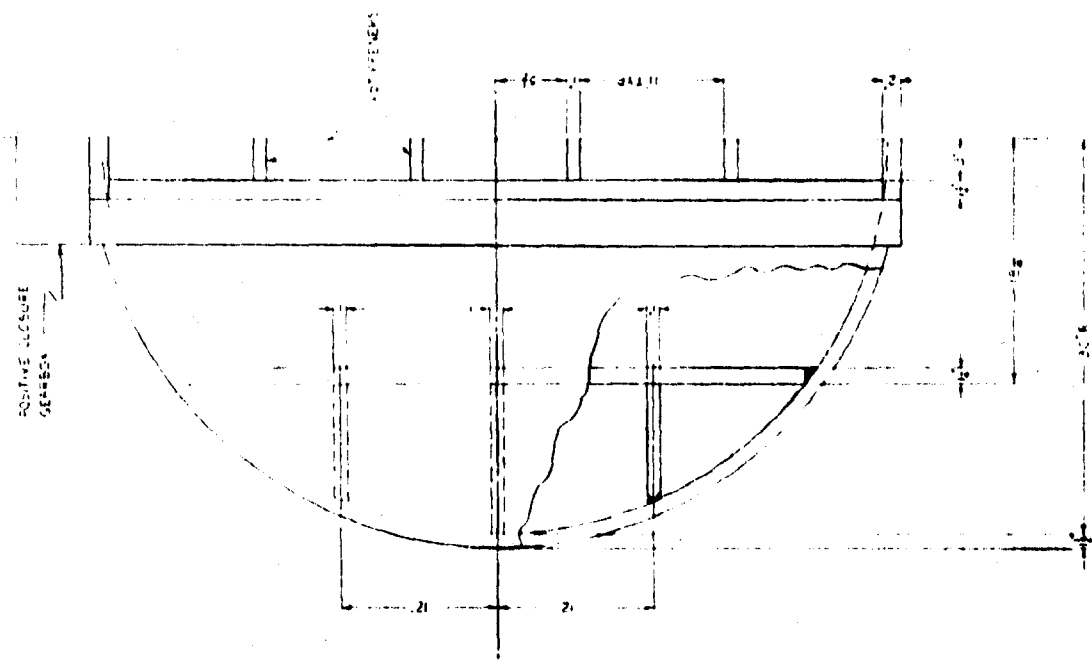
- 1. FRAME SPECS PER WORKSHEET;
- 2. GEAR MUST SLIP ON FOR PROPER SIZE OF GEAR.



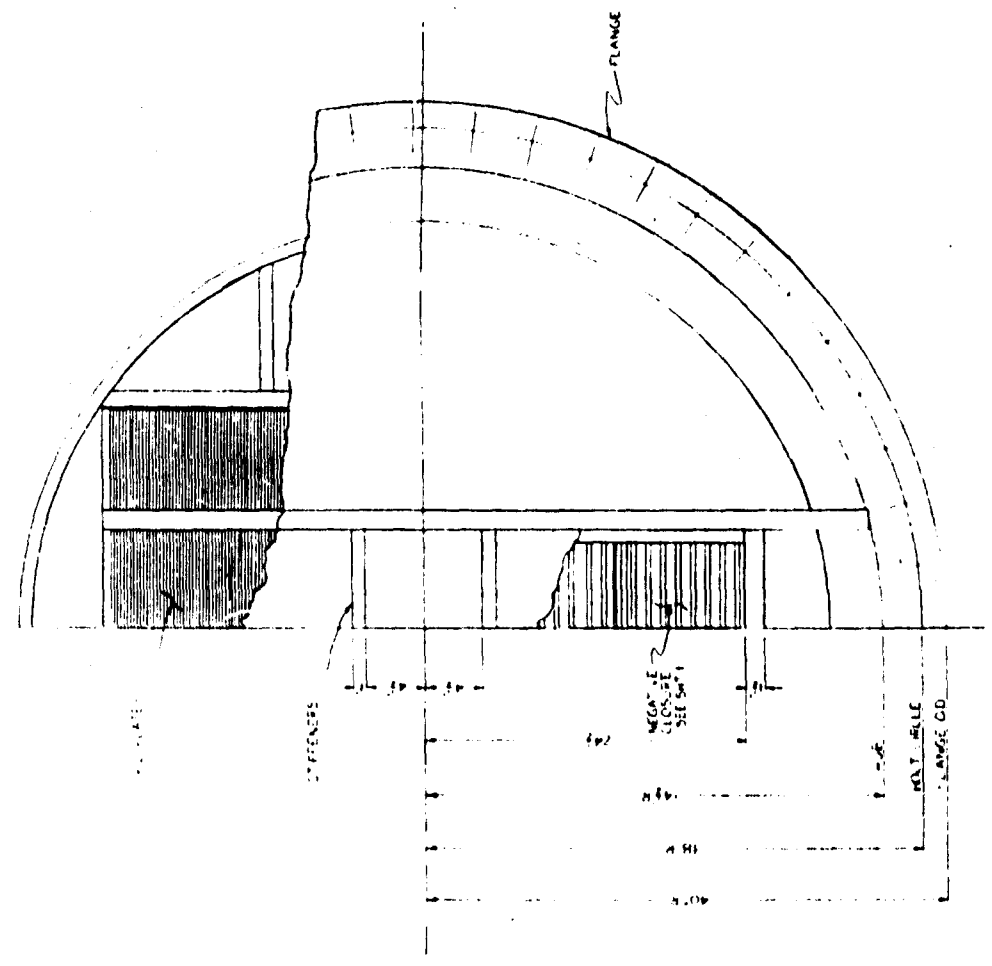
PROTOTYPE	
CLARK BLAST VA	
MATERIAL:	DESIGNED BY: [initials]
SEE ANALYSIS:	CHECKED BY: [initials]
SCALE: 1/2"	APPROVED BY: [initials]
	(C)

Figure 3 POSITIVE CLOSURE





TOP VIEW  
Scale 1/1



BOTTOM VIEW  
Scale 1/1

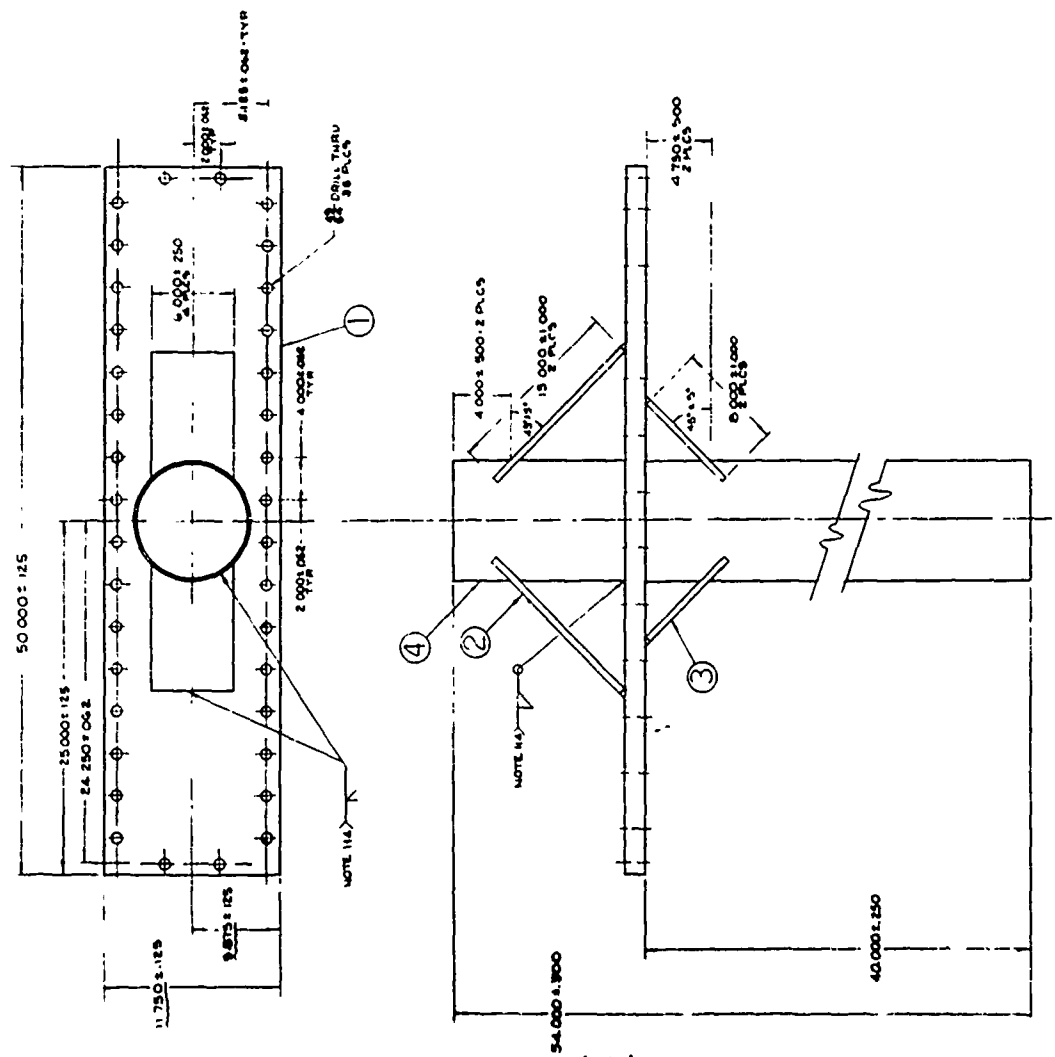
PROTOTYPE	
CLARK BLAST VA	
DRAWN BY: [initials]	CHECKED BY: [initials]
SCALE: 1/1	APPROVED BY: [initials]

Figure 5

REV	DESCRIPTION	DATE	APP
1			

**NOTES**

1. SHIELDED METAL ARC WELD USING AWS 601X
2. LOW HYDROGEN ELECTRODES
3. ALTERNATE MATERIAL: A516-70
4. INSPECTION OF WELDS PER M.R.I. INSTRUCTIONS



LIST OF MATERIALS	
1	TUBING 20" O.D. X 1/2" WALL - 1440 PL.
2	LOW CARBON HYPER STRENGTH 2" X 4" X 1/2"
3	WELLS 1/2" X 3/4" X 1/2" X 1/2"
4	OR EQUIVALENT
5	OR EQUIVALENT
6	OR EQUIVALENT
7	OR EQUIVALENT
8	OR EQUIVALENT
9	OR EQUIVALENT
10	OR EQUIVALENT
11	OR EQUIVALENT
12	OR EQUIVALENT
13	OR EQUIVALENT
14	OR EQUIVALENT
15	OR EQUIVALENT
16	OR EQUIVALENT
17	OR EQUIVALENT
18	OR EQUIVALENT
19	OR EQUIVALENT
20	OR EQUIVALENT
21	OR EQUIVALENT
22	OR EQUIVALENT
23	OR EQUIVALENT
24	OR EQUIVALENT
25	OR EQUIVALENT
26	OR EQUIVALENT
27	OR EQUIVALENT
28	OR EQUIVALENT
29	OR EQUIVALENT
30	OR EQUIVALENT
31	OR EQUIVALENT
32	OR EQUIVALENT
33	OR EQUIVALENT
34	OR EQUIVALENT
35	OR EQUIVALENT
36	OR EQUIVALENT
37	OR EQUIVALENT
38	OR EQUIVALENT
39	OR EQUIVALENT
40	OR EQUIVALENT
41	OR EQUIVALENT
42	OR EQUIVALENT
43	OR EQUIVALENT
44	OR EQUIVALENT
45	OR EQUIVALENT
46	OR EQUIVALENT
47	OR EQUIVALENT
48	OR EQUIVALENT
49	OR EQUIVALENT
50	OR EQUIVALENT
51	OR EQUIVALENT
52	OR EQUIVALENT
53	OR EQUIVALENT
54	OR EQUIVALENT
55	OR EQUIVALENT
56	OR EQUIVALENT
57	OR EQUIVALENT
58	OR EQUIVALENT
59	OR EQUIVALENT
60	OR EQUIVALENT
61	OR EQUIVALENT
62	OR EQUIVALENT
63	OR EQUIVALENT
64	OR EQUIVALENT
65	OR EQUIVALENT
66	OR EQUIVALENT
67	OR EQUIVALENT
68	OR EQUIVALENT
69	OR EQUIVALENT
70	OR EQUIVALENT
71	OR EQUIVALENT
72	OR EQUIVALENT
73	OR EQUIVALENT
74	OR EQUIVALENT
75	OR EQUIVALENT
76	OR EQUIVALENT
77	OR EQUIVALENT
78	OR EQUIVALENT
79	OR EQUIVALENT
80	OR EQUIVALENT
81	OR EQUIVALENT
82	OR EQUIVALENT
83	OR EQUIVALENT
84	OR EQUIVALENT
85	OR EQUIVALENT
86	OR EQUIVALENT
87	OR EQUIVALENT
88	OR EQUIVALENT
89	OR EQUIVALENT
90	OR EQUIVALENT
91	OR EQUIVALENT
92	OR EQUIVALENT
93	OR EQUIVALENT
94	OR EQUIVALENT
95	OR EQUIVALENT
96	OR EQUIVALENT
97	OR EQUIVALENT
98	OR EQUIVALENT
99	OR EQUIVALENT
100	OR EQUIVALENT

**TOP PLATE ASSY**

DRAWN BY: [Signature]

CHECKED BY: [Signature]

APPROVED BY: [Signature]

DATE: [Date]

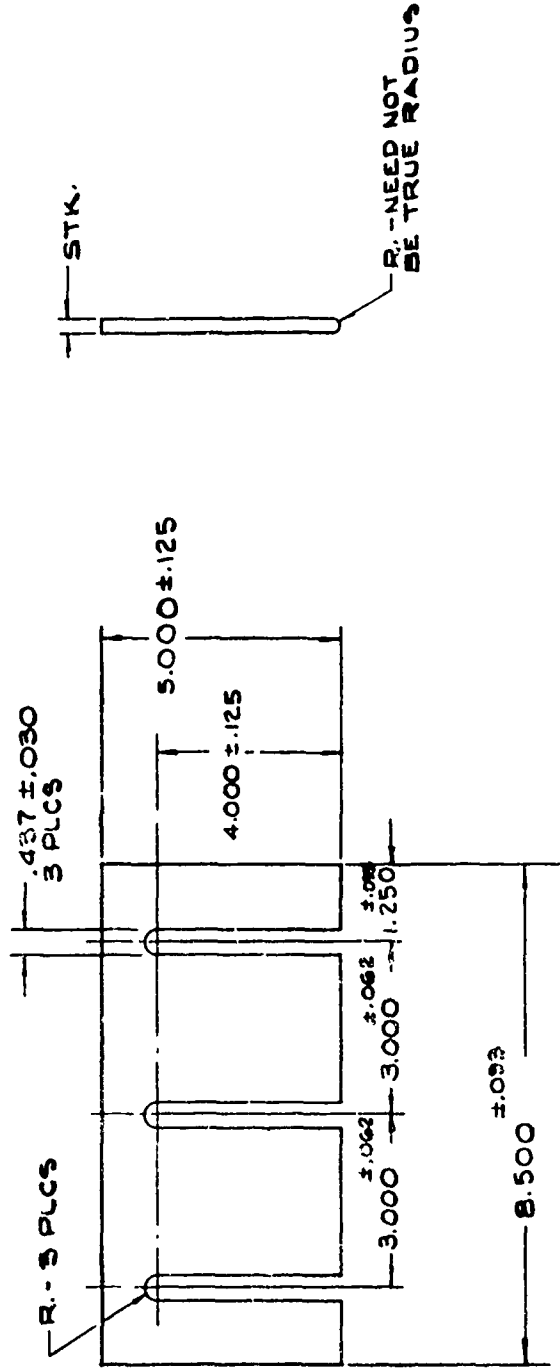
SCALE: [Scale]

FIG. NO. [Number]

Figure 6



REVISIONS		
SYM	DESCRIPTION	DATE
A	ORIG. ISSUE	APP



SPACER,  
PISTON PLATE

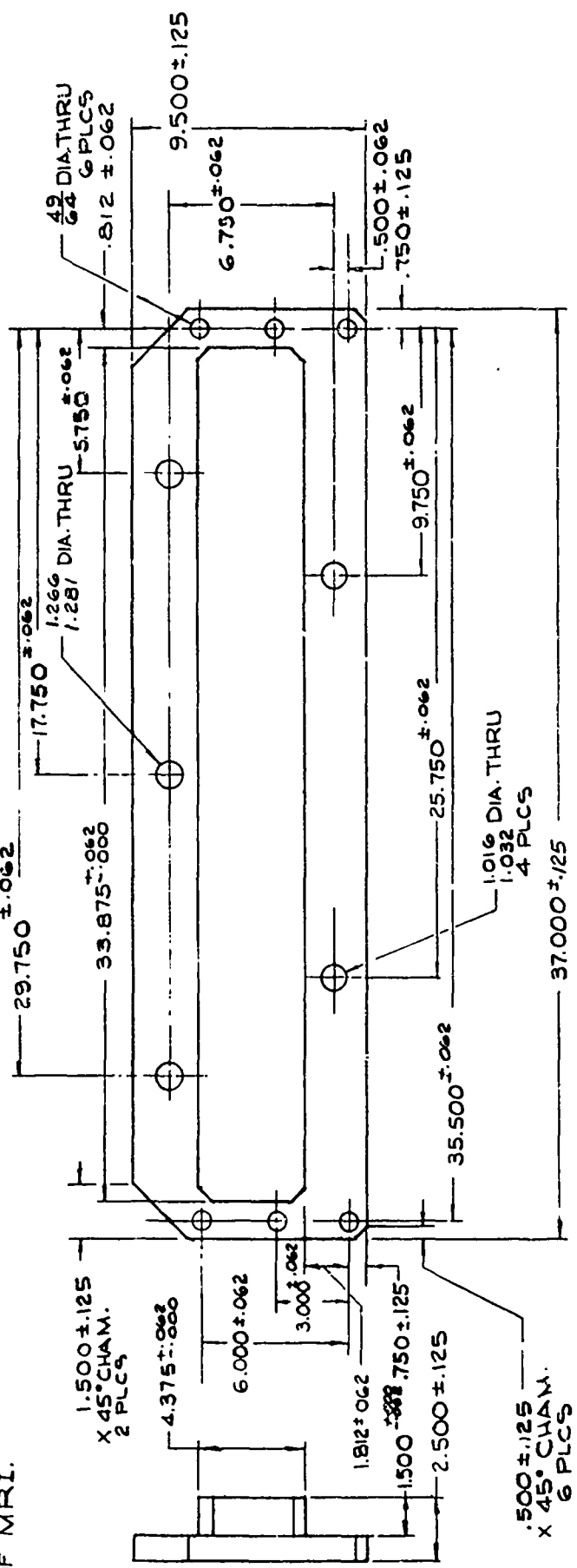
MATERIAL: MILD STEEL .250 STK	SCALE: 1/2	DRAWN BY: <i>JMN</i>	③
		CHECKED BY: <i>J. Rosenberg</i>	
		APPROVED BY:	

Figure 8

123

NOTES

1. MAT'L: LOW CARBON-HIGH STRENGTH STEEL,  
U.S.S.-T1, ARMO SSS-100 OR EQUIVALENT  
(100,000 PSI MIN YIELD)
2. 2 PC WELDMENT OPTIONAL UPON APPROVAL  
OF MRI.



REVISIONS		
SYM	DESCRIPTION	DATE
A		APP

ACCESS DOOR

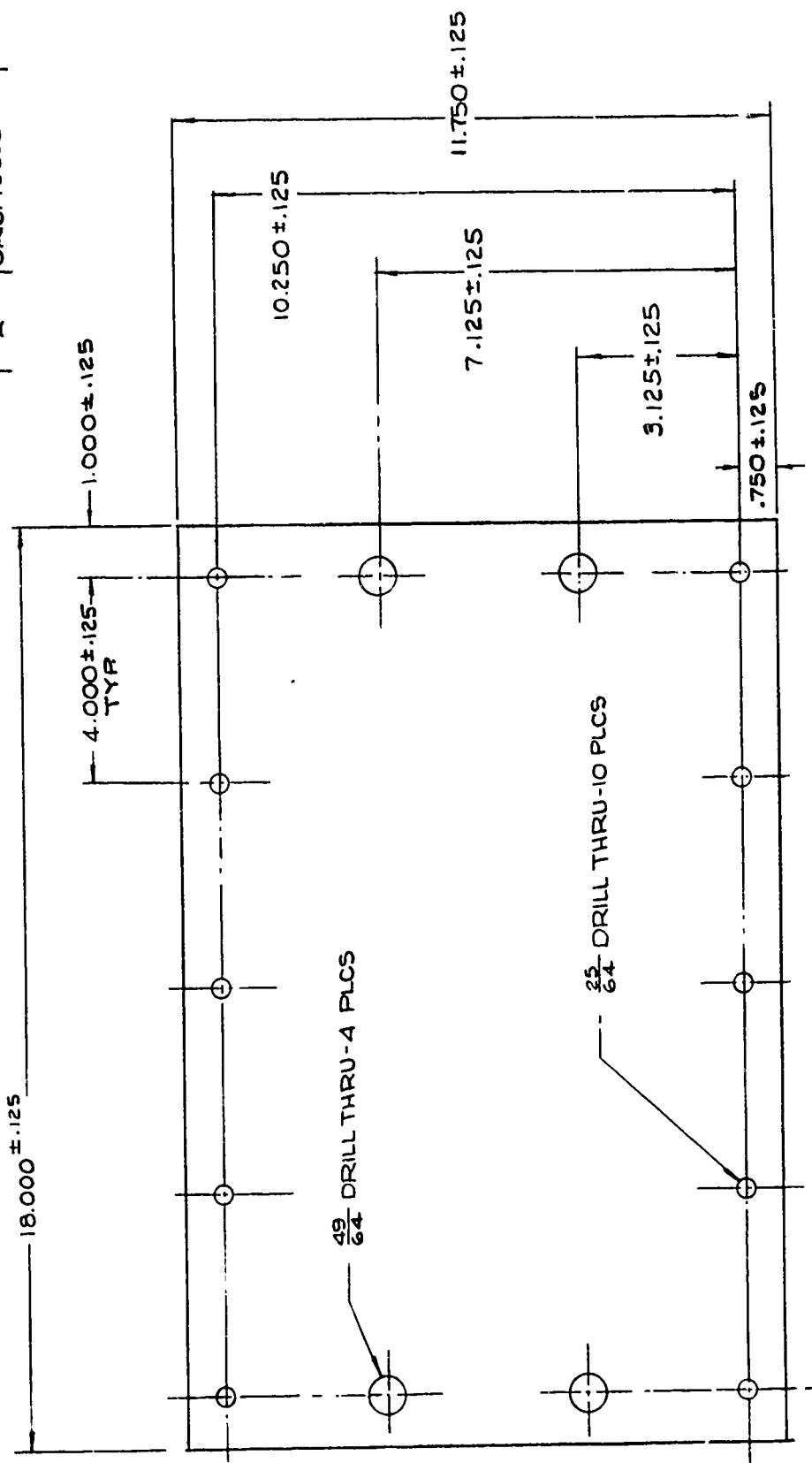
MATERIAL:	DRAWN BY: <i>San</i>
SEE NOTES	CHECKED BY: <i>d. Romberg</i>
SCALE: 1/4	APPROVED BY:

4

Figure 9

124

REVISIONS		
SYM	DESCRIPTION	DATE
A	ORIG. ISSUE	APP

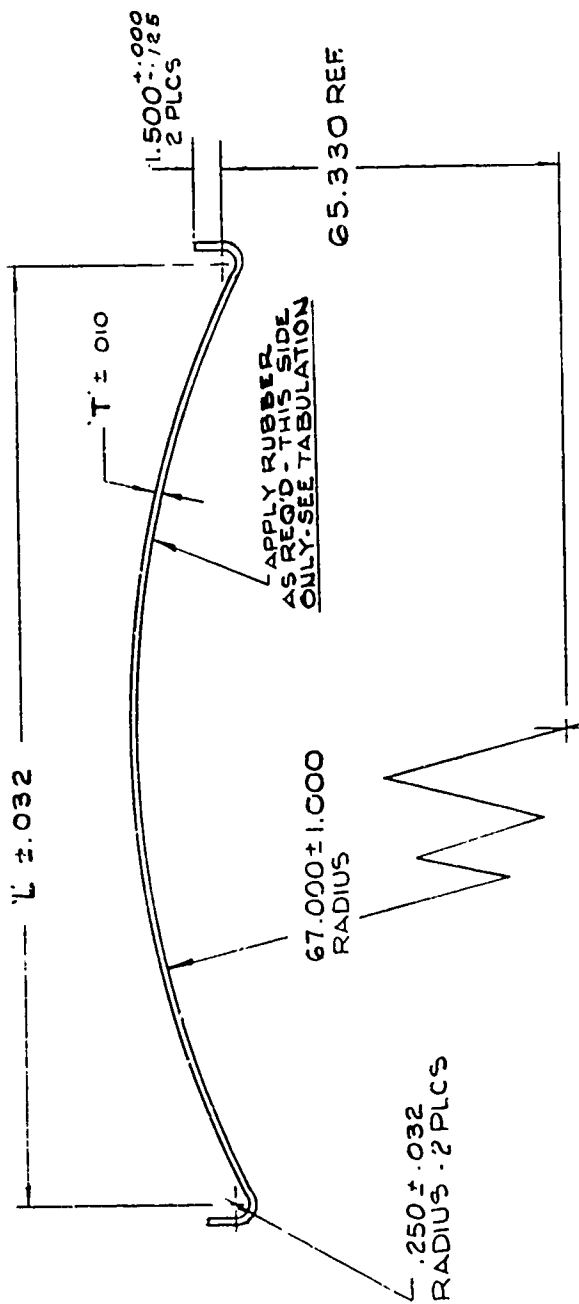


TEST DOOR		MATERIAL	DRAWN BY: <i>JMM</i>	⑤
		1/2 MILD STEEL	CHECKED BY: <i>A. Remsburg</i>	
		SCALE: 1/2	APPROVED BY:	

Figure 10

125

TABULATION		REVISIONS			
PART No.	MATERIAL	DIM. "L"	DESCRIPTION	DATE	APP
A	STEEL, SAE 1074 or 1095	.080	ORIG. ISSUE		
B	STEEL, SAE 1074 or 1095	.040	CHG MAT'L A, B, C ADD NOTE 2	22/12/70	DR
C	STEEL, -AE 1074 or 1095 VULCANIZE 1/8 RUBBER TO SURFACE INDICATED	32.420			
D	ALUMINUM (AMS-4026C-T4)	32.340			



PISTON PLATE TO MOVE  
FREELY WHEN ASSEMBLED  
IN BLAST VALVE - SEE  
DWG No. 1

NOTES

1. DIMENSION 'L' IS EQUAL TO 32.500 ± .021
2. PARTS A, B, AND C TO BE HEAT TREATED TO HARDNESS TO ROCKWELL C.

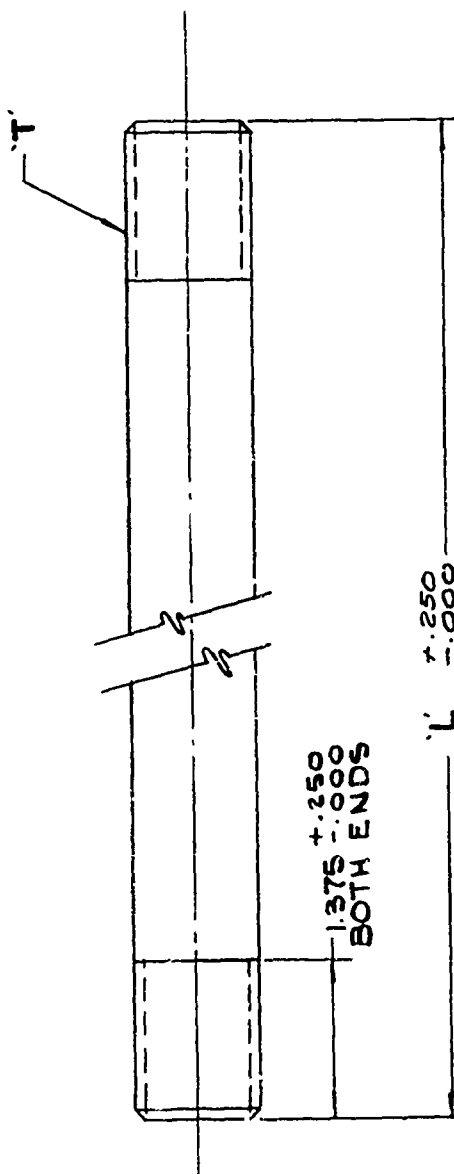
PISTON PLATE TABULATION		DRAWN BY: <i>DMU</i>	6
MATERIAL: SEE TABULATION	CHECKED BY: <i>J. Rosenberg</i>		
SCALE: NONE	APPROVED BY:		

Figure 11

**NOTES**

1. MAT'L: ALLOY STEEL (4340) AIRCRAFT QUALITY  
 ROD. HEAT TREAT TO 150,000 PSI TENSILE  
 YIELD MIN.

SYMBOL	DESCRIPTION	DATE	APP
A	ORIG. ISSUE		

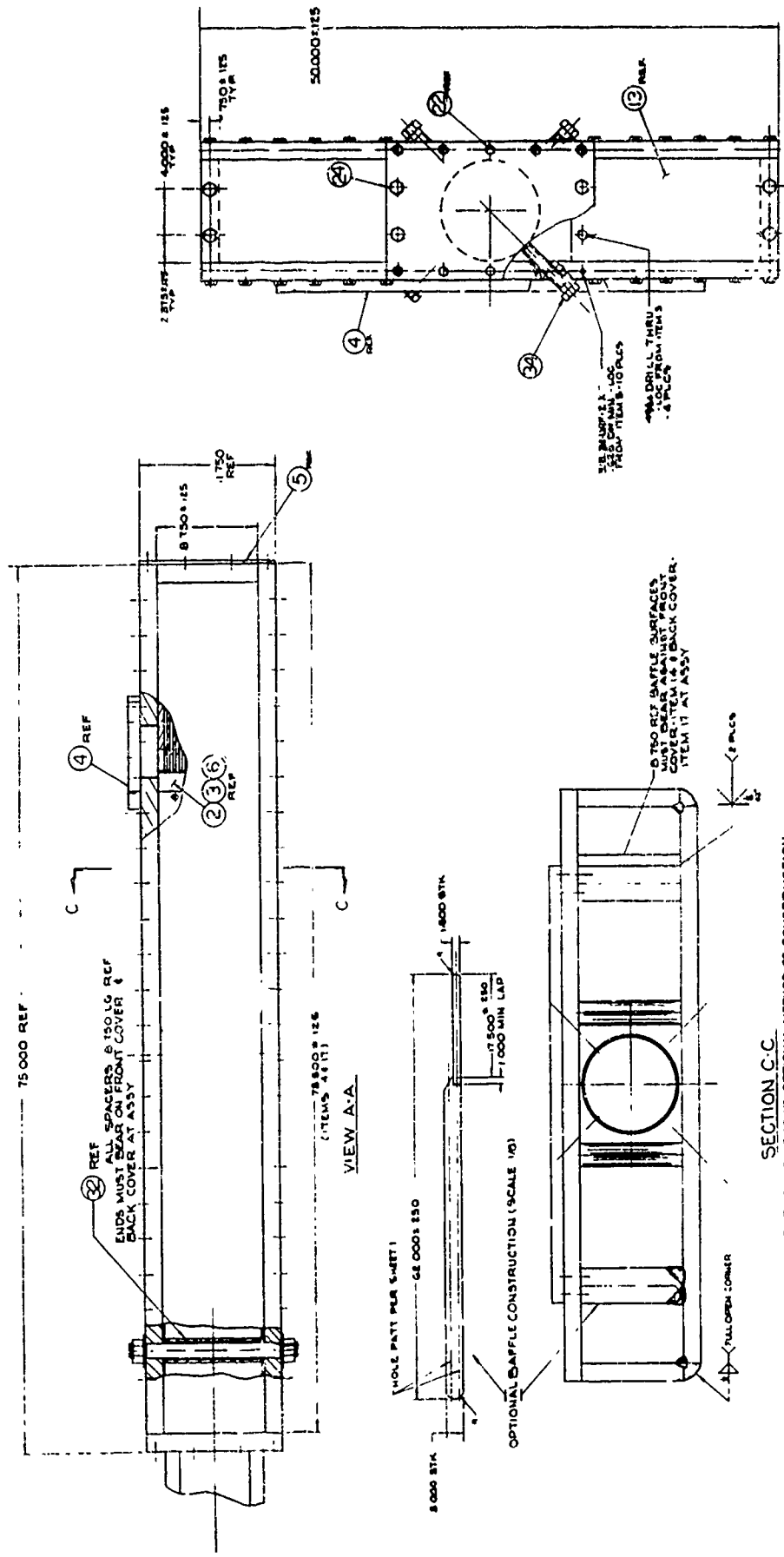


TABULATION		
PART N <sup>o</sup> .	THD 'T'	LENGTH 'L'
7-A	1/4-12UNF-3	14.500
7-B	1/4-12UNF-3	15.500
7-C	1-12UNF-3	14.000
7-D	1-12UNF-3	15.000

MATERIAL: SEE NOTES		DRAWN BY: <i>SM</i>	
		CHECKED BY: <i>d. Romberg</i>	
SCALE: NONE		APPROVED BY:	
STUD - TABULATION		7	

Figure 12





VIEW B-B

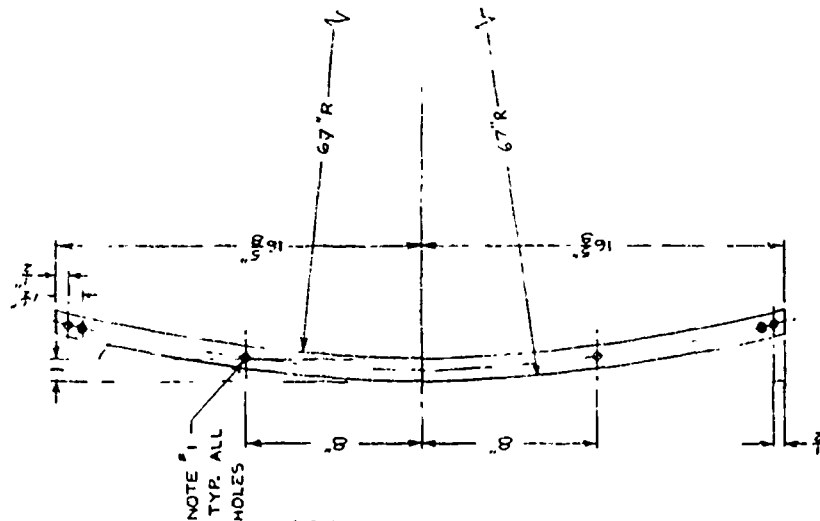
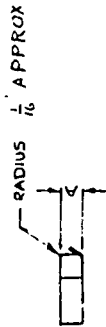
SECTION C-C

NOTE THIS VIEW SHOWS OPTIONAL METHOD OF CONSTRUCTION. WELDS AS SHOWN ARE NOT TO BE CONSIDERED. SEE ITEM 4 FOR ACCESS DOOR. ITEM 4 INSPECTION OF WELDS PER M.P.R.I. INSTRUCTIONS

ASSEMBLY	
CLARK BLAST VALVE	
DESIGNED BY	8
CHECKED BY	
SCALE	AS SHOWN BY

Figure 14

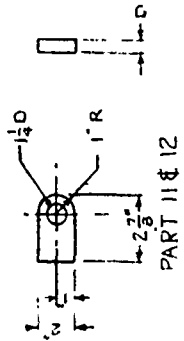
PART	A	QTY
1 & 4	1"	2 ea
2 & 5	$\frac{3}{4}$ "	6 ea
3 & 6	$\frac{1}{2}$ "	1 ea



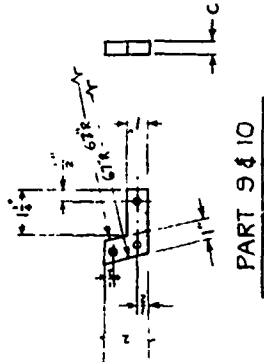
PART # 1 Thru # 3

Figure 15 Backup Grid Modification

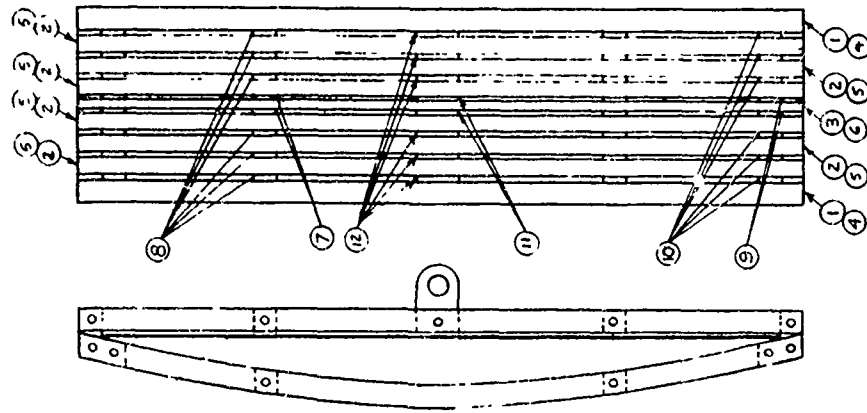
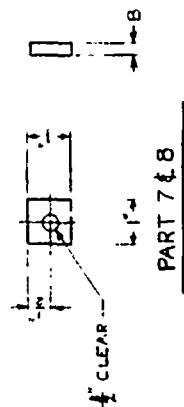
PART	D	QTY
11	$\frac{1}{2}$ "	2
12	$\frac{3}{4}$ "	6



PART	C	QTY
9	$\frac{3}{4}$ "	4
10	$\frac{1}{2}$ "	12



PART	B	QTY
7	$\frac{3}{4}$ "	4
8	$\frac{1}{2}$ "	12



ASSEMBLY INSTRUCTIONS

Notes

- 1 IN 1 (QTY) OF PARTS 1 & 4 DRILL & TAP  $\frac{1}{4}$ -13. IN REMAINDER OF PARTS DRILL CLEARANCE FOR  $\frac{1}{2}$  EXCEPT AS NOTED.
2. ALL PARTS TO BE MADE FROM C1018 OR EQUIVALENT

The Clark Valve Co  
517 Camino de la Sierra  
MESA, N.M. 87123

DRAWN BY *G. M. [Signature]*  
CHECKED BY *M. O. [Signature]*  
APPROVED BY

BLAST VALVE MODIF.

1

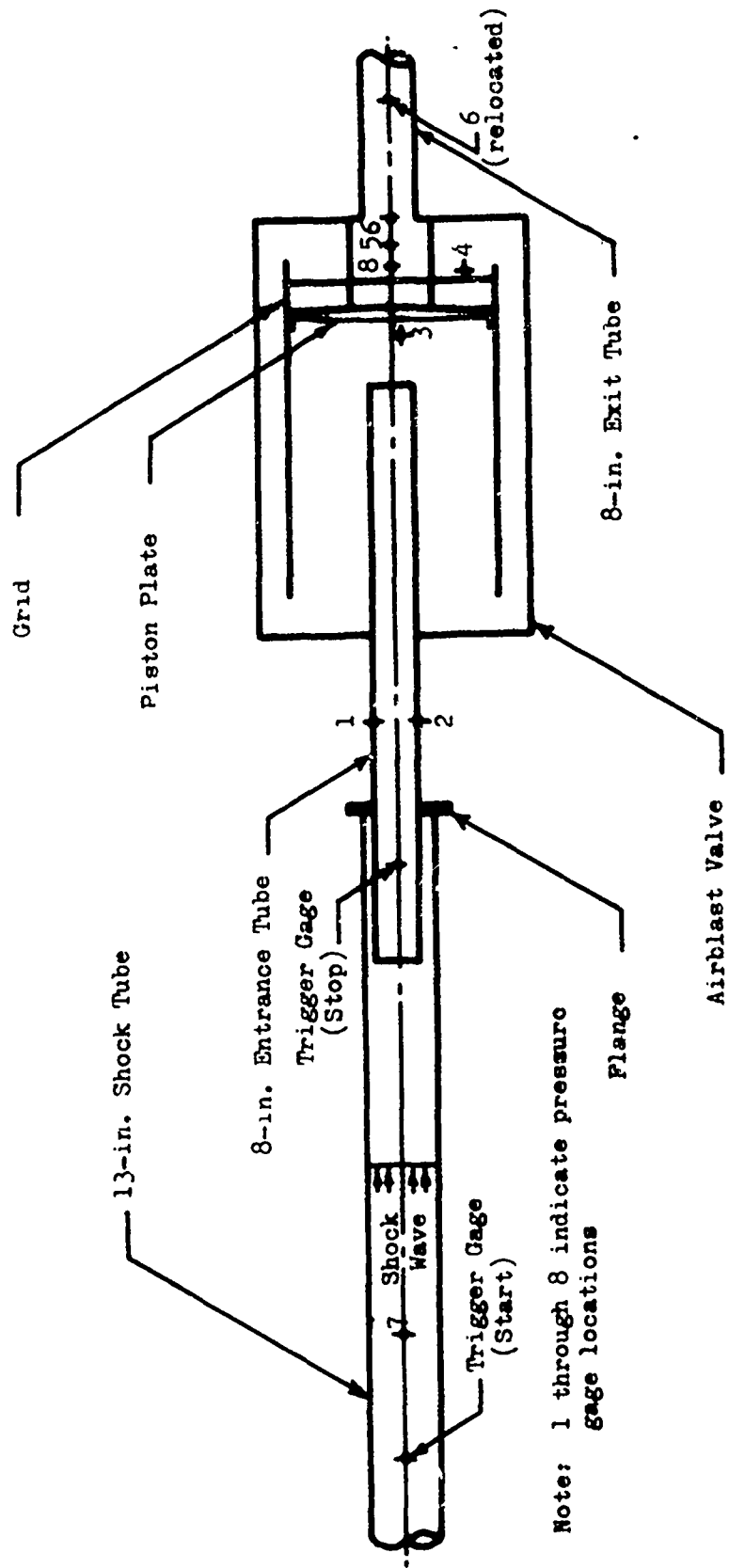
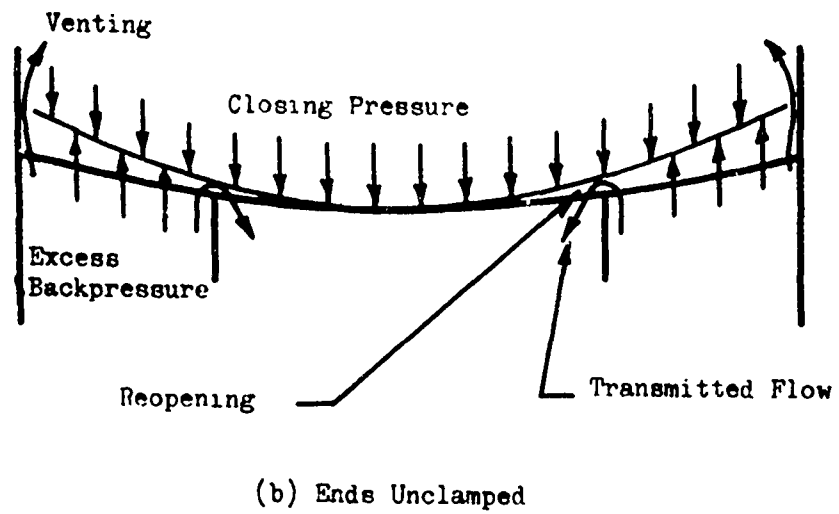
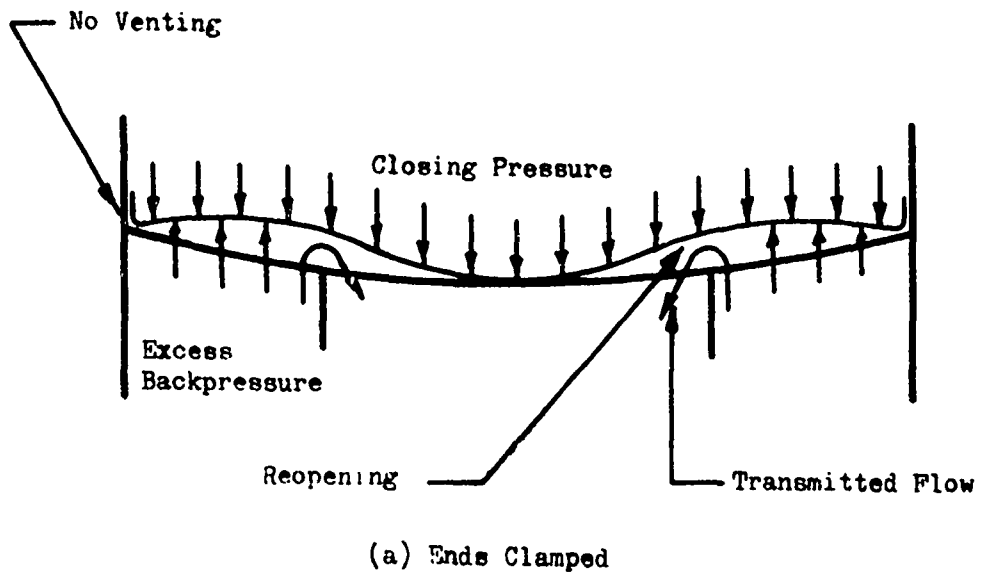


Figure 16 Plan View of Valve in Shock Tube and Pressure Gage Positions



135

Figure 17 Clamped and Free End Diaphragm Arrangements

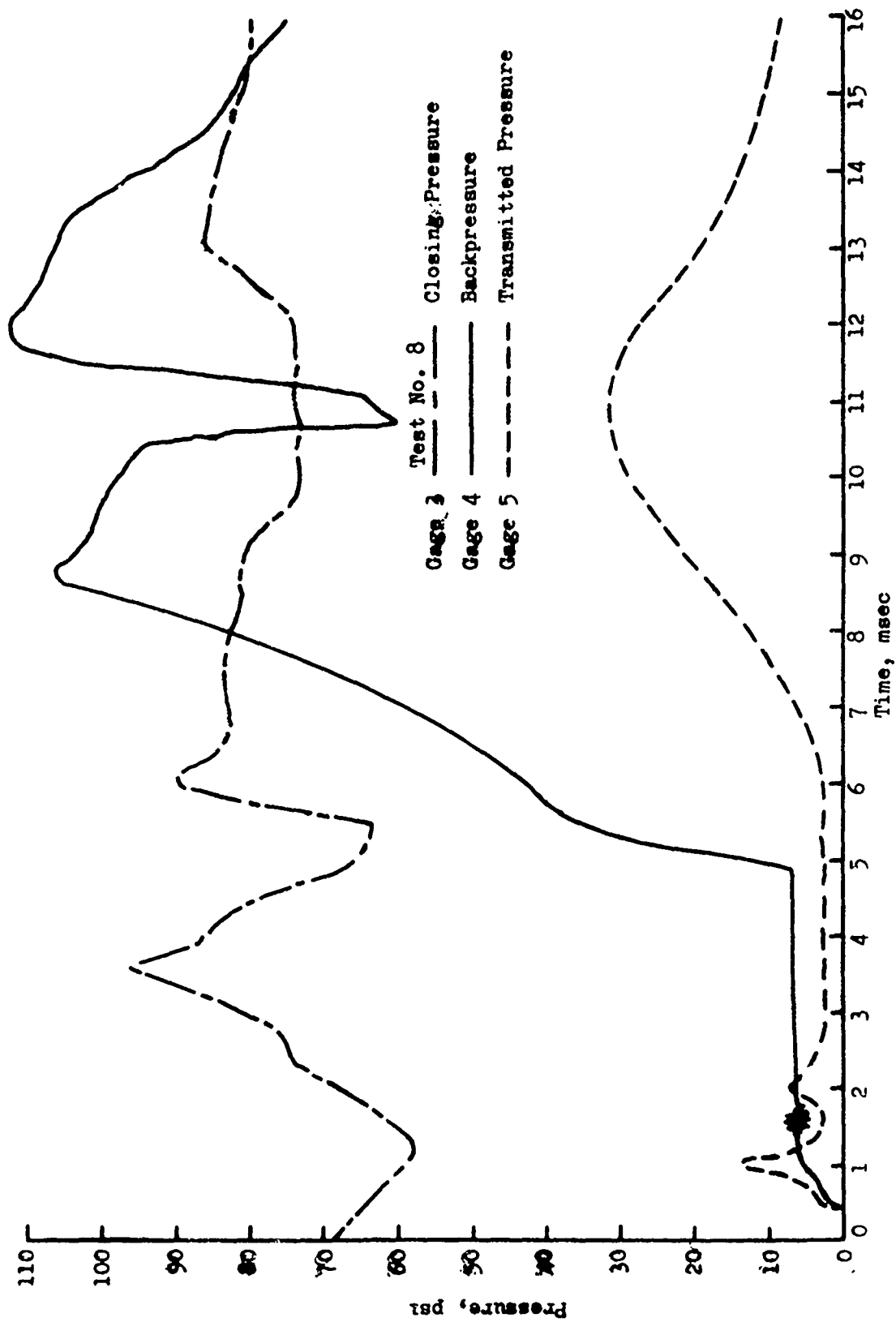


Figure 18 Development and Effects of Backpressure on Clamped End Diaphragm

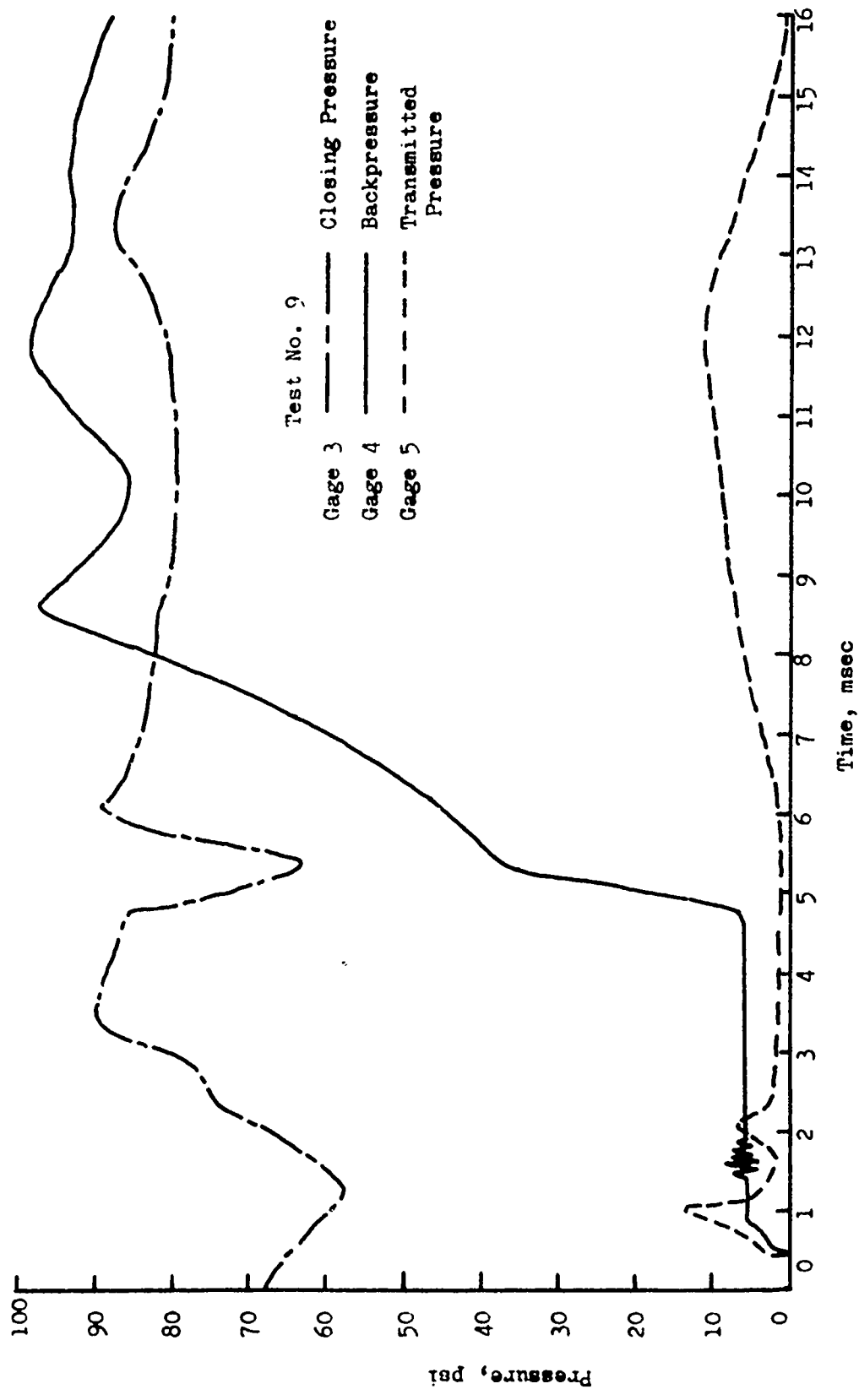


Figure 19 Development and Effects of Backpressure on Free End Diaphragm

134

$\frac{Q}{V}$  - Volume Rate of Flow in cubic feet per minute

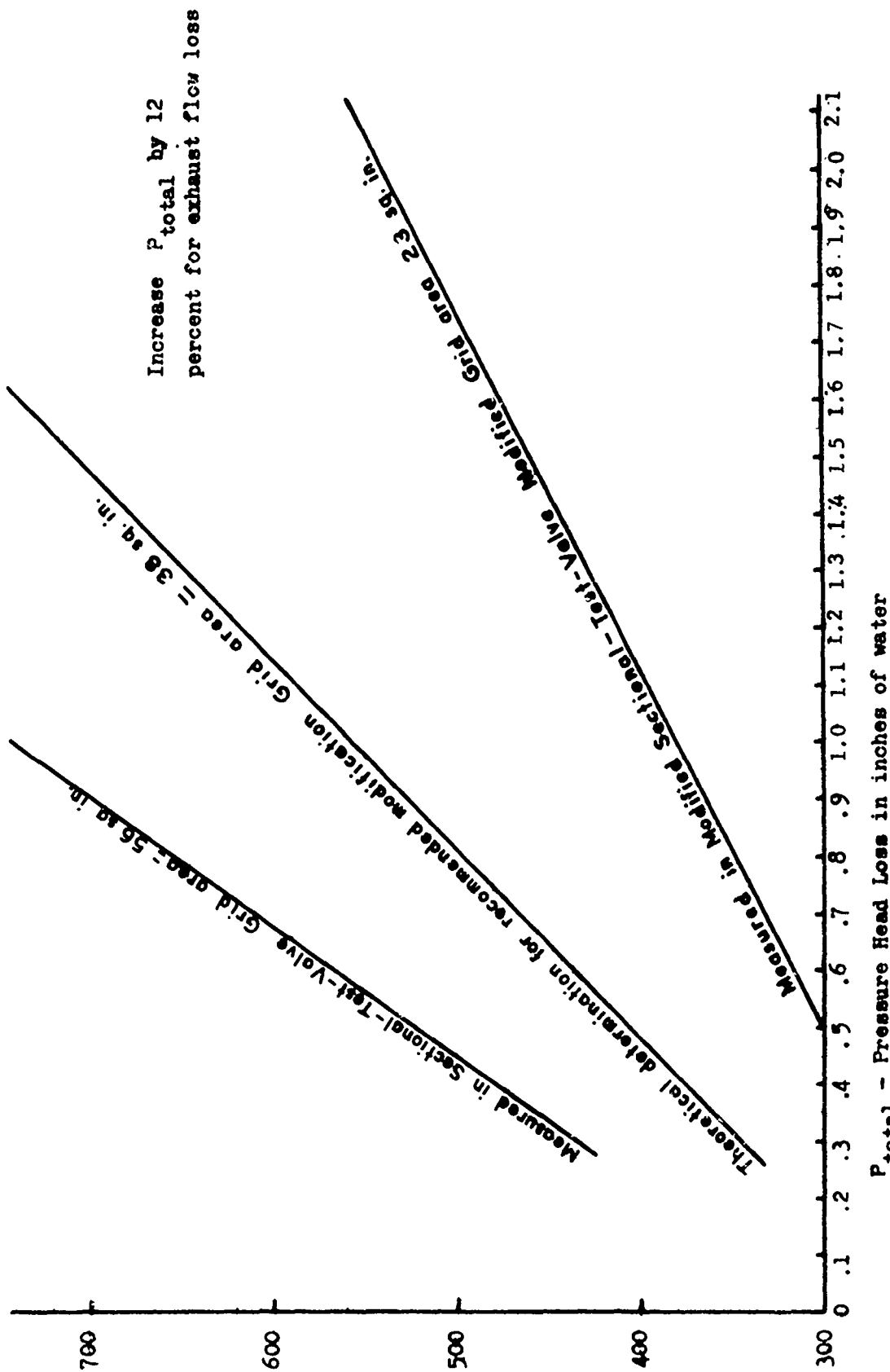


Figure 20 Pressure Head Loss versus volume rate of flow measured in test valve and calculated or prototype recommendations.